INFORMATION TO USERS

This manuscript has been reproduced from the microfilm master. UMI films the text directly from the original or copy submitted. Thus, some thesis and dissertation copies are in typewriter face, while others may be from any type of computer printer.

The quality of this reproduction is dependent upon the quality of the copy submitted. Broken or indistinct print, colored or poor quality illustrations and photographs, print bleedthrough, substandard margins, and improper alignment can adversely affect reproduction.

In the unlikely event that the author did not send UMI a complete manuscript and there are missing pages, these will be noted. Also, if unauthorized copyright material had to be removed, a note will indicate the deletion.

Oversize materials (e.g., maps, drawings, charts) are reproduced by sectioning the original, beginning at the upper left-hand corner and continuing from left to right in equal sections with small overlaps.

Photographs included in the original manuscript have been reproduced xerographically in this copy. Higher quality 6" x 9" black and white photographic prints are available for any photographs or illustrations appearing in this copy for an additional charge. Contact UMI directly to order.

Bell & Howell Information and Learning
300 North Zeeb Road, Ann Arbor, MI 48106-1346 USA
800-521-0600

UMI®

Dissertation:

Chromosome Translocations in Turtles:

A Biomarker in a Sentinel Animal for Environmental Biodosimetry

Submitted by

Brant A. Ulsh

Department of Radiological Health Sciences

In partial fulfillment of the requirements

for the degree of Doctor of Philosophy

Colorado State University

Fort Collins, Colorado

Summer 2000

Colorado State University

June 19, 2000

We hereby recommend that the dissertation prepared under our supervision by Brant A. Ulsh entitled Chromosome Translocations in Turtles – A Biomarker in a Sentinel Animal for Ecological Dosimetry, be accepted as fulfilling in part requirements for the degree of doctor of philosophy.

Committee on Graduate Work

Co-Advisor

Co-Advisor, Department Head

ABSTRACT OF DISSERTATION

Chromosome Translocations in Turtles:

A Biomarker in a Sentinel Animal for Environmental Biodosimetry

This dissertation details a new approach for determining the magnitude and genetically relevant effects of wildlife exposures to radionuclides in contaminated environments. The yellow-bellied slider turtle (*Trachemys scripta*) served as a model organism. A biomarker of radiation exposure, the frequency of symmetrical chromosome aberrations in *T. scripta* lymphocytes, was developed which correlates with cumulative lifetime exposure.

A fluorescence *in situ* hybridization probe for *T. scripta* chromosome-1 was constructed through microdissection and amplification by polymerase chain reaction. The *T. scripta* probe hybridized exclusively to chromosome-1 *T. scripta*, and in each of four other turtle species, demonstrating conservation of chromosome-1 homology in turtles over 66 million years.

The efficacy of this probe in detecting radiation-induced chromosome aberrations was demonstrated through the construction of a dose-response curve for *T. scripta* fibroblasts acutely irradiated *in vitro*. With respect to induction of chromosome interchange aberrations, human fibroblasts are approximately 1.7 times more radiosensitive than the *T. scripta* fibroblasts.

To move toward application of this biomarker in field studies, culture conditions for *T. scripta* lymphocytes, which can be sampled nonlethally, were developed. Since protracted exposures result in a reduced effect per unit dose, the extent of this effect for aberration induction in turtle cells was examined in both fibroblasts and lymphocytes.

The dose-rate below which no reduction in effect per unit dose is observed with further dose protraction was approximately 23 cGy hr^{-1}. The whole-genome spontaneous background level of complete, apparently simple symmetrical translocations in *T. scripta* lymphocytes, projected from aberrations occurring in chromosome-1 was approximately 1.20×10^{-3}/cell. Comparable spontaneous background levels reported for humans are some 5- to 30-fold higher. This relatively low background level for turtles would be a significant advantage for measurement of effects at low doses and dose-rates. Finally, the dose-response of *T. scripta* lymphocytes irradiated *in vivo* at a low dose-rate was determined. The best fit curve was $Y = (0.0015 \pm 0.0013) + (0.0058 \pm 0.0009)*D - (0.00033 \pm 0.00011)*D^2$; where Y = number of apparently simple symmetrical translocations per cell, D = dose (Gy), and errors are one Poisson standard deviation. This dose-response relationship can serve as a calibration curve for environmental biodosimetry field studies.

Brant Allan Ulsh
Department of Radiological Health Sciences
Colorado State University
Fort Collins, Colorado 80523
Summer, 2000

FOREWARD

Each chapter in this dissertation covers a different aspect of my research project on environmental biodosimetry in *T. scripta*. Chapter one is an introductory chapter on the history of biological dosimetry, and the ecological applications biodosimetric techniques. Chapter two reports the development of a whole-chromosome fluorescence *in situ* hybridization (FISH) probe for *T. scripta* chromosome-1 and use of the probe for comparative genomics. Chapter three covers the initial testing of the probe in *T. scripta* fibroblasts, and the determination of a dose-response curve for acute, high-dose rate irradiation of fibroblast cultures *in vitro*. Chapter four describes the development of *T. scripta* lymphocyte culture techniques. Chapter five investigates the dose-rate effect for chromosome aberration induction in *T. scripta* fibroblasts and lymphocytes, and develops a dose-response calibration curve for low dose-rate, chronic irradiation of *T. scripta* lymphocytes *in vivo*.

This dissertation is written so that each chapter is a stand-alone document suitable for submission for publication. The chapters are organized to reflect the steps of this project in the order in which they were addressed, rather than the order in which the chapters were written and submitted for publication, therefore an occasional reference to other chapters as manuscripts submitted or in preparation may be found. The reader may also notice repetition of some text, particularly in the introduction and discussion sections of the various chapters. This was necessary to make each paper submitted for publication complete and self-contained. Only minimal formatting changes for the sake of consistency were made to the manuscripts for inclusion in this dissertation. Upon the advice of my graduate committee, this dissertation (but not the manuscripts submitted for

publication) is written in first person singular. However, I feel it is necessary to explicitly state that the studies contained herein could not have been accomplished without the considerable help provided by the individuals mentioned in the Acknowledgements.

SUMMARY

One of the fundamental problems of ecological risk assessment and biomonitoring is the current difficulty in directly linking observed effects in wildlife populations to exposure to environmental contaminants such as chemicals or radionuclides, particularly at the low doses and dose rates typical of environmental exposures. Most often, fate and transport modeling and tissue residue analyses are used to provide exposure estimates for selected species. But such estimates suffer from several shortcomings including: 1) only a snapshot picture at a given point in time is provided – no information can be ascertained on cumulative exposure; 2) only internal exposures are estimated – no information is provided on external exposures (e.g. from ionizing radiation); 3) assumptions regarding movements of animal species through contaminated areas and the duration of exposures are required; 4) it can be difficult, particularly in sublethal ranges, to correlate a given level of a contaminant in a given tissue to ecologically relevant effects.

My overall objective was to begin to address these problems by extending the techniques of biodosimetry to environmental contamination situations. I did this by developing a biomarker of exposure to radionuclides in a model wildlife species, the yellow-bellied slider turtle (*Trachemys scripta*), which is known to have a maximum life-span of at least 22 years. Turtles were chosen because a long-lived animal would best serve the need for the study of low level, prolonged chronic exposure conditions such as those typical of contaminated environments.

As a biomarker, I used the frequency of radiation-induced symmetrical chromosome translocations in *T. scripta* fibroblasts and lymphocytes, as detected by fluorescence *in situ* hybridization (FISH) whole chromosome painting. The objective of

chapter 1 is to provide a discussion of the past uses of this biodosimetric technique, and how it may be applied to environmental contamination situations. Biodosimetric techniques are widely applied in humans acutely exposed as a result of accidents or for clinical purposes, but they have not been utilized in organisms chronically exposed to radionuclides in contaminated environments. The application of biodosimetry, the estimation of received doses by determining the frequency of radiation-induced chromosome aberrations, to environmental exposure scenarios could greatly improve the accuracy and reduce the uncertainties of ecological risk assessments and biomonitoring studies, because no assumptions are required regarding external exposure rates and the movement of organisms into and out of contaminated areas. Furthermore, unlike residue analyses of environmental media or biota tissues, environmental biodosimetry provides a genetically relevant biomarker of cumulative lifetime exposure. Symmetrical chromosome translocations can impact reproductive success when they occur in gametes, and could therefore eventually prove to be ecologically relevant as well.

The objective of chapter 2 was to discuss the development of the FISH probe, and its application in comparative genomics. After preparing a whole chromosome-1 specific DNA library from a *T. scripta* fibroblast cell line (the first such library prepared for any reptile), a FISH painting probe was prepared and hybridized to cells from four other species of turtle ranging from a desert tortoise to a loggerhead sea turtle. This resulted in specific and exclusive hybridization to chromosome-1 in each species. Previous observations of conservation in the giemsa banding pattern and chromosome morphology and number among turtles are thus extended to the DNA sequence level, revealing a cytogenetic stability of chromosome-1 in these turtles during the past 66-144 million

years. This contrasts with the situation for various hominoid species where, in many instances, extensive chromosomal rearrangements have been reported in one third of that time period.

The objective of chapter 3 was to test the probe for use in radiation biodosimetry. The efficacy of the probe for detection of chromosome aberrations was demonstrated by the establishment of a dose-response curve for chromosome interchange aberrations in acutely irradiated *T. scripta* fibroblasts. This was compared to the dose-response for human fibroblasts treated under similar conditions in this laboratory. With respect to induction of chromosome interchange aberrations, human fibroblasts were approximately 1.7 times more sensitive than the *T. scripta* fibroblasts. The relative radioresistance of turtles may be the result of evolved cellular defenses against reperfusion injury when turtles recover from hypoxic conditions encountered during diving and hibernating.

The objective of chapter 4 was to develop culture techniques for *T. scripta* lymphocytes. Since lymphocytes can be sampled nonlethally, they are the cell type of choice for environmental studies of animal species. However, culture techniques for turtle and other reptilian lymphocytes are not well established. I examined a variety of conditions and parameters relevant to turtle lymphocyte culture including: different mitogenic agents, alone and in combination; lymphocyte separation protocols; culture volume; time required to stimulate lymphocytes to mitosis; importance of humidity and gas exchange in culture incubation; suitability of different culture media; effects of varying serum concentrations; ability of interleukin-2 (IL-2) to stimulate lymphocyte growth and prevent apoptosis; and feasibility of inducing premature chromosome condensation. The best conditions and parameters of those I studied for obtaining mitotic

cells were (1) the combined use of phytohemagglutinin-M form (2%) and lipopolysaccharides (0.55 $\mu g ml^{-1}$), (2) the use of 5% autologous turtle serum (as opposed to fetal bovine serum), and (3) collection of mitotic cells around 96 hours after mitogenic stimulation. Human, recombinant IL-2 did not increase the fraction of lymphocytes in mitosis over the range of concentrations tested and calyculin A was not effective at inducing premature chromosome condensation in turtle lymphocytes over the range of concentrations tested.

Finally, the objective of chapter 5 was to take the last steps to ready this technique for use in environmental biodosimetry experiments. I investigated the dose-rate effect for radiation-induced symmetrical translocations in *T. scripta* fibroblasts and lymphocytes. The dose-rate below which no reduction in effect per unit dose was observed with further dose protraction was approximately 23 cGy hr^{-1}.

I estimated the whole-genome spontaneous background level of complete, apparently simple symmetrical translocations in *T. scripta* lymphocytes projected from aberrations occurring in chromosome-1 to be approximately 1.20×10^{-3} /cell. Comparable spontaneous background levels reported for humans are some 5- to 30-fold higher, ranging from about 6×10^{-3} to 3.4×10^{-2} per cell. This relatively low background level for turtles would be a significant advantage for measurement of effects at low doses and dose-rates.

I also chronically irradiated turtles over a range of doses from 0-8 Gy delivered at approximately 5.5 cGy hr^{-1}, and constructed a lymphocyte dose-response curve for complete, apparently simple symmetrical translocations (Y_T) suitable for use with animals chronically exposed to radiation in contaminated environments. The best fit

calibration curve (not constrained through the zero dose estimate) was of the form $Y_{as} = c + aD + bD^2$, where Y_{as} was the number of apparently simple symmetrical translocations per cell, D was the dose (Gy), a = (0.0058 ± 0.0009), b = (-0.00033 ± 0.00011), and c = (0.0015 ± 0.0013), and errors were one Poisson standard deviation. This calibration curve should facilitate field studies with *T. scripta* inhabiting radionuclide-contaminated ponds, reservoirs and streams.

Taken together, the results of the experiments reported in this dissertation demonstrate the feasibility of environmental biodosimetry in determining cumulative lifetime exposures organisms receive from environments contaminated with radionuclides. With additional whole-chromosome probes to improve sensitivity, environmental biodosimetry using stable chromosome translocations could provide a practical and genetically relevant measurement endpoint for ecological risk assessments and biomonitoring programs.

ACKNOWLEDGEMENTS

I would first like to thank my Co-Advisors, Ward Whicker and Joel Bedford. I spent innumerable hours in each of their offices discussing various technical issues and questions, and their guidance, patience, and friendship throughout the course of this project has been unfailing. I must also thank my "unofficial advisor", Maria Mühlmann-Díaz, who patiently showed me the ropes and guided me through my early days in Joel's lab.

The members of my graduate committee, Tom Hinton, Bill Lauenroth, and Dave Rowan spent many hours in my student seminars, reviewing manuscripts and drafts, and participating in my dissertation defense. This dissertation is a stronger document, and its author is a better scientist because of your efforts. Thank you!

I would also like to thank a few faculty members, fellow students and lab-mates for their insightful discussions, suggestions, and assistance: Ryan Alexander for the countless hours of computer and statistical advice, Larry Dugan, Ryuichi Okayasu, and Allen Christian for advice and discussion of various cytogenetic issues and techniques, Dianne Vannais and Elizabeth McNiel for suggestions on turtle lymphocyte stimulation, Jeanne Robinson for assistance with chromosome banding, Brad Gersey and Steve Guetersloh for statistical advice, and Mike Fox and Leslie Armstrong-Lea for assistance with flow cytometry.

And finally, I would like to thank my family, Celeste and Eli, for the moral support, financial sacrifice, and tolerance of my absence during the many long hours, days, and nights I spent in the lab over the past five years. Thank you for letting me pursue my dream!

TABLE OF CONTENTS

LIST OF TABLES AND FIGURES

Chapter 1

Environmental Biodosimetry: A Genetically Relevant Tool for Biomonitoring and Ecological Risk Assessment

Abstract:

Biodosimetry, the estimation of received doses by determining the frequency of radiation-induced chromosome aberrations, is widely applied in humans acutely exposed as a result of accidents or for clinical purposes, but biodosimetric techniques have not been utilized in organisms chronically exposed to radionuclides in contaminated environments. The application of biodosimetry to environmental exposure scenarios could greatly improve the accuracy and reduce the uncertainties of ecological risk assessments and biomonitoring studies, because no assumptions are required regarding external exposure rates and the movement of organisms into and out of contaminated areas. Furthermore, unlike residue analyses of environmental media, environmental biodosimetry provides a genetically relevant biomarker of cumulative lifetime exposure. Symmetrical chromosome translocations can impact reproductive success, and could therefore prove to be ecologically relevant as well. I describe my experience studying aberrations in the yellow-bellied slider turtle as an example of environmental biodosimetry.

Introduction:

Humans and other organisms are continuously exposed to ionizing radiation from natural background sources in the environment including cosmic radiation, ^{222}Rn and it's daughter products, actinides and their decay products, and from internal sources including ^{40}K and ^{14}C. This unavoidable exposure is not without consequence, as ionizing radiation exposure is known to deliver a variety of insults to nuclear DNA.

Unfortunately, natural background is not the only source of ionizing radiation to which organisms are exposed. Numerous sites across the U.S. (1) and the rest of the world have been contaminated with radionuclides as a result of anthropogenic activity. Human exposures can be minimized by limiting access to contaminated areas, but this is generally not feasible for nonhuman organisms, and resulting exposures can be significantly higher than those from natural background sources.

Ecological risk assessments for sites contaminated with radionuclides usually rely on indirect methods for estimating exposures to species of concern. Either screening calculations, which generally compare radionuclide levels in various environmental media against regulatory limits, and/or fate and transport modeling, is used to estimate doses that these species might receive. There are many uncertainties associated with such estimates (2). Similarly, most current biomonitoring programs for sites with radionuclide contamination consist of sampling of environmental media and tissue residue analyses of various biota (3). These types of data can often be useful in determining which species are being exposed to certain radionuclides via internal uptake, but external exposures cannot be determined. Tissue residue analyses also provide only a snapshot picture of current internal exposure rates. They reveal nothing about the cumulative exposure an organism has received, therefore many ecologically relevant effects cannot be estimated based solely on such analyses. Use of a direct biomarker of genetically relevant damage in species of concern as a measurement endpoint could remove much of the uncertainty associated with current ecological risk assessments and biomonitoring programs and provide a meaningful indicator of biological damage. Furthermore, if this biological or

genetic damage has potential reproductive effects, the biomarker could be an ecologically relevant assessment endpoint as well.

In this chapter, I discuss one such measure, the frequency of symmetrical chromosome translocations, which is ideally suited to serve as a biomarker of cumulative radiation exposure. The term "dosimetry" is generally used to refer to the determination of dose by the observation of a radiation-induced effect. The use of cytogenetic techniques to observe chromosome aberrations in humans (and a few rodent species), is termed biodosimetry, and is well-developed and widely applied. The application of these same techniques to organisms chronically exposed to radionuclides in their environment, which I call environmental biodosimetry, could provide a sensitive and biologically relevant measurement endpoint for ecological risk assessments and biomonitoring programs. Further studies to link the incidence of symmetrical translocations in a species of concern to reproductive effects could make this biomarker an ecologically relevant assessment endpoint.

The formation of chromosome aberrations:

The interaction of ionizing radiation with DNA either directly, or indirectly through intermediate reactive oxygen species, creates a spectrum of damage including oxidized and methylated bases, DNA adducts, and single- and double-strand breaks (4). Of all the products of radiation interaction with DNA, double strand breaks (DSBs) are thought to be the most detrimental and resistant to repair. There are three possible outcomes of DSBs: (1) they can be repaired, with no lasting effect on the cell, (2) they can remain unrepaired, resulting in cell death, or (3) they can be mis-repaired, leading to

the formation of chromosome aberrations. In turn, chromosome aberrations can be fatal to the cell if the aberration results in a loss of genetic material, as is the case with asymmetrical chromosome interchanges (dicentrics) (Figure 1.1).

It was suggested over 30 years ago that the incidence of radiation-induced chromosome aberrations in human lymphocytes could be used to determine the magnitude of an unknown, accidental exposure. This technique is known as biodosimetry (5). Estimating dose involves construction of a dose-response, or calibration curve for chromosome aberrations against which aberration frequencies in exposed individuals are compared to determine the received dose. Accidental exposures are typically acute, and occur at a known point in time. Therefore, the decline of unstable aberrations from a lymphocyte population of an accidentally exposed person can be quantified as $Y(t) = Y(0) * \exp(-t/t_m)$; where $Y(0)$ is the initial frequency of unstable aberrations, t is time since exposure, and t_m is the mean lymphocyte lifetime. Unstable aberrations were easier to detect with early cytogenetic techniques than were stable aberrations, therefore the frequency of dicentrics and rings in lymphocytes of exposed individuals was the biodosimetric method of choice. However, the use of unstable aberrations for biodosimetry precluded application of this technique to chronic exposure situations, since the behavior over time of unstable aberrations under chronic irradiation conditions is much more complicated than is the case with acute exposures. The frequency of unstable aberrations induced by chronic irradiation at any point in time reflects a balance between continuous induction caused by ongoing exposure, and deletion of cells bearing these aberrations from the cell population.

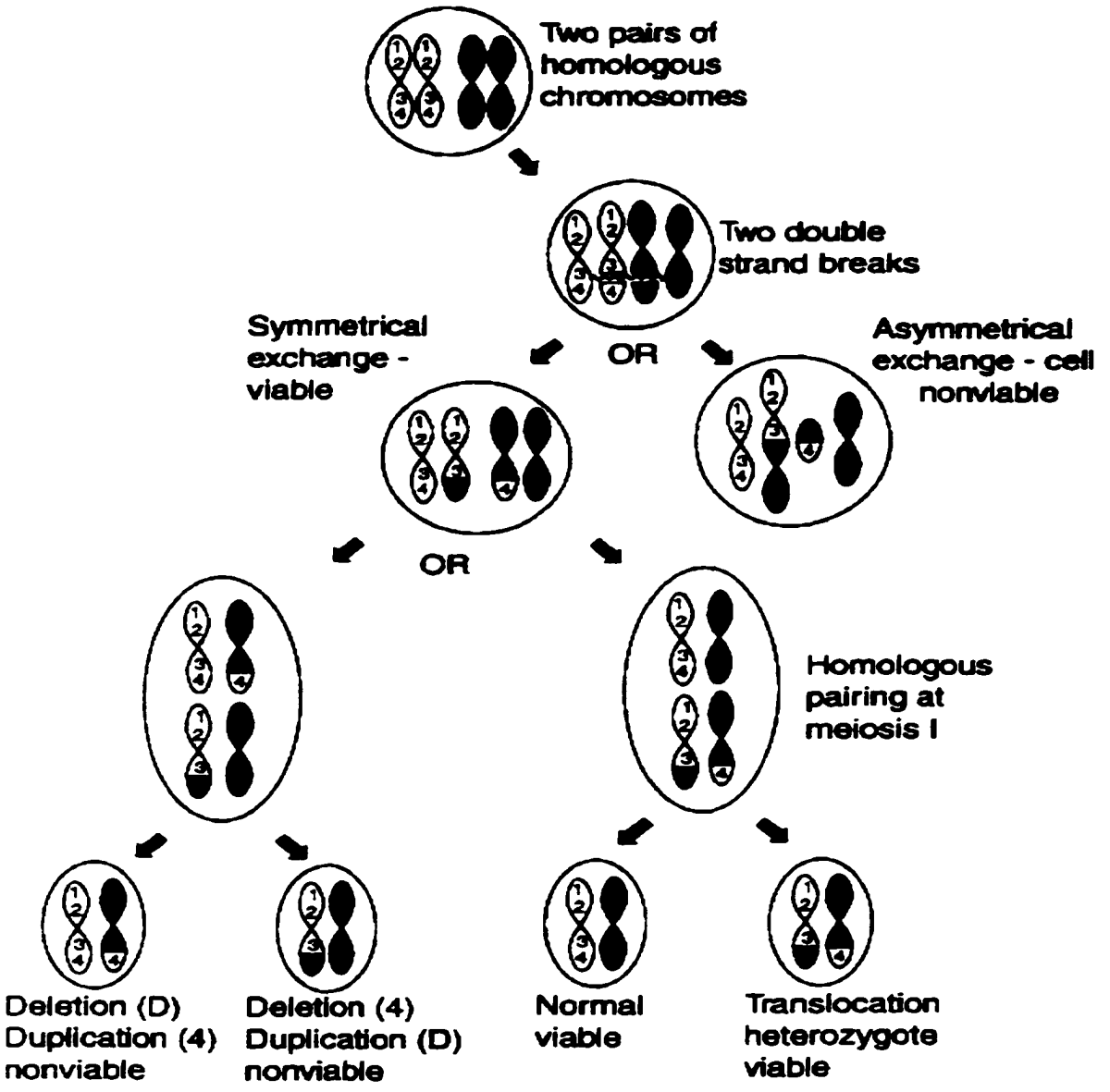

Figure 1.1:
Chromosome interchange aberrations are formed when DSBs in two (or more) chromosomes interact and are mis-repaired. Asymmetrical aberrations involve the loss of genetic material (essential genes are represented by letters and numbers inside the chromosomes), and are therefore fatal to the cell. Symmetrical aberrations involve no such loss, and therefore they have the potential to be stable. If a symmetrical translocation occurs in a germline stem cell, translocation heterozygosity can lead to a 50% reduction in reproductive success (any zygote which has a deficit of essential genetic material will be nonviable). Of the viable offspring produced by translocation heterozygotes, half will be normal, and half will also be translocation heterozygotes.

Not all chromosome aberrations are fatal to the cells carrying them. Symmetrical chromosome interchanges (translocations) do not result in a loss of genetic material (Figure 1.1), therefore they have the potential to be stable. Unless such aberrations, in and of themselves, result in a selective disadvantage relative to other cells in the population or they are coexist with unstable aberrations (6), their frequency in the cell population is not predicted to decline. The decline and disappearance of asymmetrical aberrations has been widely observed and is not in dispute (7-10), however the evidence on the stability of symmetrical aberrations is more equivocal. Although some authors have observed an initial decline in symmetrical translocations immediately following irradiation (11-14), others have not observed such a decline (15-17). Regardless of whether an initial decline in translocation frequency was observed, all these studies found that at least a fraction of the symmetrical translocations remain stable over time, and the frequency of these aberrations increases with increasing dose. In organisms subjected to chronic exposures, such as those received as a result of inhabiting radionuclide-contaminated environments, stable chromosome translocations should accumulate over time, therefore this type of aberration is best-suited to serve as a biomarker of cumulative radiation exposure. Chromosome inversions and certain more complex aberrations are also stable, but methods suitable for their routine measurement are only recently being developed.

The dose-rate effect:

There is a complication in the application of biodosimetry to chronic exposures: the dependence of the frequency of chromosome aberrations on dose-rate, in addition to total dose. Numerous studies using diverse endpoints in humans (18-24) and in a variety of other organisms (25-28) have shown that for sparsely ionizing radiation delivered at moderate dose-rates, there is a reduction in the effect caused by a given dose when the dose is protracted in time (Figure 1.2). At very high and very low dose-rates, the effect per unit dose appears to be independent of dose-rate.

The dose-rate effect for chromosome aberration induction is generally interpreted as arising from the requirement for more than one lesion or chromosome break to produce an exchange and that breaks rejoin (restitution) or mis-rejoin (exchange) with time. If for a given dose, the dose-rate is high (a few thousands of cGy hr^{-1} or more), so that all the breaks are produced at the same time or within a few minutes of each other, every break that is near enough to another to have some possibility of mis-rejoining to form an exchange will have the opportunity to do so. If the same dose is delivered at a lower dose-rate (hundreds of cGy hr^{-1} to a few tens of cGy hr^{-1}), even though the same total number of breaks are produced, some will be produced early and will have rejoined or restituted so they are no longer present to have the opportunity to mis-rejoin to produce exchanges with breaks occurring later during the protracted dose delivery. When each of these breaks is produced by an independent event, which for sparsely ionizing radiation would be the passage of a single electron track, and these interact

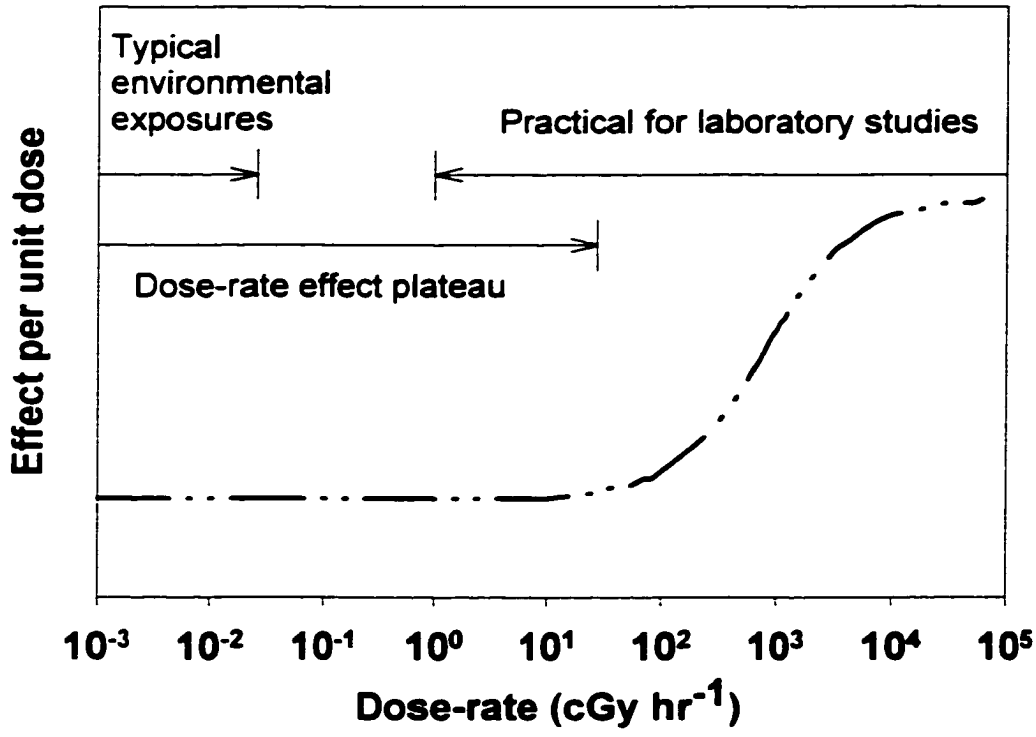

Figure 1.2:
A lower response is observed for a given dose of ionizing radiation when the dose is administered at a low dose-rate than when the same dose is administered at a high dose-rate. When the dose-rate is lowered beyond a minimum value (usually on the order of 20-60 cGy hr^{-1}), no further reduction in response per unit dose is observed. In this low dose-rate plateau, the response is independent of dose-rate, and depends only on the total received dose. At very high dose-rates (thousands of cGy hr^{-1}), the response again reaches a plateau, and becomes independent of dose-rate. Most environmental exposures occur at dose-rates in the low dose-rate plateau. To ensure their relevancy to field conditions, dose-responses curves generated in the laboratory for use in environmental dosimetry should also use dose-rates in the low dose-rate plateau.

pairwise when one occurs within a certain range of another, then the number of potentially interacting lesion-pairs would increase in proportion to the square of the number of lesions present (the latter being directly proportional to dose). The yield of exchanges from two independently produced breaks, Y_2, would increase according to the expression $Y_2 = \beta D^2$; where β is a constant relating to both the number of lesions per unit dose, and the probability that two lesions within a certain distance of each other will interact to form an exchange. As the dose-rate is reduced, the probability that two independently produced lesions will be produced within a sufficient period of time to interact will become smaller and smaller, depending on their rate of restitution and the yield of exchanges from these independent events, and finally will disappear altogether. It is known from experimental observation that the yield of exchanges for a given dose does not disappear altogether in the limit (less than a few cGy hr^{-1}) with decreasing dose-rate (25,26,29,30) and it is thought that this results because lesion-pairs or break-pairs can be produced by even the smallest possible radiation event, which is the passage of a single electron track. The production of these would, of course, be independent of dose-rate since each of the two breaks of a break-pair is produced simultaneously. The yield from this single event break-pair production, Y_1, would increase linearly with dose according to the expression $Y_1 = \alpha D$; where α is a constant relating to the number of potentially interacting break-pairs per unit dose and the probability that such a break pair will yield an exchange. The response per unit dose in this lower plateau is independent of dose-rate. The total yield of exchanges, Y_T, is then just the sum of Y_1 and Y_2, so $Y_T = \alpha D + \beta D^2$; where βD^2 is the dose-rate dependent term and αD is the dose-rate independent term.

The dose-rate effect has important implications for environmental biodosimetry. Environments contaminated with low to moderate levels of radionuclides are typically characterized by dose-rates low enough to fall into the lower dose-rate plateau region. The application of a calibration curve constructed using a dose-rate above the lower dose-rate effect plateau will result in underestimation of the doses received by organisms inhabiting such environments, as illustrated in Figure 1.3.

The effects of symmetrical translocations:

While symmetrical translocations do not result in loss of genetic material followed by cell death, they do result in the relocation of sections of DNA which almost certainly contain genes essential to the organism's survival. This can potentially lead to consequences far more serious for the organism than the death of a limited number of cells. Symmetrical translocations have been implicated in carcinogenesis when they occur in somatic (non-germline) cells. When translocations occur in germline stem cells, they can result in a condition known as translocation heterozygosity, as illustrated in Figure 1.1. Every cell in the offspring produced by a germline cell containing a symmetrical translocation will contain the translocation. Translocation heterozygotes are semi-sterile, and their reproductive success is reduced by 50%. Of the viable offspring they do produce, half will be normal, and half will also be translocation heterozygotes. The potential of symmetrical translocations to lead to translocation heterozygosity, with the concomitant reduction in reproductive success, gives the frequency of these aberrations direct ecological relevance. Therefore, the endpoint of symmetrical

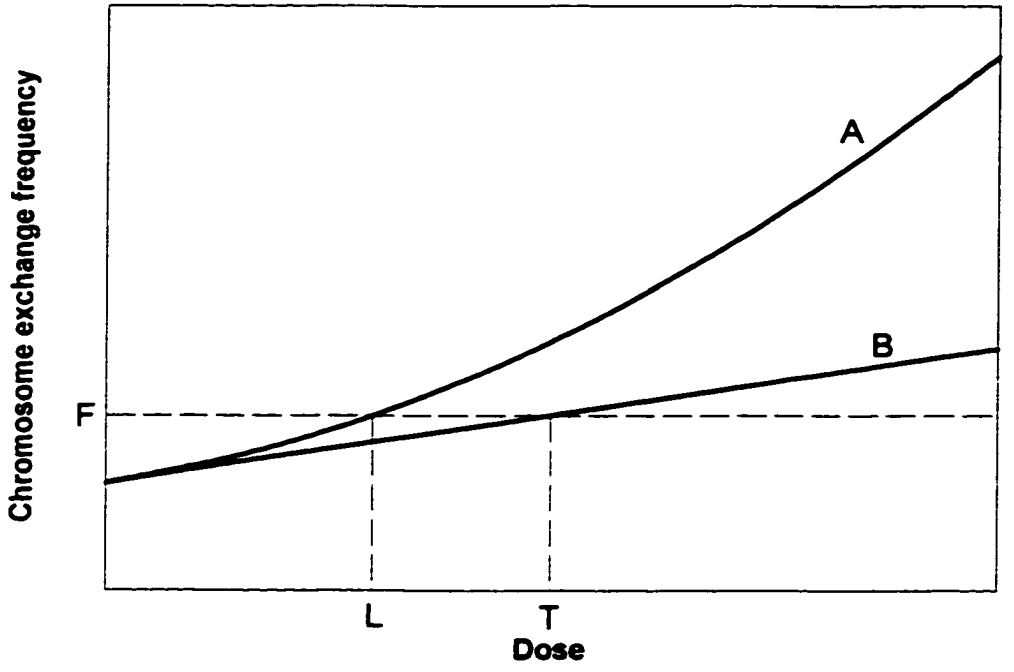

Figure 1.3:
Hypothetical curves showing a curvilinear dose-response relationship resulting from administration of the dose at a dose-rate where the dose-rate-dependent component is greater than zero (curve A), and a linear relationship resulting from administration of the dose at a chronic dose-rate where the dose-rate-dependent component has disappeared (curve B). Assume an organism receives a dose from a contaminated environment, resulting in a chromosome exchange frequency, F. Using curve A as a calibration curve for such an organism would result in an erroneously low estimate of dose (L), while the true dose received (T) would be obtained by using curve B.

translocation frequency may be more sensitive and relevant than traditional endpoints such as tissue residue analyses. Chromosome inversions, referred to previously, also have similar effects on reproduction. The goals of radiation protection of nonhuman species is maintenance of long-term population viability (31), therefore, adverse reproductive effects are of paramount concern.

Detection of chromosome aberrations:

Early cytogenetic and biodosimetric studies employed solid staining with dyes such as giemsa, orcein, or crystal violet. With these dyes, all chromosomes are stained in a single color. When cells enter mitosis, the chromosomes condense and, upon staining, they are distinctly visible under bright field illumination using a microscope. With solid staining, only asymmetrical chromosome aberrations (rings and dicentrics) are reliably detected because they involve a visible change in chromosome morphology. Symmetrical interchanges are not visible unless they involve large alterations in chromosome morphology.

Development of whole-chromosome-specific molecular probe libraries containing unique DNA sequences has facilitated significant advances in the detection of symmetrical translocations. Such probes labeled with various tags have been constructed which allow individual pairs of homologous chromosomes to be painted in unique colors. The first step in probe construction involves isolating target chromosomes from mitotic cells using either flow cytometry or microdissection techniques. This is followed by random amplification of the isolated material through the polymerase chain reaction

(PCR) (32-34), during which billions of copies of the original chromosome, each containing fluorescent marker molecules, are created. This probe library contains DNA sequences specific to the original chromosome of interest, as well as sequences repeated throughout the genome. To detect chromosome aberrations, irradiated cells are spread on glass slides, and both the chromosomes in the target cells and the DNA in the probe are denatured, or melted by heating. In this process, the DNA strands are split, much like unzipping a zipper. The probe is then "hybridized" onto the target cells, when the DNA is allowed to reanneal. The unique sequences in the probe hybridize to their unique complementary sequences in the target chromosome, while the probe is prevented from hybridizing to repetitive sequences throughout the genome by the addition of unlabeled cot DNA (highly enriched in repetitive sequences), which competitively binds to repetitive sites on the chromosomes as well as labeled repetitive DNA in the probe. Once hybridization is complete, the fluorescent probe is bound only to the specific sequences on the target chromosomes, and when viewed under a fluorescent microscope, the target chromosomes appear "painted" in a unique color distinct from the other chromosomes in the cell. This process is known as fluorescence *in situ* hybridization (FISH) whole-chromosome painting (35,36). The molecular basis for DNA melting and reannealing and its dependence on DNA sequence copy number has been reviewed on numerous occasions (e.g. (37)). When an interchange aberration involving the painted chromosome is present in a cell, a fragment of the painted chromosome appears translocated to another (unpainted) chromosome, and vice versa, and both of the chromosomes involved appear bicolored (Figure 1.4A-C). Most generally, from one to three pairs of homologous

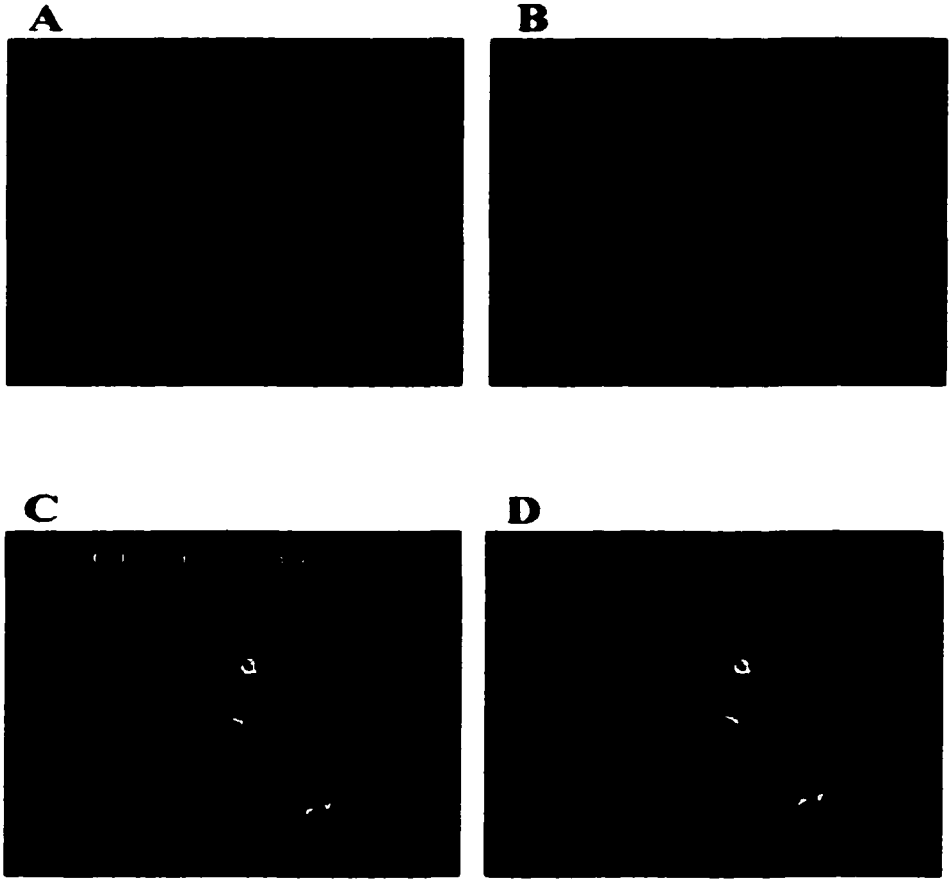

Figure 1.4:
FISH allows homologous chromosome pairs to be painted in a unique color. Panels A-C show a human AG1521A fibroblast with different homologous chromosomes painted. Depending which chromosomes happen to be painted, the cell could be scored as containing either an insertion (Panel A) or a symmetrical translocation (Panels B and C). The use of mFISH allows correct resolution of the complex aberration involving chromosomes 4, 6, and 13 (Panel D). Each pair of homologous chromosomes can be painted a unique color (Panel E), allowing maximum sensitivity for aberration detection. Application of FISH and mFISH is not limited to human cells. Panel F shows a probe for chromosome #1 of the yellow-bellied slider turtle (*Trachemys scripta*) applied to a *T. scripta* fibroblast containing one normal chromosome, and an apparently simple symmetrical translocation (identified by arrows).

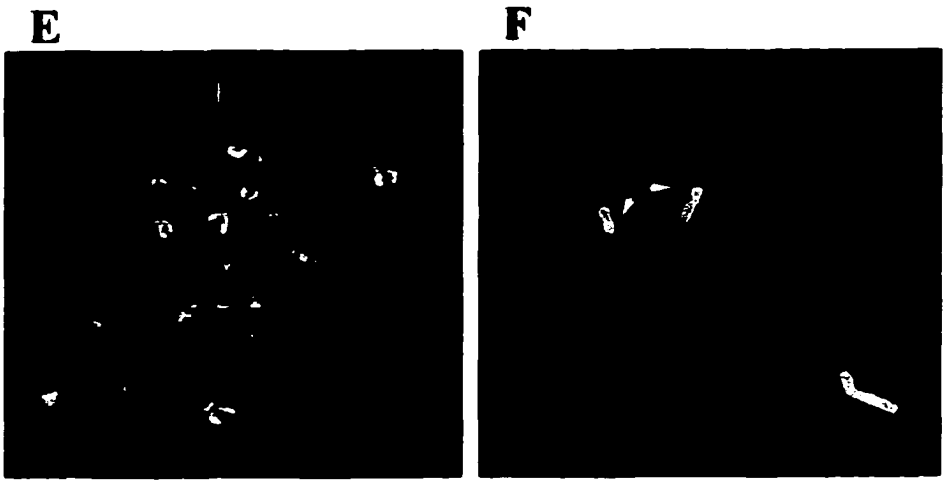

chromosomes are painted either in a single or in unique colors, and the rest of the chromosomes are counterstained in a single background color. Symmetrical translocations between chromosomes painted the same color, or among unpainted chromosomes are not visible. The FISH process is illustrated in Figure 1.5.

A further significant advance has recently been made in this technology. The application of multiple probe mixtures together in processes known as multiplex FISH (mFISH) or spectral karyotyping now allows every pair of homologous chromosomes in the human genome to be assigned a unique color (38,39). The use of mFISH for aberration detection provides dramatic potential increases in sensitivity, since chromosome interchanges involving any chromosome can be detected. At present, the analysis of each cell requires a much longer time, so the full advantage of the potential increased sensitivity will await further developments in computerized image analysis. With single color FISH, complex aberrations (those involving three or more breaks in two or more chromosomes) can be mis-scored because they appear to be simple, and the type of aberration scored depends on which chromosomes happen to be painted (Figure 1.4A-C), but with mFISH, virtually all chromosome exchange aberrations can be accurately resolved (Figure 1.4D). A human AG1521A fibroblast completely colored with mFISH is illustrated in Figure 1.4E.

Environmental biodosimetry:

Most often, biodosimetric studies have been performed on mice or rats which have received controlled exposures in the laboratory (e.g. (14,40-44), or on humans who have been exposed accidentally (16,45-51) or for therapeutic purposes (9,10,52).

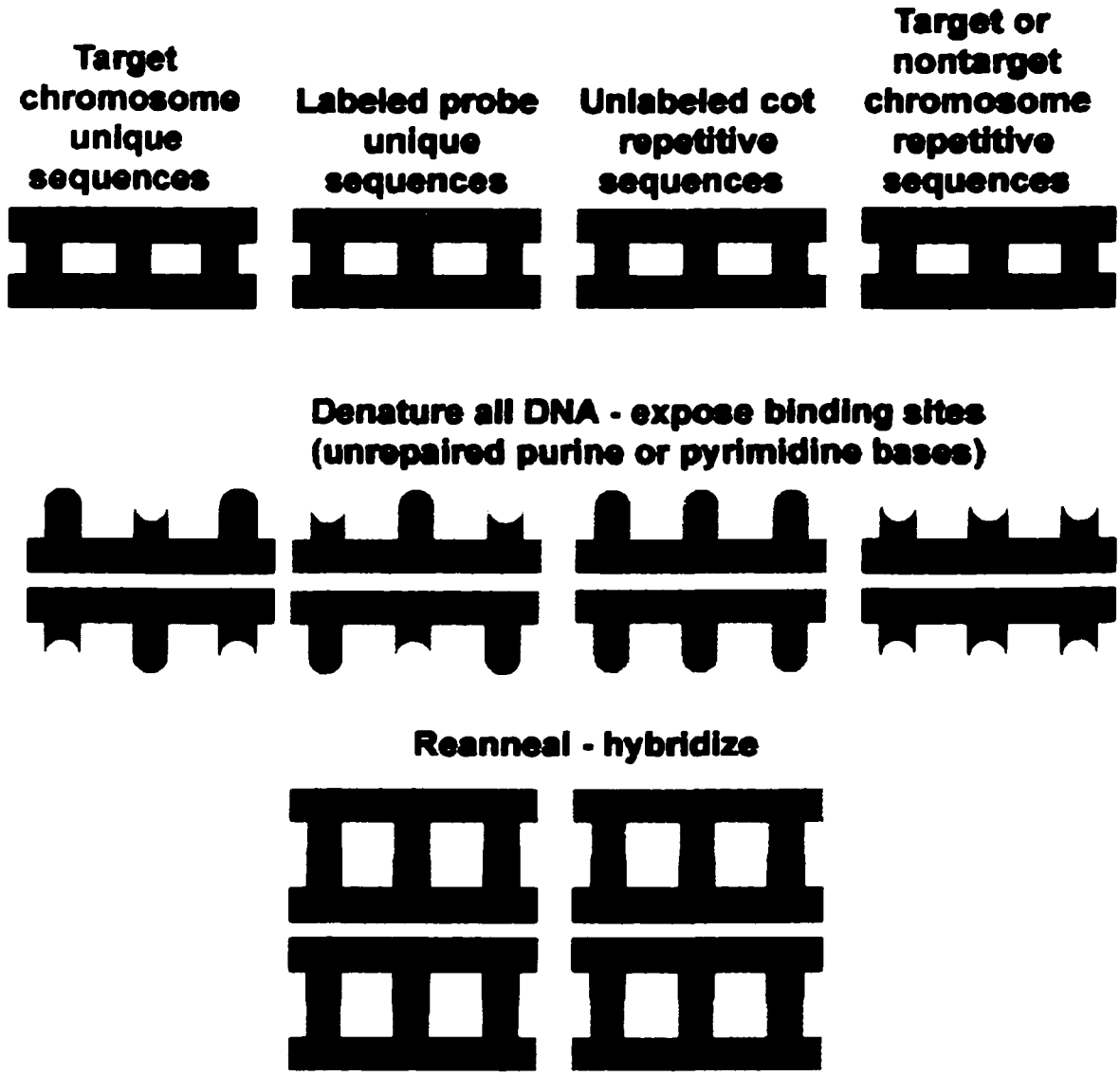

Figure 1.5:
During the FISH process, both the chromosome-specific probe and the target chromosomes are denatured. The probe is applied to the chromosomes and allowed to hybridize to the specific sequences on the target chromosomes. The probe also contains sequences repeated throughout the genome. Nonspecific hybridization to these repetitive sites is prevented by the use of unlabeled cot DNA, which is highly enriched in the repetitive sequences. The cot DNA competes with the probe for the repetitive sites and effectively blocks probe hybridization at these sites.

Only a few studies have been carried out retrospectively on humans chronically exposed to radionuclides in the environment (53-56). There are no technical limitations preventing the application of biodosimetric techniques to nonhuman organisms inhabiting environments contaminated with radionuclides, yet to my knowledge, these techniques have not previously been used for ecological applications. I have recently been performed the first such studies using yellow-bellied slider turtles (*Trachemys scripta*) (57). Figure 1.4F shows my probe for *T. scripta* chromosome #1 applied to a fibroblast containing one normal chromosome #1 and one symmetrical translocation.

Conducting environmental biodosimetry studies – step by step:

In the rest of this chapter, I discuss the steps necessary to conduct environmental biodosimetry studies, based on my experience with *T. scripta*. Each step is discussed in the order in which it arose in my project. I present this synopsis as an example of what is required to conduct these types of studies. There will no doubt be differences in other studies, depending on the endpoint species selected, but I believe these experiences may reveal the sorts of issues that may be encountered.

1) Selection of endpoint species and probe construction:

While environmental biodosimetry has the potential to be widely applicable to numerous plant and animal species, there are certain desirable traits that candidate species should possess. First, a candidate species should have a suitable karyotype, that is, they should have at least a few large and easily recognizable chromosomes. Unlike humans, for which whole-chromosome probes are commercially available, probes for

other species will have to be constructed by microdissection and PCR. For reasons discussed below, microdissection requires the presence of large, easily identifiable chromosomes, which could eliminate species with only small, indistinguishable chromosomes from consideration.

Even if limitations associated with microdissection are overcome, there is still the issue of the minimum resolution of the FISH visualization process. The minimum detectable size of a painted fragment of DNA is approximately 11 megabases (Mb) or approximately 15 Mb for unpainted fragments (58). Since chromosomes are fragmented during chromosome interchanges, species with at least a few chromosomes larger than approximately 30 Mb would make the best candidates for environmental biodosimetry studies.

There are demographic factors to consider as well. Organisms with relatively long life-spans will have the potential to accumulate significantly higher lifetime doses than those which are relatively short-lived, and therefore they will be more likely to show a measurable response to chronic radiation exposure, all other factors being equal. On the other hand, studies of reproductive effects (such as those caused by translocation heterozygosity) are difficult to conduct on long-lived, slowly-reproducing species.

Finally, candidate species should be those with some potential to be exposed. Since many environmental contaminants (including most radionuclides) are eventually deposited and sequestered in sediments (59,60), organisms which have contact with sediments could make strong candidates. Tissue residue analyses, which measure levels of contaminants in the tissues of various biota, may provide clues regarding which organisms are being exposed and what the current exposure rates might be.

It is evident that any number of plant and animal species would make strong candidates for environmental biodosimetry. Perhaps the best approach for ecological risk assessments and biological monitoring applications would be to select a suite of suitable species representing diverse ecological, economic, and aesthetic values.

2) Probe construction:

In general, the largest chromosome(s) are targeted, since the greater the fraction of the genome painted, the greater the sensitivity for detecting chromosome aberrations (61). If standard lymphocyte culture techniques work well with the species being studied, this would be the best and most direct approach for preparing chromosomes for microdissection. If this is not the case, it is easier to use fibroblasts at this stage because of the challenges in stimulating lymphocytes into mitosis. Fibroblast cell lines can be established from embryos or from tissue samples.

3) Investigation of cell culture techniques:

In conducting environmental biodosimetry studies involving animal species, it is preferable to use lymphocytes rather than fibroblasts (62). Lymphocytes offer the advantage of nonlethal sampling, which allows repeated blood sampling from individual organisms so the temporal behavior of the dose-response can be studied. Furthermore, animal welfare considerations or potential adverse impacts to endpoint populations from harvesting large numbers of individuals may also favor nonlethal sampling techniques.

The challenge in using lymphocytes is stimulating them to undergo mitosis. These cells are usually noncycling, and they must be forced into the cell cycle by

mitogenic agents. The mitogenic responses of lymphocytes from nonmammalian species is not well characterized. Therefore, factors such as which mitogenic agents are effective for a given species and the optimal concentrations of these agents, optimal culture temperature, cell cycle time, etc. will have to be determined. Of course, the available blood volume and methods for collection may provide additional challenges.

4) Determination of background symmetrical translocation frequency:

Obviously, the sensitivity of ecological applications of biodosimetry will depend on the radiosensitivity of the endpoint species. What may not be so obvious however, is that species which are more resistant, ironically, may be more sensitive indicators of radiation damage. This arises from the fact that species which are more radioresistant may also have lower background levels of symmetrical translocations, as is the case with *T. scripta*, which I found to be about twice as radioresistant as humans (57). Background frequencies of symmetrical translocations in humans have been reported as much as 30 times higher than the background I observed in *T. scripta* (63). A high background could significantly impact sensitivity, especially at the low doses and dose-rates likely to be encountered by organisms from radionuclide-contaminated environments. If the factors which make a particular species more radioresistant also depress background translocation frequencies, then the loss in sensitivity caused by higher radioresistance may be outweighed by the gain in sensitivity afforded by a lower background. In any case, some estimate of background translocation frequency will be necessary, since the organisms to be studied will have received unknown doses. Without an estimate of background, it would be unclear how much of the observed translocation frequency in

exposed animals was due to radiation exposure, and how much was due to extraneous factors. The best way to obtain an estimate of background is to score cells from numerous organisms known to be from uncontaminated environments.

5) Investigation of dose-rate effect:

As mentioned previously, it is important that the calibration curve to be used for environmental biodosimetry be determined for low dose-rate exposures. However, for practical reasons, laboratory studies will almost certainly have to be conducted at dose-rates higher than those observed in contaminated environments. The applicability of the calibration curve can only be definitively demonstrated by identification of the minimum dose-rate below which the reduction in effect per unit dose plateaus. This involves exposing whole organisms or cell cultures to the same total dose, but delivering the dose at a range of dose-rates from thousands of cGy hr^{-1} to only a few cGy hr^{-1}. For almost every organism previously studied, the lower dose-rate effect plateau begins at a rate on the order of 20-60 cGy hr^{-1}.

6) Determination of dose-response relationship:

Once an appropriate dose-rate is identified, it should be used in the construction of the calibration curve. This involves plotting the dose-response relationship over a range of doses that the organisms are expected to receive over the course of their lifetime. A preliminary estimate of the maximum dose which should be included in the calibration curve can be obtained by multiplying worst-case environmental dose-rates by the maximum expected lifespan of the endpoint species. However, the main focus should be

at the lower end of the of the dose range, since these exposures would be more typical of most environmental exposures.

7) Applying environmental biodosimetry to organisms from contaminated environments:

Upon completion of the preliminary steps outlined above, a variety of field studies are possible. These could include mark-and-recapture studies of animals, since lymphocyte sampling is nonlethal. This type of study would be particularly appropriate for biomonitoring programs and would provide useful data for ongoing exposures. For ecological risk assessments upon which remediation decisions are to be based, an extensive, one-time sampling effort might be more appropriate. An exploration of the reproductive effects caused by radiation-induced translocation heterozygosity would be particularly informative.

Conclusion:

Environmental biodosimetry studies offer several advantages over traditional approaches to biomonitoring and ecological risk assessment. Unlike dose estimates obtained by modeling, biodosimetric estimates require no assumptions regarding organism movements into and out of contaminated environments (which may be difficult to verify). Furthermore, actual doses received externally, or internally via uptake of radionuclides will be reflected in biodosimetric estimates. Another advantage of environmental biodosimetry is that an estimate of cumulative lifetime dose can be obtained, rather than the snapshot picture provided by environmental sampling and tissue residue analyses. Perhaps the most significant advantage of environmental biodosimetry,

however, is its potential relevance to ecological and biological effects in exposed populations.

While environmental biodosimetry can currently serve as a useful measurement endpoint for ecological risk assessment, completing the causal chain of events between radiation exposure, the formation of radiation-induced symmetrical translocations, and reproductive effects through translocation heterozygosity would provide an ecologically relevant assessment endpoint. Once received dose, as detected by environmental biodosimetry, can be linked to reproductive effects in exposed individuals, "ecological dosimetry" studies could be conducted on a variety of species to study effects of radiation exposure at higher levels of biological organization.

REFERENCES

1. Wolbarst, A. B., Blom, P. F., Chan, D, Cherry, R. N. Jr., Doehnert, M., Fauver, D., Hull, H. B., MacKinney, J. A., Mauro, J., Richardson, A. C. B., and Zaragoza, L., Sites in the United States contaminated with radioactivity. *Health Physics* **77**, 247-260 (2000).

2. Whicker, F. W., Shaw, G., Voigt, G., and Holm, E, Radioactive contamination: the state of the science and its application to predictive models. *Environmental Pollution* **100**, 133-149 (2000).

3. Dickerson, R. L., Hooper, M. J., Gard, N. W., Cobb, G. P., and Kendall, R. J., Toxicological foundations of ecological risk assessment: biomarker development and interpretation based on laboratory and wildlife species. *Environmental Health Perspectives* **102 Suppl 12**, 65-69 (1994).

4. Ward, J. F., Molecular mechanisms of radiation-induced damage to nucleic acids, In *Advances in Radiation Biology* (Lett, J. T. and Adler, H., Eds.), pp. 182-239. Academic Press, New York, NY, (1975).

5. Bender, M. A. and Gooch, P. C., Somatic chromosome aberrations induced by human whole-body irradiation: the "Recuplex" criticality accident. *Radiation Research* **29**, 568-582 (1966).

6. Lindholm, C., Luomahaara, S., Koivistoinen, A., Ilus, T., Edwards, A. A., and Salomaa, S., Comparison of dose-response curves for chromosomal aberrations established by chromosome painting and conventional analysis. *International Journal of Radiation Biology* **74**, 27-34 (1998).

7. Bauchinger, M., Schmid, E., and Braselmann, H., Cell survival and radiation induced chromosome aberrations. II. Experimental findings in human lymphocytes analysed in first and second post-irradiation metaphases. *Radiation & Environmental Biophysics* **25**, 253-260 (1986).

8. Bauchinger, M., Quantification of low-level radiation exposure by conventional chromosome aberration analysis. *Mutation Research* **339**, 177-189 (1995).

9. Buckton, K. E., Hamilton, G. E., Paton, L, and Langlands, A. O., Chromosome aberrations in irradiated ankylosing spondylitis patients, In *Mutagen-Induced Chromosome Damage in Man* (Evans, H. J. and Lloyd, D. C., Eds.), pp. 142-150. Edinburgh University Press, Edinburgh, Scotland, (1978).

10. Buckton, K. E., Chromosome aberrations in patients treated with X-irradiation for ankylosing spondylitis, In *Radiation-Induced Chromosome Damage in Man* (Ishihara, T. and Sasaki, M. S., Eds.), pp. 491-511. Alan R. Liss, Inc., New York, (1983).

11. Matsumoto, K., Ramsey, M. J., Nelson, D. O., and Tucker, J. D., Persistence of radiation-induced translocations in human peripheral blood determined by chromosome painting. *Radiation Research* **149**, 602-613 (1998).

12. Spruill, M. D., Ramsey, M. J., Swiger, R. R., Nath, J., and Tucker, J. D., The persistence of aberrations in mice induced by gamma radiation as measured by chromosome painting. *Mutation Research* **356**, 135-145 (1996).

13. Spruill, M. D., Nelson, D. O., Ramsey, M. J., Nath, J., and Tucker, J. D., Lifetime persistence and clonality of chromosome aberrations in the peripheral blood of mice acutely exposed to ionizing radiation. *Radiation Research* **153**, 110-121 (2000).

14. Tucker, J. D., Breneman, J. W., Briner, J. F., Eveleth, G. G., Langlois, and Moore, D. H., Persistence of radiation-induced translocations in rat peripheral blood determined by chromosome painting. *Environmental & Molecular Mutagenesis* **30**, 264-272 (1997).

15. Lindholm, C., Tekkel, M., Veidebaum, T., Ilus, T., and Salomaa, S., Persistence of translocations after accidental exposure to ionizing radiation. *International Journal of Radiation Biology* **74**, 565-571 (1998).

16. Lucas, J. N., Poggensee, M., and Straume, T., The persistence of chromosome translocations in a radiation worker accidentally exposed to tritium. *Cytogenetics & Cell Genetics* **60**, 255-256 (1992).

17. Lucas, J. N., Hill, F. S., Burk, C. E., Cox, A. B., and Straume, T., Stability of the translocation frequency following whole-body irradiation measured in rhesus monkeys. *International Journal of Radiation Biology* **70**, 309-318 (1996).

18. Bauchinger, M., Schmid, E., and Dresp, J., Calculation of the dose-rate dependence of the dicentric yield after Co γ-irradiation of human lymphocytes. *International Journal of Radiation Biology* **35**, 229-233 (1979).

19. Bedford, J. S. and Hall, E. J., Survival of HeLa cells cultured *in vitro* and exposed to protracted gamma-irradiation. *International Journal of Radiation Biology* **7**, 377-383 (1963).

20. Brewen, J. G. and Luippold, H. E., Radiation-induced human chromosome aberrations: *in vitro* dose rate studies. *Mutation Research* **12** , 305-314 (1971).

21. Liniecki, J., Bajerska, A., Wyszynsja, K, and Cisowska, B., Gamma-radiation-induced chromosomal aberrations in human lymphocytes: dose-rate effects in stimulated and non-stimulated cells. *Mutation Research* **43**, 291-304 (1977).

22. Lloyd, D. C. and Edwards, A. A., Chromosome aberrations in human lymphocytes: effect of radiation quality, dose, and dose rate. In *Radiation-Induced Chromosome Damage in Man* (Ishihara, T. and Sasaki, M. S., Eds.), pp. 23-49. Alan R. Liss, Inc., New York, (1983).

23. Lloyd, D. C., Purrott, R. J., Dolphin, G. W., Bolton, D, and Edwards, A. A., The relationship between chromosome aberrations and low LET radiation dose to human lymphocytes. *International Journal of Radiation Biology* **28**, 75-90 (1999).

24. Mitchell, J. B., Bedford, J. S., and Bailey, S. M., Dose-rate effects in plateau-phase cultures of S3 HeLa and V79 cells. *Radiation Research* **79**, 552-567 (1979).

25. Hall, E. J. and Bedford, J. S., A comparison of the effects of acute and protracted gamma-radiation on the growth of seedlings of *Vicia faba* Part I. Experimental observations. *International Journal of Radiation Biology* **8**, 467-474 (1964).

26. Sax, K., The time factor in X-ray production of chromosome aberrations. *Proceedings of the National Academy of Sciences of the United States of America* **25**, 225-233 (1939).

27. Searle, A. G., Mutation induction in mice. In *Advances in Radiation Biology* (Lett, J. T., Adler, H., and Zelle, M., Eds.), pp. 131-207. Academic Press, San Diego, CA, (1974).

28. Wells, R. L. and Bedford, J. S., Dose-rate effects in mammalian cells. IV. Repairable and nonrepairable damage in noncycling C3H 10T 1/2 cells. *Radiation Research* **94**, 105-134 (1983).

29. Catcheside, D. G., Lea, D. E., and Thoday, J. M. The production of chromosome structural changes in *Tradescantia* microspores in relation to dosage, intensity and temperature. *Journal of Genetics* **47**, 137-149 (1946).

30. Lea, D. E., *Actions of radiations on living cells.* Cambridge University Press, London, (1955).

31. International Commission on Radiological Protection, *Recommendations of the International Commission on Radiological Protection. Publication 60.* Publication 60, Pergammon Press, Oxford and New York, (1991).

32. Bussey, K. J., Chromosome microdissection: on the cutting edge. *Applied Cytogenetics* **22**, 30-36 (1996).

33. Guan, X. Y., Meltzer, P. S., Cao, J., and Trent, J. M., Rapid generation of region-specific genomic clones by chromosome microdissection: isolation of DNA from a region frequently deleted in malignant melanoma. *Genomics* **14**, 680-684 (1992).

34. Lillington, D. M., Cotter, F. E., and Riddle, P. N., Microdissection of human metaphase chromosomes. In *Human Cytogenetics: A Practical Approach* (Rooney, D. E. and Czepulkowski, B. H., Eds.), pp. 254-268. Oxford University Press, Oxford, (1992).

35. Lichter, P., Cremer, T., Borden, J., Manuelidis, L., and Ward, D. C., Delineation of individual human chromosomes in metaphase and interphase cells by in situ suppression hybridization using recombinant DNA libraries. *Human Genetics* **80**, 224-234 (1988).

36. Pinkel, D., Straume, T., and Gray, J. W., Cytogenetic analysis using quantitative, high-sensitivity, fluorescence hybridization. *Proceedings of the National Academy of Sciences of the United States of America* **83**, 2934-2938 (1986).

37. Lewin, B., *Genes*. Oxford University Press, New York, NY, (1997).

38. Speicher, M. R., Gwyn, Ballard S., and Ward, D. C., Karyotyping human chromosomes by combinatorial multi-fluor FISH. *Nature Genetics* **12**, 368-375 (1996).

39. Speicher, M. R. and Ward, D. C., The coloring of cytogenetics. *Nature Medicine* **2**, 1046-1048 (1996).

40. Boei, J. J., Balajee, A. S., de Boer, P., Rens, W., Aten, J. A., Mullenders, L. H., and Natarajan, A. T., Construction of mouse chromosome-specific DNA libraries and their use for the detection of X-ray-induced aberrations. *International Journal of Radiation Biology* **65**, 583-590 (1994).

41. Boei, J. J. and Natarajan, A. T., Combined use of chromosome painting and telomere detection to analyse radiation-induced chromosomal aberrations in mouse splenocytes. *International Journal of Radiation Biology* **73**, 125-133 (1998).

42. Hande, M. P., Boei, J. J., Granath, F., and Natarajan, A. T., Induction and persistence of cytogenetic damage in mouse splenocytes following whole-body X-irradiation analysed by fluorescence in situ hybridization. I. Dicentrics and translocations. *International Journal of Radiation Biology* **69**, 437-446 (1996).

43. Tucker, J. D., Sorensen, K. J., Chu, C. S., Nelson, D. O., Ramsey, M. J., Urlando, C., and Heddle, J. A., The accumulation of chromosome aberrations and Dlb-1 mutations in mice with highly fractionated exposure to gamma radiation. *Mutation Research* **400**, 321-335 (1998).

44. Xiao, Y., Darroudi, F., Grigorova, M., and Natarajan, A. T., Induction and persistence of chromosomal exchanges in mouse bone marrow cells following whole-body exposure to X-rays. *International Journal of Radiation Biology* **75**, 1119-1128 (1999).

45. Granath, F., Darroudi, F., Auvinen, A., Ehrenberg, L., Hakulinen, Natarajan, A. T., Rahu, M., Rytomaa, T., Tekkel, M., and Veidebaum, T., Retrospective dose

estimates in Estonian Chernobyl clean-up workers by means of FISH. *Mutation Research* **369**, 7-12 (1996).

46. Littlefield, L. G., McFee, A. F., Salomaa, S. I., Tucker, J. D., Inskip, P. D., Sayer, A. M., Lindholm, C., Makinen, S., Mustonen, R., Sorensen, K., Tekkel, M., Veidebaum, T., Auvinen, A., and Boice, J. D., Jr., Do recorded doses overestimate true doses received by Chernobyl cleanup workers? Results of cytogenetic analyses of Estonian workers by fluorescence in situ hybridization. *Radiation Research* **150**, 237-249 (1998).

47. Moore, D. H., Tucker, J. D., Jones, I. M., Langlois, R. G., Pleshanov, P., Vorobtsova, I., and Jensen, R., A study of the effects of exposure on cleanup workers at the Chernobyl nuclear reactor accident using multiple end points. *Radiation Research* **148**, 463-475 (1997).

48. Salassidis, K., Georgiadou-Schumacher, V., Braselmann, H., Muller, P., Peter, R. U., and Bauchinger, M., Chromosome painting in highly irradiated Chernobyl victims: a follow-up study to evaluate the stability of symmetrical translocations and the influence of clonal aberrations for retrospective dose estimation. *International Journal of Radiation Biology* **68**, 257-262 (1995).

49. Salomaa, S., Sevan'kaev, A. V., Zhloba, A. A., Kumpusalo, E., Makinen, S., Lindholm, C., Kumpusalo, L., Kolmakow, S., and Nissinen, A., Unstable and stable chromosomal aberrations in lymphocytes of people exposed to Chernobyl fallout in Bryansk, Russia. *International Journal of Radiation Biology* **71**, 51-59 (1997).

50. Snigiryova, G., Braselmann, H., Salassidis, K., Shevchenko, V., and Bauchinger, M., Retrospective biodosimetry of Chernobyl clean-up workers using chromosome painting and conventional chromosome analysis. *International Journal of Radiation Biology* **71**, 119-127 (1997).

51. Tucker, J. D., Tawn, E. J., Holdsworth, D., Morris, S., Langlois, R., Ramsey, M. J., Kato, P., Boice, J. D., Jr., Tarone, R. E., and Jensen, R. H., Biological dosimetry of radiation workers at the Sellafield nuclear facility. *Radiation Research* **148**, 216-226 (1997).

52. Littlefield, L. G., Kleinerman, R. A., Sayer, A. M., Tarone, R., and Boice, J. D., Jr., Chromosome aberrations in lymphocytes--biomonitors of radiation exposure. *Progress in Clinical & Biological Research* **372**, 387-397 (1991).

53. Bauchinger, M., Schmid, E., Braselmann, H., and Kulka, U., Chromosome aberrations in peripheral lymphocytes from occupants of houses with elevated indoor radon concentrations. *Mutation Research* **310**, 135-142 (1994).

54. Bauchinger, M., Braselmann, H., Kulka, U., Huber, R., and Georgiadou-Schumacher, V., Quantification of FISH-painted chromosome aberrations after domestic radon exposure. *International Journal of Radiation Biology* **70**, 657-663 (1996).

55. Pohl-Ruling, J. and Fischer, P., Chromosome aberrations in inhabitants of areas with elevated natural radioactivity. In *Radiation-Induced Chromosome Damage in Man* (Ishihara, T. and Sasaki, M. S., Eds.), pp. 527-560. Alan R. Liss, Inc., New York, (1983).

56. Pohl-Ruling, J., Haas, O. A., Obe, G., Brogger, A., Roscher, U., Daschil, F., Atzmuller, C., and Natarajan, A. T., The Chernobyl fallout in Salzburg/Austria and its effect on blood chromosomes. *Acta Biologica Hungarica* **41**, 215-222 (1990).

57. Ulsh, B. A., Muhlman-Diaz, M., Whicker, F. W., Hinton, T. G., Congdon, J. D, and Bedford, J. S., Chromosome translocations in turtles: a biomarker in a sentinel animal for ecological dosimetry. *Radiation Research* **153**, 752-759 (2000).

58. Kodama, Y., Nakano, M., Ohtaki, K., Delongchamp, R., Awa, A. A., and Nakamura, N., Estimation of minimal size of translocated chromosome segments detectable by fluorescence in situ hybridization. *International Journal of Radiation Biology* **71**, 35-39 (1997).

59. Blaylock, B. G., Mohrbacher, D. A., and Frank, M. L., Radioecology of White Oak Lake. In *Second annual report on the ORNL biological monitoring and abatement program. ORNL/TM-10399* (Loar, J. M., Eds.), pp. 290-298. Oak Ridge National Laboratory, Oak Ridge, TN, (1987).

60. Whicker, F. W., Pinder, J. E. III, Bowling, J. W., Alberts, J. J, and Brisbin, I. L. Jr., Distribution of long-lived radionuclides in an abandoned reactor cooling reservoir. *Ecological Monographs* **60**, 471-496 (1990).

61. Lucas, J. N., Awa, A., Straume, T., Poggensee, M., Kodama, Y., Nakano, M., Ohtaki, K., Weier, H. U., Pinkel, D., and Gray, J., Rapid translocation frequency analysis in humans decades after exposure to ionizing radiation. *International Journal of Radiation Biology* **62**, 53-63 (1992).

62. Fossi, M. C., Nondestructive biomarkers in ecotoxicology. *Environmental Health Perspectives* **102 Suppl 12**, 49-54 (1994).

63. Barquinero, J. F., Cigarran, S., Caballin, M. R., Braselmann, H., Ribas, M., Egozcue, J., and Barrios, L., Comparison of X-ray dose-response curves obtained by chromosome painting using conventional and PAINT nomenclatures. *International Journal of Radiation Biology* **75**, 1557-1566 (1999).

Chapter 2

Conservation of Chromosome-1 in Turtles over 66 Million Year

Abstract:

Fluorescence *in situ* hybridization (FISH) of a whole chromosome-1-specific probe from the yellow-bellied slider turtle (*Trachemys scripta*) to cells from four other species of turtle ranging from a desert tortoise to a loggerhead sea turtle resulted in specific and exclusive hybridization to chromosome-1 in all five species. Previous observations of conservation in the giemsa banding pattern and chromosome morphology and number among turtles are thus extended to the DNA sequence level, revealing a cytogenetic stability of chromosome-1 in these turtles during the past 66-144 million years. This contrasts with the situation for various hominoid species where, in many instances, extensive chromosomal rearrangements have been reported in one third of that time period. My probe, which was prepared by microdissecting whole chromosomes from embryonic *T. scripta* fibroblasts and amplifying using DOP-PCR, is the first report of a whole-chromosome FISH probe for any reptile.

Introduction:

The availability of whole-chromosome-specific DNA libraries, first from humans and later from other mammals has had wide application (1,2). One application of particular interest to me is comparative cytogenetics and genomics (3,4).

The use of whole-chromosome libraries in comparative cytogenetics holds great potential for clarifying evolutionary relationships. Such libraries have been used in studies of mammalian evolution (5-8), but wider application has been hindered by the lack of whole-chromosome libraries for non-mammalian species (6). The isolation of a

few chromosome libraries for birds has been reported (4,9), but beyond this, virtually nothing is available.

I prepared a turtle chromosome-1-specific DNA library as a potential tool for sketching evolutionary history using cytogenetic phylogenies. To the best of my knowledge, this is the first report of a whole-chromosome library for a reptilian species. Previous reports have suggested long-term genomic stability among turtle species, both in chromosome number (10) and in banded chromosome morphology (11). However, conservation of chromosome number and G-banding patterns over time does not establish conservation of DNA sequences within chromosomes (4,7). In this study, I use FISH test the hypothesis that the remarkable stability of the G-banded karyotypes in turtles extends to the DNA sequence level in chromosome-1.

Methods:

Cell culture:

A fibroblast line of *T. scripta* (yellow-bellied slider turtle) cells was established by primary explant from *T. scripta* embryos. Fibroblasts were maintained at 29°C [the preferred *T. scripta* body temperature (12)] in an atmosphere of 5% CO_2 in air. Cells were cultured in αMEM containing 10% fetal calf serum, gentamycin (Gibco, Grand Island, Illinois, final concentration 25 μg ml^{-1}), fungizone (Gibco, 0.5 μg ml^{-1}), streptomycin sulfate (68 μg ml^{-1}), and penicillin G (31 μg ml^{-1}). Mitotic fibroblasts were obtained by applying a colcemide (Gibco, 0.15 μg ml^{-1}) block for 12 hours, followed by selective detachment by agitation. Cells were fixed in 3:1 methanol/glacial acetic acid according to standard procedures (13,14) and dropped onto cold, cleaned, wet microscope

slides. *Terrapene carolina* (Eastern box turtle) and *Chrysemys picta* (painted turtle) lymphocyte cultures were prepared from turtles housed at the Savannah River Ecology Laboratory in Aiken, South Carolina. A *Gopherus agassizii* (desert tortoise) lymphocyte culture was prepared from an animal at the Colorado State University Veterinary Teaching Hospital and a *Caretta caretta* (loggerhead sea turtle) lymphocyte sample came from an animal at SeaWorld in Orlando, Florida. Samples for blood cultures were collected from the dorsal coccygeal vein (15) using syringes containing sodium heparin. Samples were then sent overnight to Colorado State University. Lymphocyte cultures were established and incubated under conditions similar to those of the fibroblast cultures with the following changes; 1) two percent phytohemagglutinin-M form (PHA-M) (Gibco) and 2) 55 $\mu g\ ml^{-1}$ lipopolysaccharides (Sigma, St. Louis, Missouri) were added to the cultures to stimulate the lymphocytes into the cell cycle, and 3) lymphocytes were cultured in Cellgro medium (Mediatech, Herndon, Virginia) supplemented with autologous serum used was from the turtle blood sample rather than the fetal bovine serum used for fibroblasts. Colcemide was added at 90 hours post-stimulation, and cells were harvested at 102 hours post-stimulation. Prior to fixation, lymphocytes were isolated by centrifugation in a ficoll gradient.

Karyotype:

Images were produced for karyotyping following a D/C-R banding procedure developed in this laboratory and which was described previously (16). Chromosomes from mitotic embryonic fibroblasts and from mitotic lymphocytes were stained simultaneously with 4,6-diamidino-2-phenylindole (DAPI) and chromomycin A3. A

Photometrics camera combined with the Universal Imaging MetaMorph software package was then used to generate one image taken with a DAPI excitation filter and one image taken with a chromomycin A3 excitation filter. A triple band pass filter designed for viewing fluorescence at the appropriate wavelengths was also in place. Intensity values from the DAPI image were then divided pixel-by-pixel by those from the chromomycin A3 image to generate patterns which are very similar to R-banding.

Probe preparation:

Chromosome spreads from log-phase cultures were prepared on coverslips for microdissection (17-19). About 10 whole-chromosome-1 (largest chromosome, sub-metacentric) samples were microdissected and placed together in a microfuge tube for PCR, to which was added 10 μl UV sterilized water, 2 μl of 10x thermosequenase reaction buffer, 4 μl of dNTP stock (2.5 mM each), 2 μl DOP primer solution, 5' CCG ACT CGA GNN NNN NAT GTG G 3' (100 μM) and 2 μl thermosequenase (4 U μl^{-1}). The solution was overlaid with mineral oil and the following PCR program was applied: 95° C for 3 minutes followed by 10 cycles of 94° C for 1.5 minutes, 30° C for 3 minutes and ramping to 72° C over 4 minutes (approximately 0.18° C s^{-1}), and then 50 cycles of 94° C for 1.5 minutes, 56° C for 1.5 minutes, and 72° C for 1.5 minutes. Small aliquots of the stock product were then labeled for the FISH procedure by repeating 10 cycles of the final, 94° C, 56° C, 72° C PCR reaction but in the presence of 100 μM biotin dUTP.

Fluorescence in situ hybridization:

The FISH was carried out essentially as described previously (20,21). Approximately 35 µl of the hybridization mixture containing 50% formamide, 10% dextran sulfate, 1 µg μl^{-1} herring sperm DNA, about 300 ng of PCR labeled probe and 5 µg of turtle cot DNA was denatured by boiling for 5 to 10 minutes, reannealed for 20 minutes, and the probe hybridization mixture was then placed on the slide (denatured as described below), covered by a 22 x 50 mm coverslip and sealed with rubber cement. Hybridization then proceeded overnight at 37°C. The turtle cot DNA was prepared (22) from *T. scripta* liver DNA which, after isolation, was sonicated to approximately 500 bp. A tube containing 1 µg μl^{-1} was then placed in boiling water for 30 minutes, transferred to a 65°C water bath for 4 minutes, and NaCl solution was added to achieve a final concentration of 0.3 M. Reannealing was then allowed to proceed for 6 minutes at 37°C and an equal volume of 2x S1 nuclease buffer along with 1 unit of S1 nuclease per µg of DNA was added. After digestion of the single stranded (slow annealing) sequences, the reaction was stopped by freezing and the cot DNA was precipitated with ammonium acetate and ethanol. The hybridization probe was placed on target slides prepared by denaturing the chromosomes on the slides in a coplin jar containing 70% formamide in 2 x SSC (sodium saline citrate) at pH 7.0 for 2 minutes at 68°C. The slide was then quickly transferred to ice cold 70% ethanol for 1 minute with agitation, followed by transfer to 90% and then 100% ice cold ethanol and finally by drying with a clean air jet. After probe hybridization to the denatured chromosomes, the coverslips were removed, the slides were washed in two changes of 50% formamide in 2 x SSC, pH 7.0, at 45°C and then were washed twice more in 2 x SSC and 3 times in PN buffer for 3 minutes

each, also at 45°C. For probe detection, PN buffer containing 5% non-fat dry milk was applied for 5 minutes at room temperature, the solution was drained from the slide and a solution of 5 $\mu g\ ml^{-1}$ avidin FITC in PN in 5% non-fat dry milk was applied (approximately 5 $\mu l\ cm^{-2}$ of the slide) and the slide was incubated 20 minutes at 37°C. The slide was then rinsed in 3 changes of PN buffer at 45°C for 2 minutes each. Further signal amplification was sometimes used as necessary. For microscopy, the slides were counterstained with a solution of antifade containing DAPI and/or propidium iodide (PI) at a concentration of 0.5 $\mu g\ \mu l^{-1}$ under a coverslip. Slides were then viewed under a fluorescence microscope with appropriate excitation and emission filters. Photographs were prepared with a Photometrics camera combined with the Universal Imaging MetaMorph software package.

Results:

The D/C R-banded karyotype for the *T. scripta* embryonic fibroblast cell line is shown in Figure 2.1A. The reported (diploid) chromosome number for *T. scripta*, 2n=50 (10,23), whereas I found that for this fibroblast cell line, the modal chromosome number was 48. Figure 2.1B is the D/C-R-banded karyotype constructed from *T. scripta* lymphocytes, which agreed with the reported karyotype for this species (2n=50). My use of fibroblast cultures yielded karyotypes that matched well with that for lymphocytes, except for a deficit in the number of microchromosomes.

Figure 2.2A shows a metaphase chromosome spread from a *T. scripta* cell which was labeled by FISH with biotinylated chromosome-1 probe library and detected with FITC avidin. Counter-staining was with propidium iodide. I then applied the labeled *T.*

scripta chromosome-1 probe to metaphase lymphocytes from other turtle species. Figures 2.2 B, C, D, and E are lymphocyte metaphase chromosome spreads from: *Chrysemys picta* (painted turtle), *Terrapene carolina* (Eastern box turtle), *Gopherus agassizii* (desert tortoise), and *Caretta caretta* (loggerhead sea turtle) respectively. All show exclusive hybridization of the probe to chromosome-1 of each species examined.

Discussion:

In the *T. scripta* karyotypes pictured in Figures 2.1A and B, regions of preferential DAPI staining (AT-rich, heterochromatin) are lighter, while the darker regions represent regions of preferential chromomycin A3 staining (GC-rich, euchromatin). By this criterion, the microchromosomes appear to be highly euchromatic, while the macrochromosomes contain larger blocks of heterochromatin. This is especially interesting in light of the fact that differences in the numbers of microchromosomes account for much of the variations observed among giemsa-stained karyotypes from different cryptodiran (head-retracting) turtle species (as opposed to pleurodiran, or side-necked species). Many pleurodires have substantially lower chromosome numbers (24,25)]. It also appears that in the macrochromosomes, subtelomeric and pericentromeric regions are more euchromatic. These patterns of euchromatin and heterochromatin distribution are also evident in previous reports of G-banded karyotypes from a variety of turtle species (25-31) and contrasts with the pattern for humans and other mammals where many chromosomes contain pericentromeric heterochromatin. The *T. scripta* genome has a DNA content similar to that of humans (32,33).

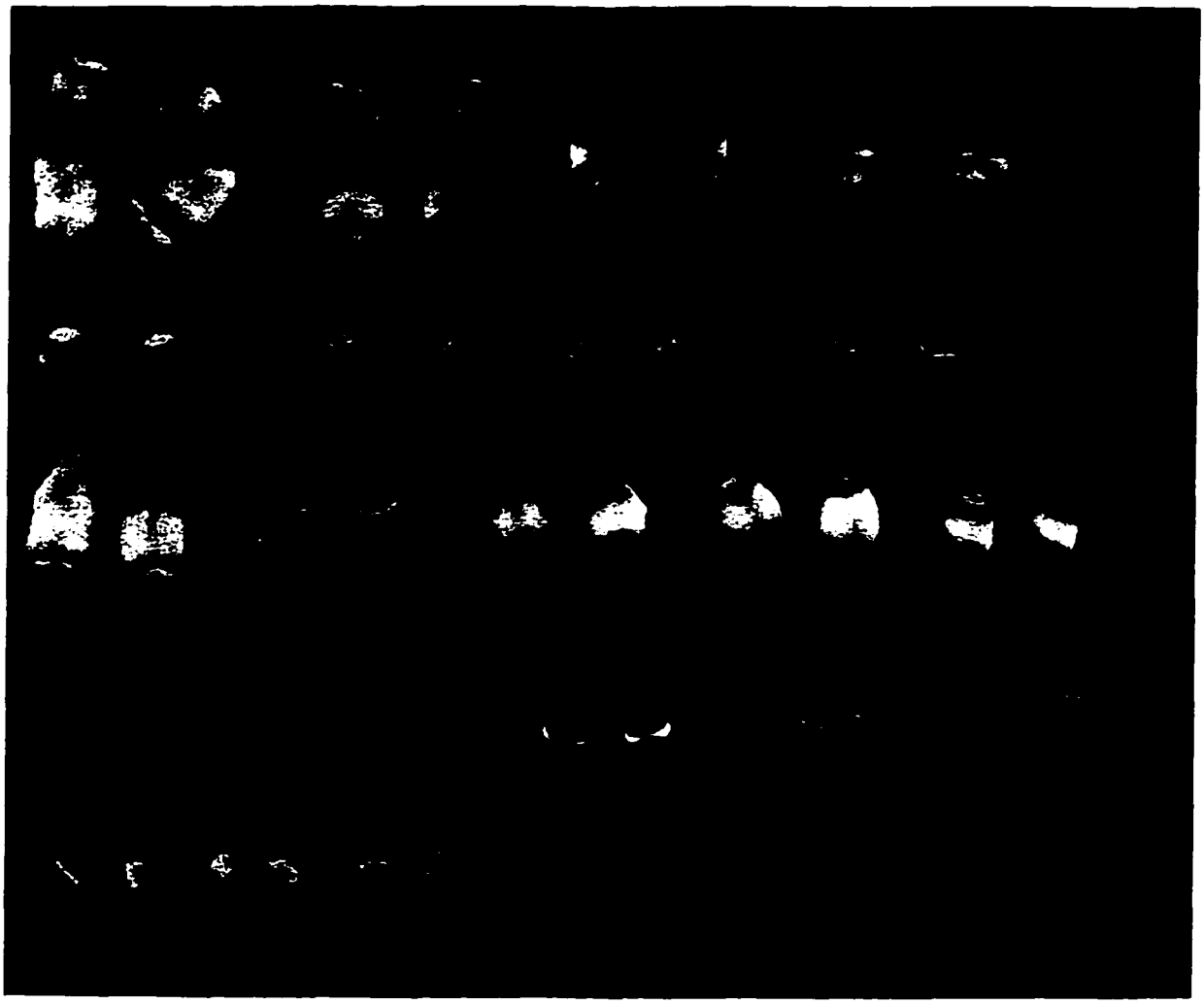

Figure 2.1A:
Karyotype of *T. scripta* embryonic fibroblast cell line. Image was created by D/C R-banding (16) and pseudocoloring.

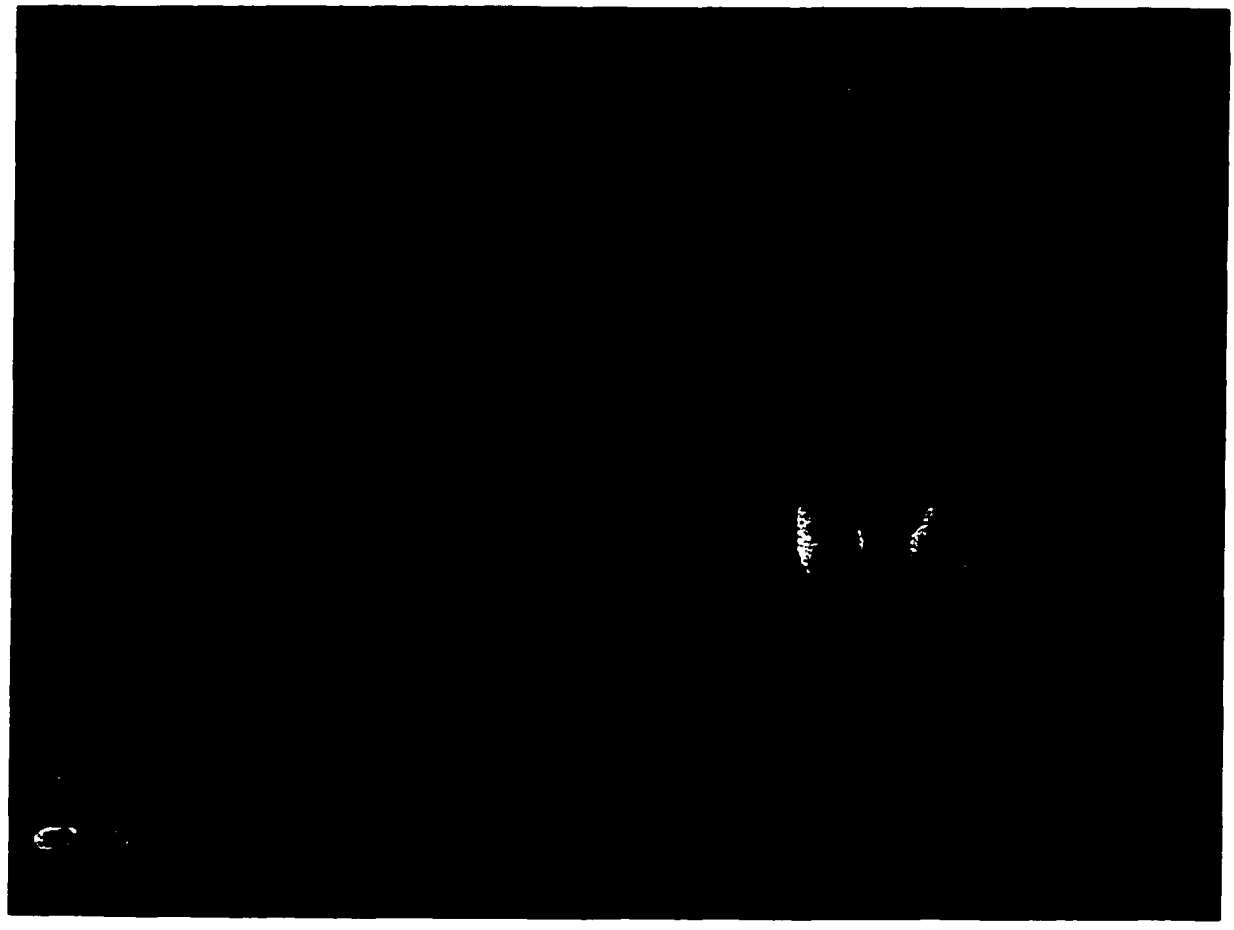

Figure 2.1B:
Karyotype of *T. scripta* lymphocyte. Image was created by D/C R-banding (16).

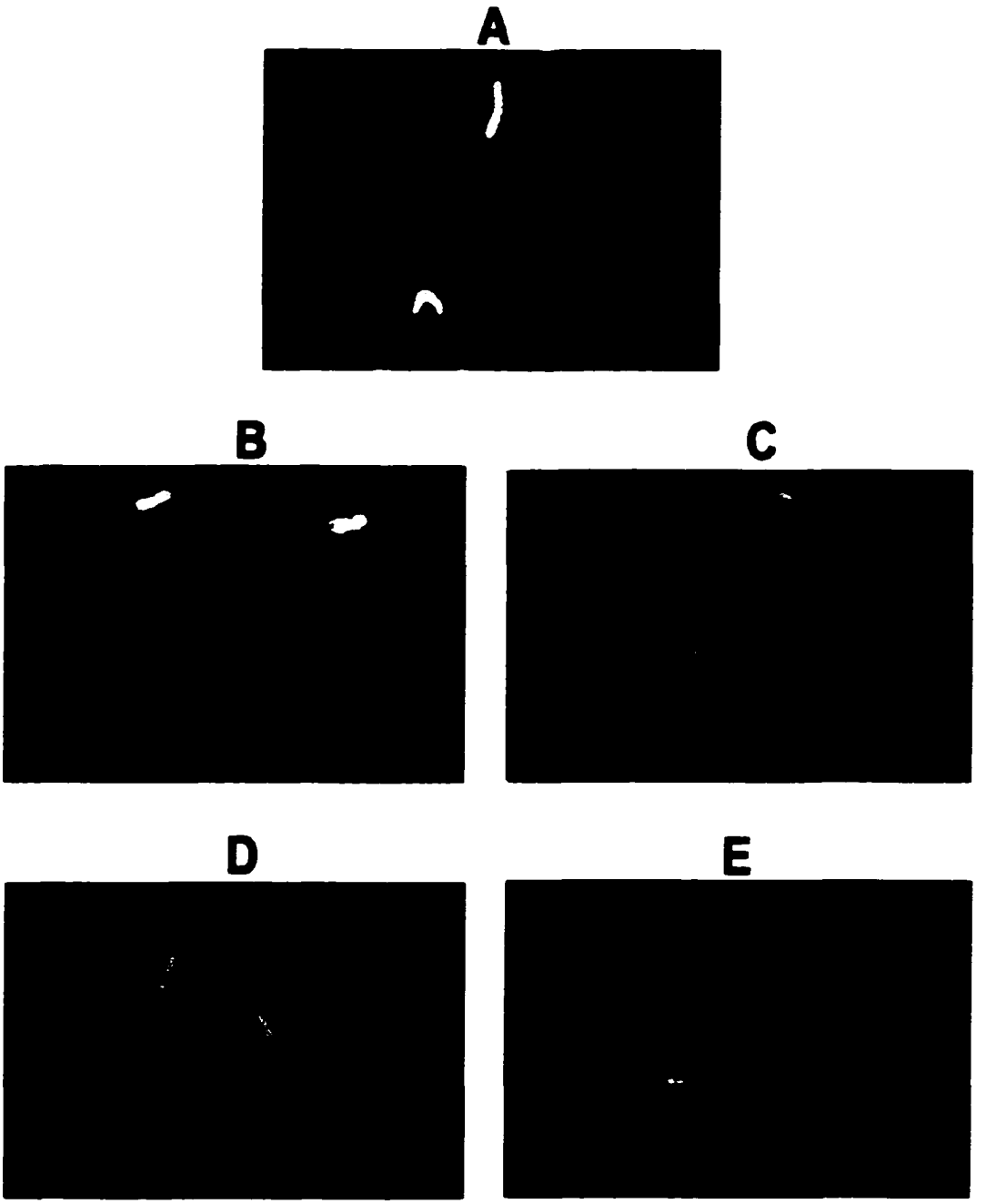

Figure 2.2:
Whole chromosome painting by fluorescence *in situ* hybridization (FISH) using a *T. scripta* chromosome-1 library obtained by microdissection and DOP-PCR. Chromosome-1 probe labeling and detection was with biotin dUTP and FITC avidin (yellow-green chromosomes). Panel A illustrates the *T. scripta* chromosome-1-specific probe library hybridized onto *T. scripta* mitotic cells. Panels B, C, D, and E utilized the same probe, but with hybridization onto *C. picta* (B), *T. carolina* (C); *G. agassizii* (D); or *C. caretta* (E) mitotic cells. Counterstaining was with propidium iodide (PI).

Turtles (order Testudines) appear in the fossil record about 200 million years ago. Body form is conservative. *T. scripta*, *C. picta*, and *T. carolina* are members of the family Emydidae (Figure 2.3), which is the largest and most diverse family of living turtles that occupy North Africa, Asia, Indonesia, the Philippines, Europe and the Americas. The family is currently comprised of two subfamilies: Batagurinae (Old World) and Emydinae (New World) pond turtles (34). The Batagurinae and Emydinae have similar chromosome numbers (2n=52 and 2n=50, respectively) (26). There are 33 genera and approximately 90 species in the family Emydidae. The earliest known fossils of Emydine turtles in North America are from approximately 65 million year old Paleocene deposits. *G. agassizii* is a member of the family Testudinidae, and *C. caretta* is a member of the family Cheloniidae (Figure 2.3)(35,36). Based on skeletal characteristics and the fossil record, these families diverged during the Cretaceous period, approximately 66.4-144 million years ago (35).

There are numerous lines of evidence suggesting slow rates of evolution in turtles. The rate of change in Testudine mitochondrial DNA base sequences is eight times slower than in other higher vertebrates, which show a rate of change of about 2% per million years (37). Homologous loci have been found in six marine turtle species within two families (Cheloniidae and Dermochelydidae) and one freshwater species (*T. scripta*). indicating conservation of flanking microsatellite loci (38) since the Cretaceous period (~144 million years). Sporadic natural viable hybrids among sea turtle (family Cheloniidae) genera occur. The species involved in the hybridization events represent lineages thought to have diverged 10-75 million years ago. Thus they appear to represent the oldest diverged lineages documented to hybridize. By implication, changes in the

genomes of species have remained small (39). Karyologic comparisons of Testudine groups have revealed extensive similarity in chromosome numbers among diverse members of a majority of turtle families, including the species considered in this study: *T. scripta*, $2n$=50 ($2n$=48 in the embryonic fibroblast cell line used in this study); *T. carolina*, $2n$=50; *C. picta*, $2n$=50; *G. agassizii*, $2n$=52; and *C. caretta*, 2n=56 (10,23). Previous reports comparing G-banding patterns for primarily macrochromosomes among diverse turtle species had suggested chromosomal stability over an evolutionary time scale of millions of years (11,26,40). Whereas banding patterns from giemsa staining may suggest chromosome stability and conservation, such banding does not demonstrate a conservation of DNA sequences within chromosomes (4,7).

That the entire chromosome-1 of all four species was uniquely and exclusively labeled with the probe derived from chromosome-1 of *T. scripta* demonstrates that this chromosome has maintained a remarkable stability with regard to translocations or other rearrangements in species as diverse as desert tortoises and loggerhead sea turtles. This contrasts with the situation for certain hominoid species where extensive chromosomal rearrangements have been reported (3,4) during the past 20 million years (41,42), despite a considerable degree of linkage conservation. The reason for a greater genomic stability in turtles is not known, but one possibility might be the lower rate of oxidative free radical production related to lower metabolic rate (37). The development of whole-chromosome probes for a turtle species is especially timely, as considerable debate currently exists over the evolutionary relationship between turtles, other reptilian species, and avian species. Recent molecular evidence appears to be at odds with phylogenies

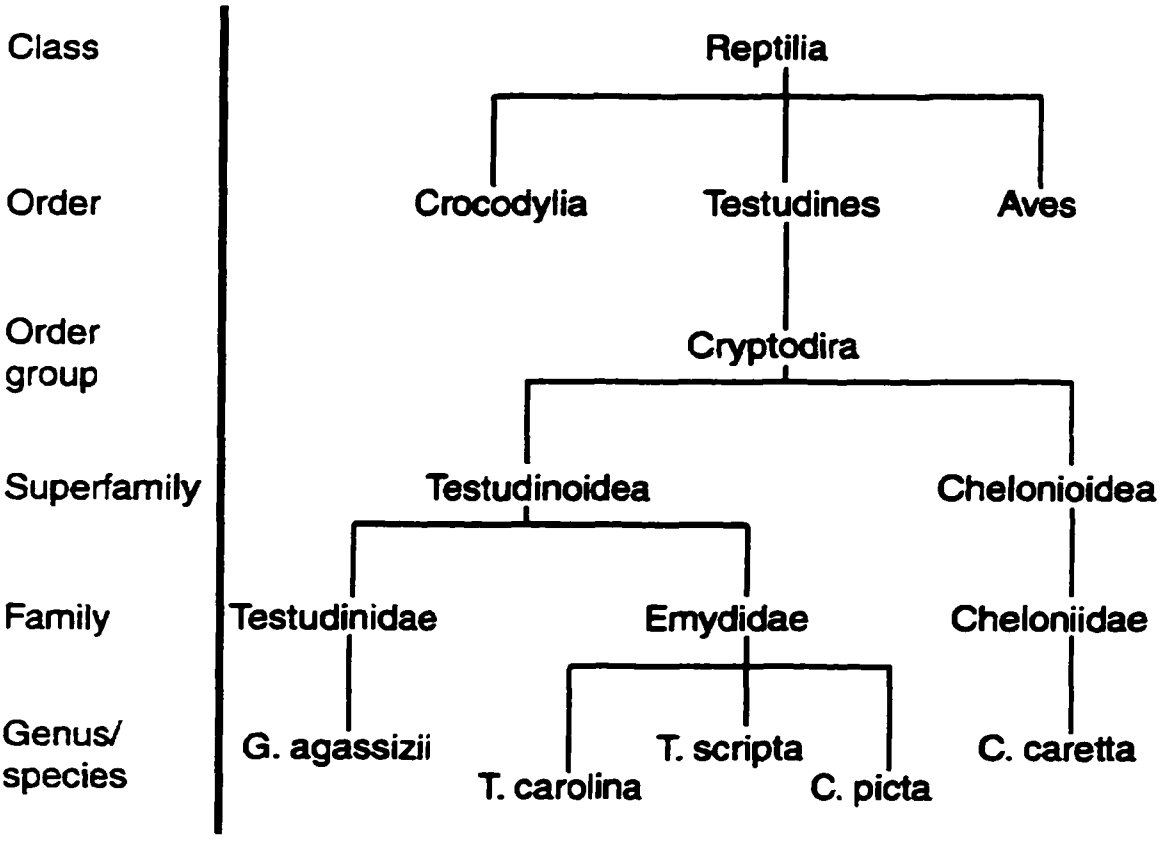

Figure 2.3:
A partial phylogeny of turtles. Note that only the branches which include species discussed in this chapter are detailed in this figure. *T. scripta, C. picta,* and *T. carolina* are members of the family Emydidae, which first appeared in the fossil record during the Eocene period (36.6-57.8 million years ago), while *G. agassizii* is a member of the family Testudinidae, which also first appeared in the Eocene, and *C. caretta* is a member of the family Cheloniidae, which first appeared in the Cretaceous period, 66.4-144 million years ago (35).

based on the fossil record and on morphology (43). The development of whole-chromosome libraries for turtles can provide independent cytogenetic evidence of genomic relationships and contribute to this debate.

I am currently attempting to examine an even broader range of turtle species, and to develop probes for other turtle chromosomes. A larger number of whole-chromosome libraries would be very useful for comparative genomics, as it would allow a more complete investigation of chromosome homology and linkage patterns among the genomes of diverse turtle species, and among turtles and other organisms; especially other reptiles and birds, for example. Full comparisons of relative stability cannot be made at present because I do not have whole-chromosome-specific DNA libraries for every chromosome.

The utility of whole-chromosome libraries for nonhuman organisms is not limited to comparative cytogenetics. I have also used the chromosome-1 probe to examine the clastogenic effects of ionizing radiation on *T. scripta* fibroblasts (44), and I am currently extending the techniques of biological dosimetry to turtles exposed to radionuclides in contaminated natural environments.

The application of microdissection, PCR and FISH to generate whole-chromosome libraries for nonmammalian organisms will greatly expand the tools available for comparative genomics, help to clarify evolutionary relationships, and expand the reach of genetic ecotoxicology to important species of organisms not previously examined.

Acknowledgements:

This work was supported by the Department of Energy grant RR267-055/4895914 to University of Georgia, Savannah River Ecological Laboratory and subcontract to Colorado State University, and a grant from the NIH, National Cancer Institute, 5 T32 CA09236 to Colorado State University.

The *Caretta caretta* blood sample was supplied by Dr. Dan Odell of Sea World, Inc., and was authorized by the Florida Fish and Wildlife Conservation Commission.

REFERENCES

1. Lucas, J. N., Awa, A., Straume, T., Poggensee, M., Kodama, Y., Nakano, M., Ohtaki, K., Weier, H. U., Pinkel, D., and Gray, J., Rapid translocation frequency analysis in humans decades after exposure to ionizing radiation. *International Journal of Radiation Biology* **62**, 53-63 (1992).

2. Rowley, J. D., Molecular cytogenetics: Rosetta stone for understanding cancer--twenty-ninth G. H. A. Clowes memorial award lecture. *Cancer Research* **50**, 3816-3825 (1990).

3. Wienberg, J. and Stanyon, R., Chromosome painting in mammals as an approach to comparative genomics. *Current Opinion in Genetics & Development* **5**, 792-797 (1995).

4. Wienberg, J. and Stanyon, R., Comparative painting of mammalian chromosomes. *Current Opinion in Genetics & Development* **7**, 784-791 (1997).

5. Arnold, N., Stanyon, R., Jauch, A., O'Brien, P., and Wienberg, J., Identification of complex chromosome rearrangements in the gibbon by fluorescent in situ hybridization (FISH) of a human chromosome 2q specific microlibrary, yeast artificial chromosomes, and reciprocal chromosome painting. *Cytogenetics & Cell Genetics* **74**, 80-85 (1996).

6. Scalzi, J. M. and Hozier, J. C., Comparative genome mapping: mouse and rat homologies revealed by fluorescence in situ hybridization. *Genomics* **47**, 44-51 (1998).

7. Stanyon, R., Arnold, N., Koehler, U., Bigoni, F., and Wienberg, J., Chromosomal painting shows that "marked chromosomes" in lesser apes and Old World monkeys are not homologous and evolved by convergence. *Cytogenetics & Cell Genetics* **68**, 74-78 (1995).

8. Wienberg, J., Jauch, A., Stanyon, R., and Cremer, T., Molecular cytotaxonomy of primates by chromosomal in situ suppression hybridization. *Genomics* **8**, 347-350 (1990).

9. Ambady, S., Ciufo, S., Robl, J. M., Smyth, J. R., and Ponce de Leon, F. A., Development of a chicken Z-chromosome-specific DNA library. *Journal of Heredity* **88**, 247-249 (1997).

10. Stock, A. D., Karyological relationships in turtles (Reptilia: Chelonia). *Canadian Journal of Genetics & Cytology* **15**, 859-868 (1972).

11. Bickham, J. W., Two-hundred-million-year-old chromosomes: deceleration of the rate of karyotypic evolution in turtles. *Science* **212**, 1291-1293 (1981).

12. Spotila, J. R., Foley, R. E., and Standora, E. A., Thermoregulation and climate space of the slider turtle, In *Life History and Ecology of the Slider Turtle* (Gibbons, J. W., Eds.), pp. 288-298. Smithsonian Institution Press, Washington, D.C., (1990).

13. Bedford, J. S., Mitchell, J. B., Griggs, H. G., and Bender, M. A, Radiation-induced cellular reproductive death and chromosome aberrations. *Radiation Research* **76**, 573-586 (1978).

14. Cornforth, M. N. and Bedford, J. S., A quantitative comparison of potentially lethal damage repair and the rejoining of interphase chromosome breaks in low passage normal human fibroblasts. *Radiation Research* **111**, 385-405 (1987).

15. Haskell, A. and Pokras, M. A., Nonlethal blood and muscle tissue collection from redbelly turtles for genetic studies. *Herpetological Review* **25**, 11-12 (1994).

16. Christian, A., McNiel, E., Robinson, J., Drabek, R., LaRue, S., Waldren, C., and Bedford, J., A versatile image analysis approach for simultaneous chromosome identification and localization of FISH probes. *Cytogenetics & Cell Genetics* **82**, 172-179 (1998).

17. Bussey, K. J., Chromosome microdissection: on the cutting edge. *Applied Cytogenetics* **22**, 30-36 (1996).

18. Guan, X. Y., Trent, J. M., and Meltzer, P. S., Generation of band-specific painting probes from a single microdissected chromosome. *Human Molecular Genetics* **2**, 1117-1121 (1993).

19. Muhlmann-Diaz, M., Christian, A. T., and Bedford, J. S., Chromosome microdissection, In *Radiation Research 1895-1995 Congress Proceedings* (Hagen,

U., Harder, D., Jung, H., and Streffer, C., Eds.), pp. 468-469. International Congress of Radiation Research, Wurzburg,Germany, (1995).

20. Lichter, P., Cremer, T., Borden, J., Manuelidis, L., and Ward, D. C., Delineation of individual human chromosomes in metaphase and interphase cells by in situ suppression hybridization using recombinant DNA libraries. *Human Genetics* **80**, 224-234 (1988).

21. Pinkel, D., Landegent, J., Collins, C., Fuscoe, J., Segraves, R., Lucas, J., and Gray, J., Fluorescence in situ hybridization with human chromosome-specific libraries: detection of trisomy 21 and translocations of chromosome 4. *Proceedings of the National Academy of Sciences of the United States of America* **85**, 9138-9142 (1988).

22. Nisson, P. E, Watkins, P. C., and Boyle, A, Efficient mapping of mouse clones using mouse Cot-1 DNA. *Focus* **14**, 119-122 (1992).

23. Bickham, J. W. and Baker, R. J., Karyotypes of some neotropical turtles. *Copeia* **1976**, 703-708 (1976).

24. Ayres, M., Sampaio, M. M., Barros, R. M. S., Dias, L. B, and Cunha, O. R., A karyological study of turtles from the Brazilian Amazon region. *Cytogenetics* **8**, 401-409 (1969).

25. Bull, J. J. and Legler, J. M., Karyotypes of side-necked turtles (Testudines: Pleurodira). *Canadian Journal of Zoology* **58**, 828-841 (1980).

26. Bickham, J. W. and Baker, R. J., Chromosome homology and evolution of emydid turtles. *Chromosoma* **54**, 201-219 (1976).

27. Bickham, J. W., Bull, J. J., and Legler, J. M., Karyotypes and evolutionary relationships of trionychoid turtles. *Cytologia* **48**, 177-183 (1983).

28. Bickham, J. W., The karyotype and chromosomal banding patterns of the green turtle (*Chelonia Mydas*). *Copeia* **1980**, 540-543 (1980).

29. Carr, J. L., Bickham, J. W., and Dean, R. H., The karyotype and chromosomal banding patterns of the Central American river turtle *Dermatemys Mawii*. *Herpetologica* **37**, 92-95 (1981).

30. Haiduk, M. W. and Bickham, J. W., Chromosomal homologies and evolution of testudinoid turtles with emphasis on the systematic placement of *Platysternon*. *Copeia* **1982**, 60-66 (1982).

31. Stock, A. D. and Mengden, G. A., Chromosome banding pattern conservatism in birds and nonhomology of chromosome banding patterns between birds, turtles, snakes and amphibians. *Chromosoma* **50**, 69-77 (1975).

32. Atkin, N. B., Mattinson, G., Becak, W, and Ohno, S., The comparative DNA content of 19 species of placental mammals, reptiles, and birds. *Chromosoma* **17**, 1-10 (1965).

33. Mirsky, A. E. and Ris, H., Variable and constant components of chromosomes. *Nature* **163**, 666-667 (1949).

34. Russell, L. S., Fossil turtles from Saskatchewan and Alberta. *Transactions of the Royal Society of Canada* **28**, 101-111 (1934).

35. Obst, F. J., *Turtles, Tortoises and Terrapins*. Druckerei Fortschritt Erfurt, Leipzig, (1986).

36. Pough, F. Harvey, Andrews, Robin M., Cadle, John E., Crump, Martha L., Savitzky, Alan H, and Wells, Kentwood D., *Herpetology*. Prentice Hall, Upper Saddle River, NJ, (1998).

37. Avise, J. C., Bowen, B. W., Lamb, T., Meylan, A. B., and Bermingham, E., Mitochondrial DNA evolution at a turtle's pace: evidence for low genetic variability and reduced microevolutionary rate in the Testudines. *Molecular Biology & Evolution* **9**, 457-473 (1992).

38. FitzSimmons, N. N., Moritz, C., and Moore, S. S., Conservation and dynamics of microsatellite loci over 300 million years of marine turtle evolution. *Molecular Biology & Evolution* **12**, 432-440 (1995).

39. Karl, S. A., Bowen, B. W., and Avise, J. C., Hybridization among the ancient mariners: characterization of marine turtle hybirds with molecular genetic assays. *Journal of Heredity* **86**, 262-268 (1995).

40. Bickham, J. W. and Carr, J. L., Taxonomy and phylogeny of the higher categories of cryptodiran turtles based on a cladistic analysis of chromosomal data. *Copeia* **1983**, 918-932 (1983).

41. Andrews, P., Fossil evidence on human origins and dispersal. *Cold Spring Harbor Symposia on Quantitative Biology* **51 Pt 1**, 419-428 (1986).

42. Sibley, C. G. and Ahlquist, J. E., The phylogeny of the hominoid primates, as indicated by DNA-DNA hybridization. *Journal of Molecular Evolution* **20**, 2-15 (1984).

43. Hedges, S. B. and Poling, L. L., A molecular phylogeny of reptiles. *Science* **283** , 998-1001 (1999).

44. Ulsh, B. A., Muhlman-Diaz, M., Whicker, F. W., Hinton, T. G., Congdon, J. D, and Bedford, J. S., Chromosome translocations in turtles: a biomarker in a sentinel animal for ecological dosimetry. *Radiation Research* **153**, 752-759 (2000).

Chapter 3

Chromosome Translocations in Turtles:

A Biomarker in a Sentinel Animal for Environmental Biodosimetry

Abstract:

Nonhuman organisms are being exposed to ionizing radiations at radionuclide-contaminated sites around the world. Direct methods are seldom available for measuring biologically relevant doses received by these organisms. Here, I extend biological dosimetry techniques, which are much better developed for humans and a few other mammalian species, to a nonmammalian species. Turtles were chosen because a long-lived animal would best serve the need for low level, chronic exposure conditions. I chose the yellow-bellied slider turtle (*Trachemys scripta*) which is known to have a maximum life-span of at least 22 years. As reported elsewhere, I first isolated an embryonic fibroblast cell line and constructed whole-chromosome-specific DNA libraries for chromosome-1 by microdissection and PCR. A FISH painting probe was prepared and used to establish a dose-response curve for ionizing radiation-induced chromosome interchange aberrations in turtle fibroblasts. This was compared to the dose-response for human fibroblasts treated under similar conditions in this laboratory. With respect to induction of chromosome interchange aberrations, human fibroblasts were approximately 1.7 times more sensitive than the *T. scripta* fibroblasts. To the extent that symmetrical interchanges are persistent over long periods of time, this approach could eventually provide a measure of the integrated lifetime dose these organisms receive from radionuclides in their environment and give a measure of the extent of relevant genetic damage over that time.

Introduction:

Determining the effect of clastogenic agents decades after exposure is possible in humans due to the availability of whole-chromosome-specific DNA libraries, as demonstrated for example in Japanese A-bomb survivors fifty years after radiation exposure (1). Cytogenetic analysis has been greatly facilitated by fluorescence *in situ* hybridization techniques (FISH) (2), To my knowledge, whole-chromosome-specific DNA libraries have been isolated and utilized for biodosimetry only in humans exposed accidentally or other mammals clinically exposed in controlled laboratory settings (*e.g.* human studies reviewed in (3-6), rhesus monkeys (7) and rodents, *e.g.* (8-11)). FISH-based biodosimetry has not been applied to nonhuman organisms receiving radiation exposure from contaminated environments.

The aim of the present study was to extend the techniques of biodosimetry to an ecological receptor, the yellow-bellied slider turtle (*Trachemys scripta*). In this chapter, I refer to retrospective biodosimetry in nonhuman organisms continuously inhabiting contaminated environments as "environmental biodosimetry" to differentiate this type of assessment from the traditional applications of biodosimetry where humans or other mammals receive controlled doses for clinical purposes, or acute exposures in accident situations. I hypothesize that, at the very least, environmental biodosimetry could be useful in the exposure assessment stage of ecological risk assessments involving radionuclides or other clastogens. Should these techniques prove to be sufficiently sensitive and indicative of adverse biological or ecological effects, they could inspire a reexamination of currently proposed primary dose-rate limits based on less sensitive measures of biological damage such as gross mortality or reproductive impairment (12).

It is widely recognized that chromosome interchanges are particularly well-suited to serve as biomarkers of radiation exposure, as suggested by Bender and Gooch (13) more than 35 years ago. The scoring of asymmetrical chromosome interchanges (dicentrics) in peripheral blood lymphocytes has long been used for this purpose. With the development of FISH, scoring of symmetrical interchanges for biodosimetry has also become practical. Symmetrical interchanges are generally thought to be relatively more stable over time than asymmetrical interchanges, i.e. they do not kill cells bearing them and they remain in a stem cell population to produce progeny with aberrations many cell generations after exposure. While the background level of symmetrical interchanges is generally considerably higher than that of asymmetrical interchanges, they can better serve as a biomarker of cumulative radiation exposure. This higher background is presumably due to the accumulation of symmetrical interchanges caused by chronic exposure to natural radiation sources or endogenous mutagens. Asymmetrical interchanges would also be produced from such sources, but they would not accumulate due to the resultant cell lethality.

The model organism I chose, *T. scripta*, has a relatively long life span (maximum of at least 22 years (14)) and a wide geographical distribution (15), which make it an excellent sentinel animal for assessing chromosomal damage that is likely relevant to ecological risk from chronic, low-level exposure to radionuclides (and other clastogens) in the environment (16). Other turtle species are endemic to much of the United States (17,18) and are also relatively long-lived, so techniques developed for *T. scripta* could have wide application. Using FISH whole-chromosome paint probes prepared by microdissection and PCR (the development of which will be described elsewhere), I test

the hypothesis that the dose-response curve for radiation-induced chromosome interchanges in *T. scripta* is of a linear-quadratic form, and similar to one generated in this laboratory for human fibroblasts treated similarly. In doing so, I have developed a biomarker of cumulative radiation exposure for the common yellow-bellied slider turtle. This appears to be the first application of FISH-based biodosimetry to a nonmammalian organism.

Methods:

Cell culture:

A fibroblast line of *T. scripta* (yellow-bellied slider turtle) cells was established by primary explant from *T. scripta* embryos. Fibroblasts were maintained at 29°C (the preferred *T. scripta* body temperature (19)) in an atmosphere of 5% CO_2. Cells were cultured in αMEM containing 10% fetal calf serum, gentamycin (Gibco BRL, Grand Island, Ill., final concentration 25 μg ml^{-1}), fungizone (Gibco BRL, 0.5 μg ml^{-1}), streptomycin sulfate (68 μg ml^{-1}), and penicillin G (31 μg ml^{-1}).

Contact-inhibited cultures were grown for use in irradiation treatments to ensure that cells were in G_0 during irradiation and the following period of damage repair/misrepair. Contact-inhibition was verified in the fibroblast cultures by the addition of bromodeoxyuridine (BrdU) (10^{-4} M) to two replicate cultures established in parallel with the unirradiated experimental control cultures. At the conclusion of the irradiation of experimental treatments, the (unirradiated) cultures containing BrdU were immediately fixed and labeled with mouse monoclonal anti-BrdU (Amersham Pharmacia Biotech, Piscataway, NJ) followed by anti-mouse Ig, fluorescein linked whole antibody (from

sheep) (Amersham Pharmacia Biotech). One-thousand cells from each replicate were then scored using a fluorescence microscope equipped with a FITC filter. Less than 5% of the cell population were typically found to be cycling.

Irradiation:

Contact-inhibited cells were irradiated at room temperature in a 222 TBq ^{137}Cs γ irradiator (MARK-1 Model 68A, J. L. Shepherd and Associates, San Fernando, CA). ^{137}Cs γ-ray doses were 0 (control), 4, 6, 8, and 10 Gy delivered at 3.48 Gy min^{-1} (exposure rates measured using a Victoreen R-chamber traceable to the National Institute of Standards and Technology). Cultures were returned to the incubator immediately after irradiation for 24 hours to allow for the completion of repair/misrepair processes (20,21). Cells were then subcultured and fixed at 6 hour intervals beginning 30 hours after subculture (to estimate the time of the peak in first post-irradiation mitoses) or at 42 hours after subculture (for FISH experiments).

Depending on the number of mitotic cells obtained from irradiated cultures, one to three independent trials were conducted to obtain a sufficient number of scorable cells for each experimental treatment. Identical irradiation and culture conditions and the same cell line were used for all trials. The results were not statistically significantly different between trials for any dose, therefore the results were combined to yield pooled aberration frequencies.

Fixation and slide preparation:

Fixation was always preceded by a 6 hour colcemide (Gibco BRL, 0.15 μg ml^{-1} final concentration) block. The fixation procedure consisted of the following standardized protocol: 1) cells were trypsinized from the culture flasks and centrifuged; 2) the supernatant was discarded, and the cell pellet was resuspended in 8 ml 0.075 M KCl and incubated for 15 minutes at 37°C; 3) two ml fixative (3:1 methanol/glacial acetic acid) was added to the hypotonic solution; 4) cells were centrifuged, the supernatant was discarded, and the pellet was broken by agitation; 5) 4 ml of fixative was added dropwise to the cells while they were agitated to prevent clumping; 6) two more changes of fixative were performed. Cell suspensions were stored at – 20°C until use. Fixed cells were dropped onto clean, cold, wet glass slides. The slides used for FISH were hybridized within 3-7 days. Slides used for determination of mitotic index were giemsa stained and scored immediately. One thousand cells were scored for each 6 hour interval for each dose and the mitotic index (the percentage of cells in mitosis) was calculated.

Fluorescence in situ hybridization:

The whole-chromosome-1 probe used in this study was prepared by microdissection and DOP-PCR (22-24). FISH was carried out essentially as described by Pinkel and coworkers (25) and by Lichter and coworkers (26). Approximately 35 μl of the hybridization mixture containing 50% formamide, 10% dextran sulfate, 1 μg μL^{-1} herring sperm DNA, about 300 ng of probe PCR labeled with biotin and 5 μg of turtle cot DNA (see following subsection for details on cot preparation) was denatured by boiling

for 5 to 10 minutes, reannealed for 20 minutes at 37°C, and the probe hybridization mixture was then placed on the slide (denatured as described below), covered by a 22 x 50 mm coverslip and sealed with rubber cement. Hybridization then proceeded overnight at 37° C. The target slides onto which the hybridization probe was placed were prepared by denaturing the chromosomes on slides in a coplin jar containing 70% formamide in 2 x saline sodium citrate (SSC) at pH 7.0 for 2 minutes at 68° C. After this, the slide was quickly transferred to ice cold 70% ethanol for 1 minute with agitation, followed by transfer to 90% and then 100% ice cold ethanol and finally by drying with a clean air jet. After probe hybridization to the denatured chromosomes, the coverslips were removed, the slides were washed in two changes of 50% formamide in 2 x SSC, pH 7.0, at 45° C and then were washed twice more in 2 x SSC and 3 times in PN buffer for 3 minutes each, also at 45° C. For probe detection, PN buffer containing 5% non-fat dry milk was applied for 5 minutes at room temperature, then the solution was drained from the slide and a solution of 5 $\mu g\ ml^{-1}$ avidin-fluorescein isothiocyanate (FITC) in PN was applied (approximately 5 $\mu l\ cm^{-2}$ of the slide). The slide was incubated 20 minutes at 37° C, then rinsed in 3 changes of PN buffer at 45° C for 3 minutes each. Further, amplification was sometimes used. For microscopy, the slides were counterstained with a solution of antifade containing 4,6-diamidino-2-phenylindole (DAPI) and propidium iodide (PI) at a concentration of 0.5 $\mu g\ \mu L^{-1}$ under a coverslip. Slides were then viewed under a fluorescence microscope with appropriate excitation and emission filters. Photographs were prepared with a Photometrics camera combined with the Universal Imaging MetaMorph software package.

Cot preparation:

The turtle cot DNA was prepared from *T. scripta* liver DNA which, after isolation, was sonicated to approximately 500 bp. A tube containing 1 μg μL^{-1} was then placed in boiling water for 30 minutes, transferred to a 65° C water bath for 4 minutes, and NaCl solution was added to achieve a final concentration of 0.3 M. Reannealing was then allowed to proceed for 6 minutes at 37° C and an equal volume of 2x S1 nuclease buffer along with 1 unit of S1 nuclease per μg of DNA was added. After digestion of the single stranded (slow annealing) sequences, the reaction was stopped by freezing, and the cot DNA was precipitated with ammonium acetate and ethanol.

Aberration scoring:

Using a probe for chromosome-1, I determined a dose-response for the induction of interchange aberrations involving *T. scripta* chromosome-1 in cultured fibroblasts following various doses of ^{137}Cs gamma rays (Table 1). Aberrations were classified as either apparently simple and complete asymmetrical or symmetrical interchanges, or as incomplete or complex aberrations (as defined in (27)). I used the PAINT nomenclature (28) for scoring aberrations.

Results:

There was a distinct peak in mitotic index for the interval ending at 42 hours after subculture in the control and in treatments irradiated with 4 and 8 Gy (Figure 3.1). The peaks for the 6 and 10 Gy treatments were seen in the succeeding interval ending at 48 hours post-subculture. I therefore chose the 36-42 hour post-subculture interval for

harvest of cells in their first post-irradiation mitosis for the subsequent experiment (i.e. the determination of the dose-response relationship for radiation-induced interchange aberrations).

One example of the type of aberration seen at the first mitosis after irradiation of G_0 *T. scripta* cells is shown in Figure 3.2. A metaphase cell containing a normal chromosome-1 and a chromosome-1 involved in a chromosome exchange was painted using the labeled chromosome-1 probe, labeled by FISH with biotinylated chromosome-1 probe library and detected with FITC avidin. Counter-staining was with propidium iodide. This aberration was scored as an apparently simple symmetrical chromosome-type interchange. As described below, however, there is often considerable uncertainty about centromere identification after the relatively harsh chromosome treatments necessary for the *in situ* hybridization, resulting in a scoring bias toward symmetrical and against asymmetrical interchanges. A whole-genome dose-response curve was generated for apparently simple, complete, symmetrical plus asymmetrical interchanges projected from the frequency of interchanges involving chromosome-1 (Figure 3.3). For comparison, data generated in this laboratory for low-passage human fibroblasts (20) grown and irradiated under nearly identical conditions are also shown in Figure 3.3. Besides a small correction made for differences in radiation quality between the studies (X-rays (20) vs. γ-rays in the present study), a further correction was applied to estimate a whole genome equivalent for turtle cells based on measurement of interchanges solely in chromosome-1 (1). By measuring DAPI and chromomycin fluorescence on identical

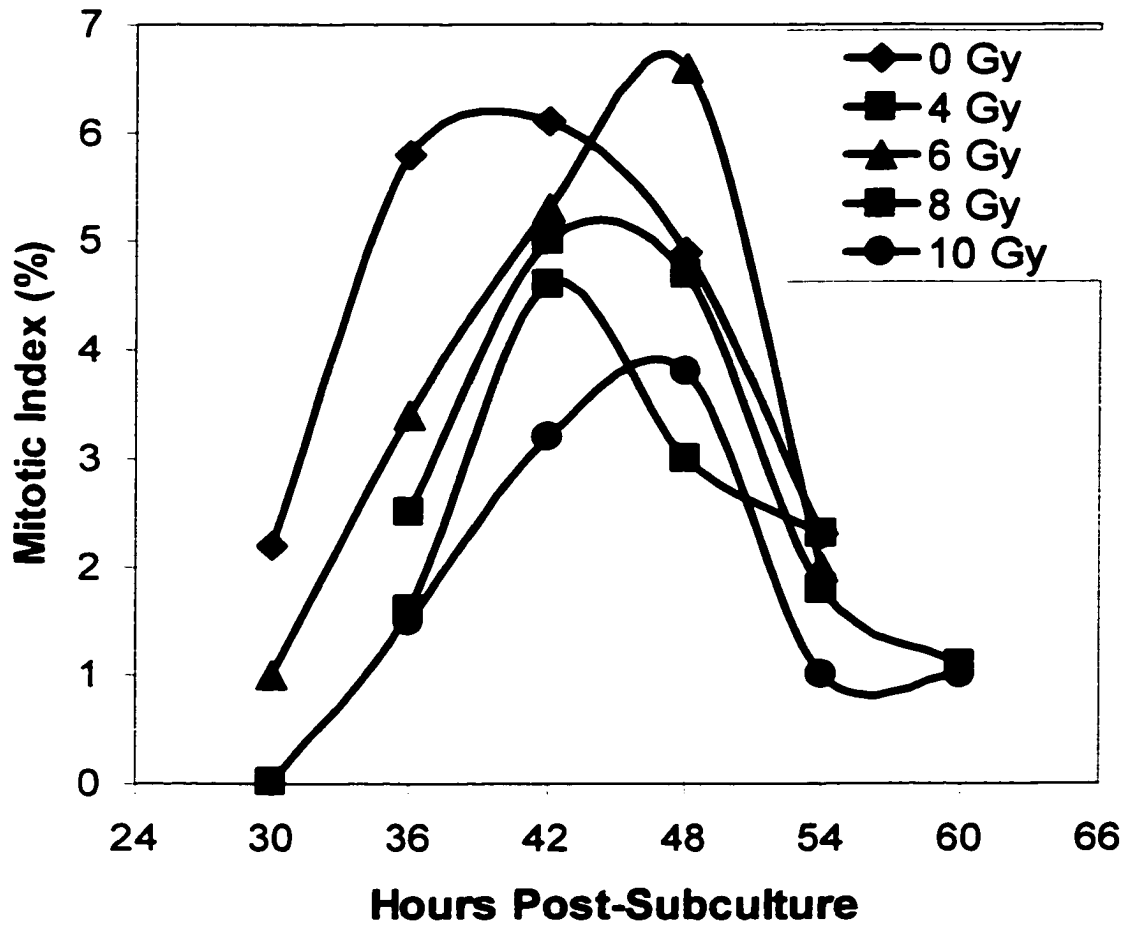

Figure 3.1:
Mitotic index at various sampling times after irradiation and subculture of contact inhibited *T. scripta* fibroblasts. Contact inhibited cells were irradiated at room temperature at the indicated doses, returned to incubators (29°C) for 24 hours to allow complete damage processing, then subcultured. Cells were then fixed (in 3:1 methanol/glacial acetic acid) at the times indicated. All fixations were preceded by a 6 hour colcemide block to accumulate cells in mitosis.

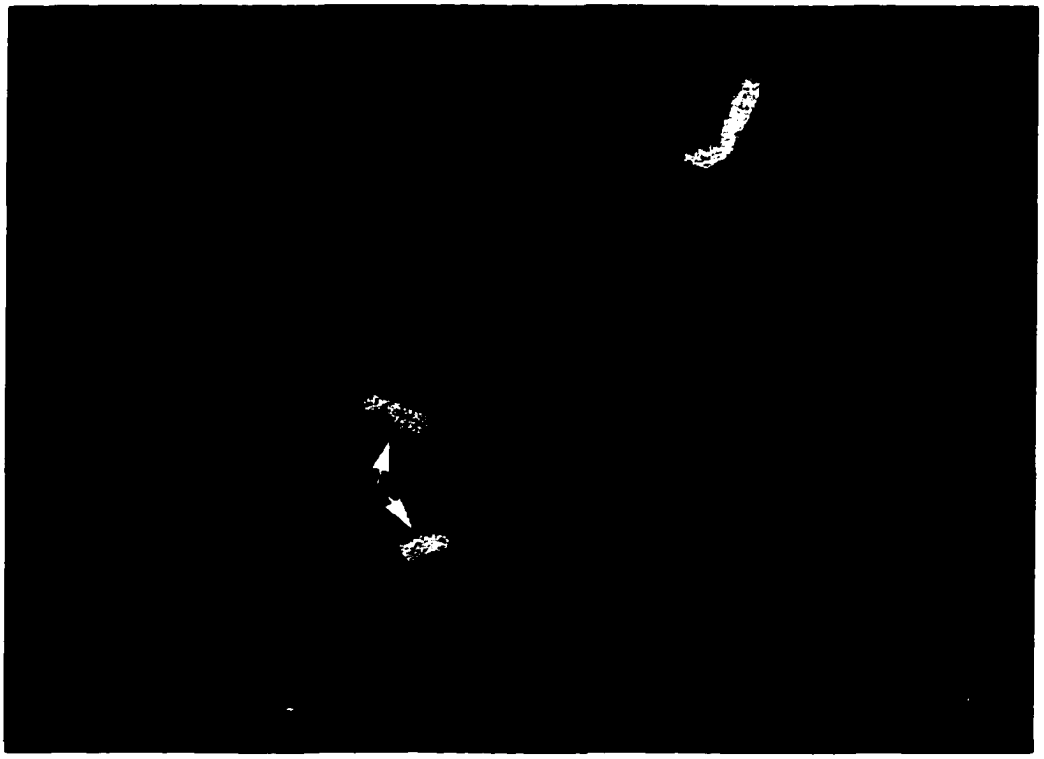

Figure 3.2:
Whole chromosome painting by fluorescence *in situ* hybridization (FISH) using *T. scripta* chromosome-1 library obtained by microdissection and DOP-PCR. Chromosome-1 probe labeling and detection was with biotin-dUTP and FITC. A chromosome interchange aberration (arrows) involving *T. scripta* chromosome-1 (yellow) and another *T. scripta* chromosome in the first metaphase after a ^{137}Cs gamma-ray dose of 4 Gy delivered to G_0 cells is visible, as well as an intact chromosome-1. Propidium iodide was used as a counterstain.

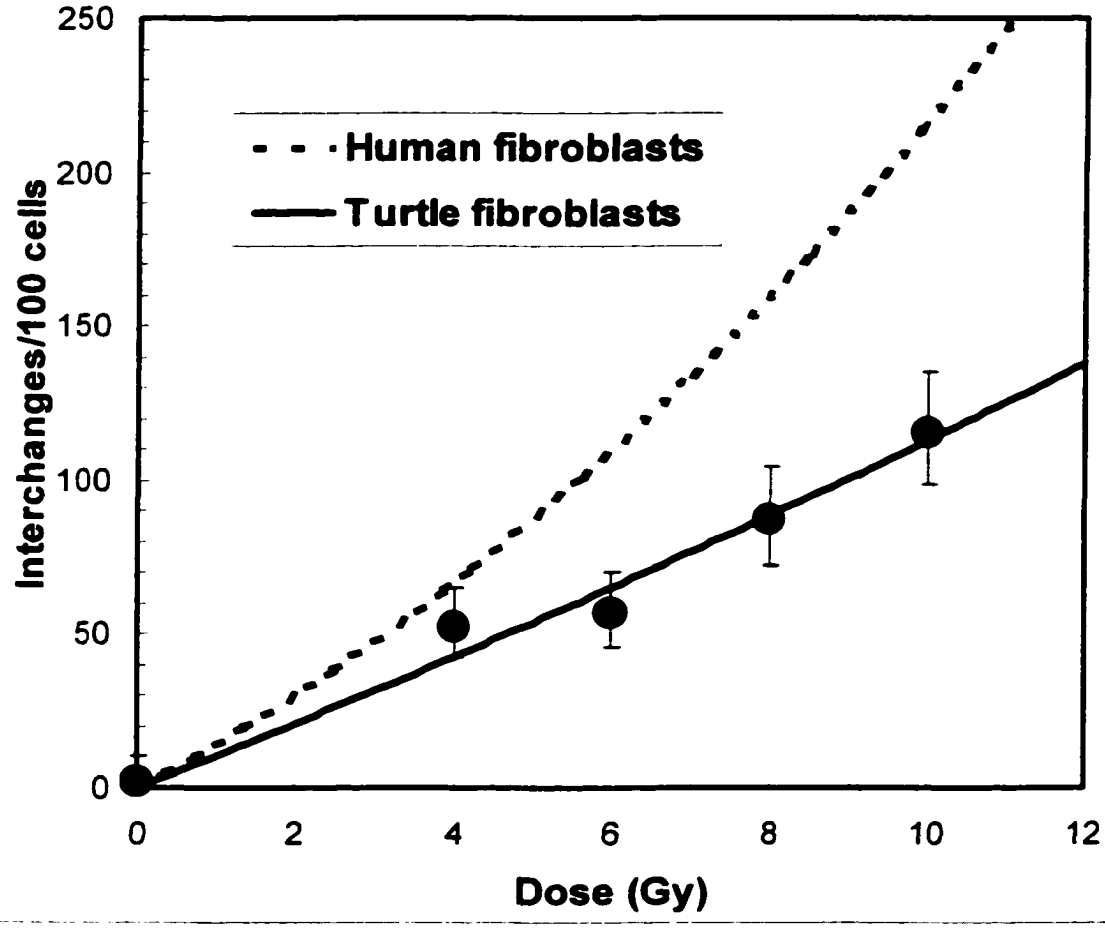

Figure 3.3:

Comparison of turtle (*T. scripta*) and human chromosomal radiosensitivity. Data (Table 1, columns four and six) on total interchange frequencies (apparently simple, complete, symmetrical and asymmetrical interchanges) involving *T. scripta* chromosome-1 (which comprises about 17% of the entire genome) were used to project the total expected frequency for the whole turtle genome. To the extent that all *T. scripta* chromosomes have the same radiosensitivity per unit of DNA as chromosome-1, the ^{137}Cs gamma-ray dose response for the induction of total chromosome-type interchanges in the first mitosis after irradiation of cultured fibroblasts in G_0 is plotted in the lower curve. Error bars indicate 95% confidence limits on the mean based on Poisson counting statistics. For comparison, the curve for human fibroblasts irradiated with X-rays, but otherwise under identical conditions, is shown as the upper curve (see text for details).

chromosomes and also by chromosome length measurements, I have estimated that chromosome-1 comprises about 17% of the turtle genome. A linear-quadratic function provided a better fit than a linear function at the 90%, but not at the 95% confidence level. The best linear fit was $Y = (11.1 \pm 0.472)*D$; $r^2 = 0.97$, $n = 5$, uncertainties are standard errors, and Y is the total interchange frequency per 100 cells and D is the dose in Gy. The best linear-quadratic fit was $Y = (10.2 \pm 2.38)*D + (0.11 \pm 0.280)*D^2$; $r^2 = 0.98$, $n = 5$. Results are presented in Table 1.

Discussion:

It has traditionally been thought that if radiation protection standards for humans are not exceeded, populations of other organisms and ecosystems will also be adequately protected, as stated by the International Commission on Radiological Protection:

> "The Commission believes that the standard of environmental control needed to protect man to the degree currently thought desirable will ensure that other species are not put at risk. Occasionally, individual members of non-human species might be harmed, but not to the extent of endangering whole species or creating imbalance between species."(29)

However, special considerations may be required for endangered species, populations with long generation times or geographically isolated populations (30). Further, there are regulatory requirements for ecological risk assessments and, where indicated, remediation of some sites contaminated by radionuclides or other genotoxic agents. Environmental sampling (*e.g.* soil, sediment, water, biota, etc.) can provide data from which a current radiation dose rate can be estimated. But this type of data reveals nothing about the total exposure an organism has received. A direct quantitative

biological assessment using a relevant genetic index of exposure would be a very useful tool, especially in long-lived organisms which may show cumulative effects of chronic exposure. My biomarker of cumulative radiation exposure for *T. scripta* is such a tool, and apparently the first FISH-based biodosimeter applicable for a free-ranging wildlife species. I chose symmetrical interchange aberrations as a biomarker mainly because they are thought to be generally stable over time (31,32), in contrast to dicentrics which decline with an estimated half-time of 1-3 years in humans (33-35). Some recent studies however, have found that even symmetrical interchanges may not be entirely stable. For example, in human peripheral blood lymphocytes exposed *in vitro* to 0 – 4 Gy, a decline of 26 - 47% in symmetrical interchange frequency was noted between days 2 and 7 post-irradiation (36). In rat peripheral blood lymphocytes exposed *in vitro* to 1 - 2 Gy, the decline was up to 35% between days 2 and 5 post-irradiation (37). And in mouse peripheral blood lymphocytes exposed to 4 Gy *in vivo*, the initial decline was approximately 33% between days 10 and 30 post-irradiation, but no decline was observed in mice exposed to lower doses (10). Nevertheless, these studies all report a subsequent plateau in symmetrical interchange frequencies above control levels, a result consistent with the long-term persistence of at least a subpopulation of cells bearing these aberrations.

I found a ratio of symmetrical interchanges to asymmetrical interchanges apparently greater than one at every dose (Table 1), but without the simultaneous use of centromere-specific probes, I cannot attribute any significance to this observation. Classical theory suggests that these aberrations should occur at equal frequency in the first post-irradiation mitosis, and there is substantial evidence to support this notion (*e.g.*

(20,34,38-44)). The harsh denaturation treatments involved in the FISH procedure can obscure centromeres, and when this occurs, some asymmetrical interchanges will be misclassified as symmetrical (45). Some recent studies have reported an excess of symmetrical versus asymmetrical interchanges even when a pancentromeric probe was used (21,46-49), or when centromeres were visible by DAPI staining (50). While I cannot rule out the possibility that there may be an excess of symmetrical interchanges in irradiated *T. scripta* fibroblasts, much of the excess I observed is almost certainly due to the fact that centromeres were not always identifiable. This is especially problematic for the *T. scripta* genome because of the presence of several microchromosomes, the centromeres of which are difficult to detect even under the best of circumstances. Definitive identification of interchange aberrations as symmetrical or asymmetrical in this organism should be possible once a pancentromeric probe becomes available. Development of such a probe is underway in this laboratory.

Since turtles are an unusual experimental species, an approximate, order-of-magnitude type comparison between turtle and human cell sensitivity may be of interest. To this end, I compared the results obtained in this study for turtle cells with data previously generated in this laboratory for normal human fibroblasts. The most appropriate comparison would include normal human fibroblasts with a similar proportion of the genome painted with a whole-chromosome FISH probe, as was done with turtle fibroblasts in this study. However studies in the literature involving human cells almost always employ lymphocytes, which tend to have a different dose-response than fibroblasts (51). Even though some extrapolation was necessary, I therefore felt it was more appropriate to compare the data generated here with the human data set

previously generated in this laboratory, especially since I could verify that the experimental conditions were similar between the two studies.

The comparison between human and turtle fibroblast sensitivity indicates that turtle cells are more resistant by a factor of about 1.7 with respect to the induction of chromosomal interchange aberrations (comparison based on the ratio of doses for the same level of effect). The difference in sensitivity cannot be accounted for by a difference in total genome size because the DNA content per cell is very nearly the same for turtle and human diploid G_1 cells (52,53). The human data were generated by scoring asymmetrical interchanges in giemsa stained metaphase spreads. Assuming that symmetrical and asymmetrical interchanges occur in equal frequency, I estimated the total interchange frequencies in the human fibroblasts by doubling the asymmetrical interchange frequency. A linear-quadratic function of dose provided a significantly better fit (54) than a linear function ($P \geq 0.95$) for the human data. The best-fit curve was $Y = (15.3 \pm 5.45)*D + (0.96 \pm 0.46)*D^2$; $r^2 = 0.97$, $n = 7$, Y = the total interchange frequency (#/100 cells), and D = dose (Gy). The lesser sensitivity of turtle fibroblasts could at least partially explain the linear dose-response seen over the range of doses from 0-10 Gy. Indeed, fitting the human data over the same range of biological effect, rather than the same range of dose, also resulted in a situation where a linear-quadratic function did not significantly improve the fit over a simple linear function.

The data plotted in Figure 3.3 for turtles are whole-genome interchange frequencies (symmetrical plus asymmetrical) projected from complete, apparently simple, chromosome interchange aberration frequencies involving chromosome-1 observed in the first post-irradiation mitosis (Table 1, columns four and six), but other aberrations which

obviously involved three or more break points in a complex interchange were also observed, as were apparently incomplete interchanges (Table 1, columns five and seven). Including these other aberrations will of course increase the sensitivity of the system for detecting chromosomal damage. Increased sensitivity could also be achieved by production of additional chromosome-specific libraries for simultaneous whole-chromosome painting of two or more chromosomes (1). Ultimately, probes for each chromosome with multi-color painting (*e.g.* mFISH (55) or spectral karyotyping (56)) would allow the maximum sensitivity and resolution for assessment of exposure to genotoxic agents in the environment. The results presented in Figure 3.3 demonstrate the feasibility of using symmetrical interchange frequency to determine received dose in *T. scripta*. The doses (and dose-rates) used were relatively high, but are not unreasonably so, considering that this species could receive cumulative doses near 100 Gy over a lifetime of 1-2 decades if exposures occurred at currently proposed dose-rate standards for populations (10 mGy day^{-1} for maximally exposed aquatic organisms, and 1 mGy day^{-1} for maximally exposed terrestrial animals (12)). The sensitivity of this system for detecting effects from low dose, low dose-rate exposures will depend on the total fraction of the genome painted, the number of uniquely colored probes available, the natural background of symmetrical translocations, the persistence of symmetrical translocations, and the number of cells scored.

Direct comparisons of total aberrations in all chromosomes using classical giemsa staining is hampered for turtle cells because it is difficult to distinguish between microchromosomes and interstitial or small terminal deletions. Even though a deletion results in an excess fragment and should be apparent in the chromosome count, there is a

small variation in modal chromosome number in my fibroblasts cultures involving especially microchromosomes, so small deletions are not unequivocally identifiable at present. These can only be resolved unequivocally by the application of centromere- and telomere-specific probes that are not currently available. Genetic deficiencies arising from the loss of acentric fragments is a major cause of cell reproductive death following ionizing radiation exposure (20,57). For risk assessments, however, the focus is on stable aberrations, which have the potential to reflect cumulative exposures. Thus, for assessing the impacts of long-term, low-level exposure over many years or decades, the stable aberrations detected by my molecular whole-chromosome painting probe, such as symmetrical interchanges or complex interchanges that do not produce acentric fragments are of principal concern.

These first steps, the construction of FISH probes for *T. scripta* and the determination of the dose-response curve for acute irradiation, demonstrate the feasibility of extending biodosimetry to ecological receptors. There is evidence that the probes I have developed in *T. scripta* will have broad applicability beyond this particular species of turtle. I have successfully hybridized the chromosome-1 probe to metaphase spreads from 4 other diverse turtle species (to be reported elsewhere). But my ultimate objective is to apply biodosimetric techniques to turtles receiving sustained, relatively low-level exposure from radionuclides in the natural environment. This will require a dose-response calibration curve for irradiation conditions similar to those turtles are experiencing in the field. I am currently conducting experiments to examine the dose-rate effect for interchange aberration induction in this organism, and to determine the dose-response relationship for chronic, rather than acute, exposures. Furthermore, it

would be especially useful to sample lymphocytes, rather than fibroblasts, so that repeated, nonlethal sampling can be conducted. To this end, development of turtle lymphocyte culture and stimulation techniques are also currently under development in this laboratory. Finally, an estimation of background frequencies of symmetrical interchanges in *T. scripta* lymphocytes due to exposure to natural radiation sources and endogenous mutagens will be necessary. This will be especially important for distinguishing effects of natural exposures from effects of low dose and low dose-rate anthropogenic exposures typical of sites contaminated with radionuclides. Experiments consisting of chronic irradiation of previously unexposed turtles, with lymphocyte samples collected both before (to provide an estimate of background) and after irradiation are underway. Additionally, I plan to resample the animals used in these experiments at various time periods after irradiation to determine the temporal stability of radiation-induced symmetrical translocations.

Environmental biodosimetry could revolutionize ecological risk assessment by providing direct, accurate, and precise methods for estimating the dose that organisms have received in the field. For obvious ethical reasons, direct investigations of the effects of chronic, low-level environmental exposures in humans is impossible. Therefore, in addition to being ecologically relevant, biodosimetric investigations could provide valuable insights into the effects of these types of exposures on humans.

Acknowledgements:

This work was supported by the Department of Energy grant RR267-055/4895914 to University of Georgia, Savannah River Ecology Laboratory and subcontract to

Colorado State University, and a grant from the NIH, National Cancer Institute, 5 T32 CA09236 to Colorado State University.

REFERENCES

1. Lucas, J. N., Awa, A., Straume, T., Poggensee, M., Kodama, Y., Nakano, M., Ohtaki, K., Weier, H. U., Pinkel, D., and Gray, J., Rapid translocation frequency analysis in humans decades after exposure to ionizing radiation. *International Journal of Radiation Biology* **62**, 53-63 (1992).

2. Pinkel, D., Landegent, J., Collins, C., Fuscoe, J., Segraves, R., Lucas, J., and Gray, J., Fluorescence in situ hybridization with human chromosome-specific libraries: detection of trisomy 21 and translocations of chromosome 4. *Proceedings of the National Academy of Sciences of the United States of America* **85**, 9138-9142 (1988).

3. Gray, J. W., Lucas, J., Kallioniemi, O., Kallioniemi, A., Kuo, W. L., Straume, T., Tkachuk, D., Tenjin, T., Weier, H. U., and Pinkel, D., Applications of fluorescence in situ hybridization in biological dosimetry and detection of disease-specific chromosome aberrations. *Progress in Clinical & Biological Research* **372**, 399-411 (1991).

4. Gray, J. W., Lucas, J. N., Pinkel, D., and Awa, A., Structural chromosome analysis by whole chromosome painting for assessment of radiation-induced genetic damage. *Journal of Radiation Research* **33 Suppl**, 80-86 (1992).

5. Lucas, J. N., Chromosome translocations: a biomarker for retrospective biodosimetry. *Environmental Health Perspectives* **105 Suppl 6**, 1433-1436 (1997).

6. Straume, T., Anspaugh, L. R., Haskell, E. H., Lucas, J. N., Marchetti, A. A., Likhtarev, Chumak, V. V., Romanyukha, A. A., Khrouch, V. T., Gavrilin, Yul, and Minenko, V. F., Emerging technological bases for retrospective dosimetry. *Stem Cells* **15 Suppl 2**, 183-193 (1997).

7. Lucas, J. N., Dose reconstruction for individuals exposed to ionizing radiation using chromosome painting. *Radiation Research* **148**, S33-S38 (1997).

8. Boei, J. J., Balajee, A. S., de Boer, P., Rens, W., Aten, J. A., Mullenders, L. H., and Natarajan, A. T., Construction of mouse chromosome-specific DNA libraries and their use for the detection of X-ray-induced aberrations. *International Journal of Radiation Biology* **65**, 583-590 (1994).

9. Hande, M. P., Boei, J. J., Granath, F., and Natarajan, A. T., Induction and persistence of cytogenetic damage in mouse splenocytes following whole-body X-irradiation analysed by fluorescence in situ hybridization. I. Dicentrics and translocations. *International Journal of Radiation Biology* **69**, 437-446 (1996).

10. Spruill, M. D., Ramsey, M. J., Swiger, R. R., Nath, J., and Tucker, J. D., The persistence of aberrations in mice induced by gamma radiation as measured by chromosome painting. *Mutation Research* **356**, 135-145 (1996).

11. Tucker, J. D., Sorensen, K. J., Chu, C. S., Nelson, D. O., Ramsey, M. J., Urlando, C., and Heddle, J. A., The accumulation of chromosome aberrations and Dlb-1 mutations in mice with highly fractionated exposure to gamma radiation. *Mutation Research* **400**, 321-335 (1998).

12. International Atomic Energy Agency, *Effects of Ionizing Radiation on Plants and Animals at Levels Implied by Current Radiation Protection Standards*. Technical reports series, 332, International Atomic Energy Agency, Vienna, (1992).

13. Bender, M. A. and Gooch, P. C., Types and rates of X-ray-induced chromosome aberrations in human blood irradiated *in vitro*. *Proceedings of the National Academy of Sciences of the United States of America* **48**, 522-532 (1962).

14. Frazer, N. B., Gibbons, J. W., and Greene, J. L., Life tables of a slider turtle population, In *Life History and Ecology of the Slider Turtle* (Gibbons, J. W., Eds.), pp. 183-200. Smithsonian Institution Press, Washington, D.C., (1990).

15. Ernst, C. H., Systematics, taxonomy, variation, and geographic distribution of the slider turtle, In *Life History and Ecology of the Slider Turtle* (Gibbons, J. W., Eds.), pp. 57-67. Smithsonian Institution Press, Washington, D.C., (1990).

16. Meyers-Schone, L., Shugart, L. R., Beauchamp, J. L, and Walton, B. T., Comparison of two freshwater turtle species as monitors of radionuclide and chemical contamination: DNA damage and residue analysis. *Environmental Toxicology and Chemistry* **12**, 1487-1496 (1993).

17. Obst, F. J., *Turtles, Tortoises and Terrapins*. Druckerei Fortschritt Erfurt, Leipzig, (1986).

18. Pough, F. Harvey, Andrews, Robin M., Cadle, John E., Crump, Martha L., Savitzky, Alan H, and Wells, Kentwood D., *Herpetology*. Prentice Hall, Upper Saddle River, NJ, (1998).

19. Spotila, J. R., Foley, R. E., and Standora, E. A., Thermoregulation and climate space of the slider turtle, In *Life History and Ecology of the Slider Turtle* (Gibbons, J. W., Eds.), pp. 288-298. Smithsonian Institution Press, Washington, D.C., (1990).

20. Cornforth, M. N. and Bedford, J. S., A quantitative comparison of potentially lethal damage repair and the rejoining of interphase chromosome breaks in low passage normal human fibroblasts. *Radiation Research* **111**, 385-405 (1987).

21. Darroudi, F., Fomina, J., Meijers, M., and Natarajan, A. T., Kinetics of the formation of chromosome aberrations in X-irradiated human lymphocytes, using PCC and FISH. *Mutation Research* **404**, 55-65 (1998).

22. Bussey, K. J., Chromosome microdissection: on the cutting edge. *Applied Cytogenetics* **22**, 30-36 (1996).

23. Guan, X. Y., Trent, J. M., and Meltzer, P. S., Generation of band-specific painting probes from a single microdissected chromosome. *Human Molecular Genetics* **2**, 1117-1121 (1993).

24. Muhlmann-Diaz, M., Christian, A. T., and Bedford, J. S., Chromosome microdissection, In *Radiation Research 1895-1995 Congress Proceedings* (Hagen, U., Harder, D., Jung, H., and Streffer, C., Eds.), pp. 468-469. International Congress of Radiation Research, Wurzburg,Germany, (1995).

25. Pinkel, D., Straume, T., and Gray, J. W., Cytogenetic analysis using quantitative, high-sensitivity, fluorescence hybridization. *Proceedings of the National Academy of Sciences of the United States of America* **83**, 2934-2938 (1986).

26. Lichter, P., Cremer, T., Borden, J., Manuelidis, L., and Ward, D. C., Delineation of individual human chromosomes in metaphase and interphase cells by in situ suppression hybridization using recombinant DNA libraries. *Human Genetics* **80**, 224-234 (1988).

27. Savage, J. R. and Simpson, P. J., FISH "painting" patterns resulting from complex exchanges. *Mutation Research* **312**, 51-60 (1994).

28. Tucker, J. D., Morgan, W. F., Awa, A. A., Bauchinger, M., Blakey, D., Cornforth, M. N., Littlefield, L. G., Natarajan, A. T., and Shasserre, C., A proposed system for scoring structural aberrations detected by chromosome painting. *Cytogenetics & Cell Genetics* **68**, 211-221 (1995).

29. International Commission on Radiological Protection, *Recommendations of the International Commission on Radiological Protection. Publication 60.* Publication 60, Pergammon Press, Oxford and New York, (1991).

30. Whicker, F. W. and Bedford, J. S., Environmental impact of radioactive releases. In *Proceedings of an International Symposium on Environmental Impact of Radioactive Releases* pp. 561-567. International Atomic Energy Agency, Vienna, (1995).

31. Lindholm, C., Tekkel, M., Veidebaum, T., Ilus, T., and Salomaa, S., Persistence of translocations after accidental exposure to ionizing radiation. *International Journal of Radiation Biology* **74**, 565-571 (1998).

32. Lucas, J. N., Hill, F. S., Burk, C. E., Cox, A. B., and Straume, T., Stability of the translocation frequency following whole-body irradiation measured in rhesus monkeys. *International Journal of Radiation Biology* **70**, 309-318 (1996).

33. Bauchinger, M., Quantification of low-level radiation exposure by conventional chromosome aberration analysis. *Mutation Research* **339**, 177-189 (1995).

34. Buckton, K. E., Chromosome aberrations in patients treated with X-irradiation for ankylosing spondylitis, In *Radiation-Induced Chromosome Damage in Man* (Ishihara, T. and Sasaki, M. S., Eds.), pp. 491-511. Alan R. Liss, Inc., New York, (1983).

35. Bauchinger, M., Schmid, E., and Braselmann, H., Cell survival and radiation induced chromosome aberrations. II. Experimental findings in human lymphocytes analysed in first and second post-irradiation metaphases. *Radiation & Environmental Biophysics* **25**, 253-260 (1986).

36. Matsumoto, K., Ramsey, M. J., Nelson, D. O., and Tucker, J. D., Persistence of radiation-induced translocations in human peripheral blood determined by chromosome painting. *Radiation Research* **149**, 602-613 (1998).

37. Tucker, J. D., Breneman, J. W., Briner, J. F., Eveleth, G. G., Langlois, and Moore, D. H., Persistence of radiation-induced translocations in rat peripheral blood determined by chromosome painting. *Environmental & Molecular Mutagenesis* **30**, 264-272 (1997).

38. Bahari, I. B., Bedford, J. S., Giaccia, A. J., and Stamato, T. D., Measurement of the relative proportion of symmetrical and asymmetrical chromosome-type interchanges induced by gamma radiation in human-hamster hybrid cells. *Radiation Research* **123**, 105-107 (1990).

39. Boei, J. J. and Natarajan, A. T., Combined use of chromosome painting and telomere detection to analyse radiation-induced chromosomal aberrations in mouse splenocytes. *International Journal of Radiation Biology* **73**, 125-133 (1998).

40. Fernandez, J. L., Campos, A., Goyanes, V., Losada, C., Veiras, C., and Edwards, A. A., X-ray biological dosimetry performed by selective painting of human chromosomes 1 and 2. *International Journal of Radiation Biology* **67**, 295-302 (1995).

41. Finnon, P., Lloyd, D. C., and Edwards, A. A., Fluorescence in situ hybridization detection of chromosomal aberrations in human lymphocytes: applicability to biological dosimetry. *International Journal of Radiation Biology* **68**, 429-435 (1995).

42. Kanda, R. and Hayata, I., Comparison of the yields of translocations and dicentrics measured using conventional Giemsa staining and chromosome painting. *International Journal of Radiation Biology* **69**, 701-705 (1996).

43. Lindholm, C., Luomahaara, S., Koivistoinen, A., Ilus, T., Edwards, A. A., and Salomaa, S., Comparison of dose-response curves for chromosomal aberrations established by chromosome painting and conventional analysis. *International Journal of Radiation Biology* **74**, 27-34 (1998).

44. Lucas, J. N., Chen, A. M., and Sachs, R. K., Theoretical predictions on the equality of radiation-produced dicentrics and translocations detected by chromosome painting. *International Journal of Radiation Biology* **69**, 145-153 (1996).

45. Straume, T. and Lucas, J. N., A comparison of the yields of translocations and dicentrics measured using fluorescence in situ hybridization. *International Journal of Radiation Biology* **64**, 185-187 (1993).

46. Barquinero, J. F., Knehr, S., Braselmann, H., Figel, M., and Bauchinger, M., DNA-proportional distribution of radiation-induced chromosome aberrations analysed by fluorescence in situ hybridization painting of all chromosomes of a human female karyotype. *International Journal of Radiation Biology* **74**, 315-323 (1998).

47. Bauchinger, M., Schmid, E., Zitzelsberger, H., Braselmann, H., and Nahrstedt, U., Radiation-induced chromosome aberrations analysed by two-colour fluorescence in situ hybridization with composite whole chromosome-specific DNA probes and a pancentromeric DNA probe. *International Journal of Radiation Biology* **64**, 179-184 (1993).

48. Knehr, S., Zitzelsberger, H., Braselmann, H., Nahrstedt, U., and Bauchinger, M., Chromosome analysis by fluorescence in situ hybridization: further indications for a non-DNA-proportional involvement of single chromosomes in radiation-induced structural aberrations. *International Journal of Radiation Biology* **70**, 385-392 (1996).

49. Knehr, S., Huber, R., Braselmann, H., Schraube, H., and Bauchinger, M., Multicolour FISH painting for the analysis of chromosomal aberrations induced by 220 kV X-rays and fission neutrons. *International Journal of Radiation Biology* **75**, 407-418 (1999).

50. Dominguez, I., Boei, J. J., Balajee, A. S., and Natarajan, A. T., Analysis of radiation-induced chromosome aberrations in Chinese hamster cells by FISH using chromosome-specific DNA libraries. *International Journal of Radiation Biology* **70**, 199-208 (1996).

51. Virsik-Peuckert, P., Rave-Frank, M., Langebrake, U., and Schmidberger, H., Differences in the yields of dicentrics and reciprocal translocations observed in the chromosomes of irradiated human skin fibroblasts and blood lymphocytes from the same healthy individuals. *Radiation Research* **148**, 209-215 (1997).

52. Menton, M. L., Willms, M., and Wright, W. D, Nucleic acid content of splenic lymphocytes in normal and leukemic mice. *Cancer Research* **13**, 729-732 (1953).

53. Mirsky, A. E. and Ris, H., Variable and constant components of chromosomes. *Nature* **163**, 666-667 (1949).

54. Snedecor, G. W., *Statistical Methods*. The Iowa State University Press, Ames, IA, (1956).

55. Speicher, M. R., Gwyn, Ballard S., and Ward, D. C., Karyotyping human chromosomes by combinatorial multi-fluor FISH. *Nature Genetics* **12**, 368-375 (1996).

56. Schrock, E., du, Manoir S., Veldman, T., Schoell, B., Wienberg, J., Ferguson, Smith, Ning, Y., Ledbetter, D. H., Bar-Am, I., Soenksen, D., Garini, Y., and Ried, T., Multicolor spectral karyotyping of human chromosomes. *Science* **273**, 494-497 (1996).

57. Revell, S. H., Relationships between chromosome damage and cell death, In *Radiation-Induced Chromosome Damage in Man* (Ishihara, T. and Sasaki, M. S., Eds.), pp. 215-233. Alan R. Liss, Inc., New York. (1983).

Chapter 4

Culture Methods for Turtle Lymphocytes

Abstract:

Culture techniques for turtle and other reptilian lymphocytes are not well established. Optimization of lymphocyte culture techniques is essential for facilitating cytogenetic and immunologic research for these animals. I have examined a variety of conditions and parameters relevant to turtle lymphocyte culture including: different mitogenic agents, alone and in combination; lymphocyte separation protocols; culture volume; time required to stimulate lymphocytes to mitosis; importance of humidity and gas exchange in culture incubation; suitability of different culture media; effects of varying serum concentrations; ability of interleukin-2 (IL-2) to stimulate lymphocyte growth and prevent apoptosis; and feasibility of inducing premature chromosome condensation. The best conditions and parameters of those I studied for obtaining mitotic cells were (1) the combined use of phytohemagglutinin-M form (2%) and lipopolysaccharides (0.55 $\mu g\ ml^{-1}$), (2) the use of 5% autologous turtle serum (as opposed to fetal bovine serum), and (3) collection of mitotic cells around 96 hours after mitogenic stimulation. Human, recombinant IL-2 did not increase the fraction of lymphocytes in mitosis over the range of concentrations tested and calyculin A was not effective at inducing premature chromosome condensation in turtle lymphocytes over the range of concentrations tested.

Introduction:

The expanding field of comparative cytogenetics requires adequate techniques for lymphocyte culture to prepare chromosome spreads, at least for vertebrates. Further, turtles have been utilized as sentinel species in chemical and radionuclide uptake studies

(1,2). While it is often useful to know contaminant levels in the tissues of organisms, a more complete picture is gained by an examination of biologically relevant effects, such as chromosome damage, caused by contaminant exposures (3). There have been several cytogenetic studies involving turtles to establish karyotypes including the early studies of standard, non-banded karyotypes (4-12) as well as other studies of banded karyotypes (13-18). Most of these early studies obtained mitotic cells from cultured spleen, heart, or kidney tissue. Collection of these tissues is obviously not conducive to repeated sampling. Furthermore, routine sampling from such tissues would be totally unsuitable, especially for species which are either threatened or endangered (such as most Chelonioid species) since sacrifice of the animals is required.

I am involved in research to examine the induction of chromosome aberrations in turtles by chronic, low-level exposure to radioactivity. The research requires that samples be repeatedly collected from exposed animals, therefore nonlethal sampling techniques are necessary. Furthermore, it is necessary to stimulate cells into the cell cycle, and to harvest them in mitosis for assessment of aberration induction. Finally, in contrast to karyotyping where only a few mitotic cells are necessary, large numbers of mitotic cells are required, since induced frequencies of aberrations per cell are relatively low. Sampling lymphocytes is an obvious way to satisfy these requirements, which is my motivation for optimizing turtle lymphocyte culture techniques.

The results of these experiments would also be of interest to researchers in comparative and veterinary immunology. Lymphocytes mediate immune response, and they are therefore used in immunologic assays. The inclusion of turtles in immunologic studies could provide a valuable perspective on the response of these animals to

xenobiotic exposures, as impairment of the immune system is frequently a component of the stress response elicited by such exposures (19).

Blood culture techniques for humans and other mammals are well established, but these techniques may not be optimal for reptilian lymphocytes. One major difference between reptiles and mammals is that reptiles have nucleated erythrocytes. Other physiological differences could also lead to variations in optimum blood culture conditions between reptiles and mammals. Some studies in this regard have been conducted using Florida alligators (*Alligator mississippiensis*), and it does appear that like mammals, reptiles, or at least alligators, have T- and B-lymphocytes (20) which are responsive to mitogenic stimulation (21).

Peripheral blood lymphocytes are normally in the G_0, or resting phase of the cell cycle. Therefore, performance of some immunologic and all cytogenetic assays requires culture techniques which provide not only for the viability of lymphocytes, but for stimulation into the cell cycle. This is usually accomplished using mitogens, but even among mammals, the effectiveness of different mitogens varies across species. The effectiveness of the various mitogens in stimulating turtle lymphocytes remains largely untested.

In the interest of facilitating the inclusion of reptiles in general, and turtles in particular, in immunologic and cytogenetic studies, work was undertaken to determine suitable conditions for the culture and stimulation of turtle lymphocytes. I examined several important variables including: protocols for separating lymphocytes from whole blood; the effectiveness of the most common mitogens; the efficacy of different culture

media; the lymphocyte cycle time (time to reach first post-stimulation mitosis); and the feasibility of utilizing premature chromosome condensation to address cytogenetic issues.

Materials and methods:

General methods:

All animals included in this study were adult yellow-bellied slider turtles (*Trachemys scripta*). They were captured with hoop traps from a farm pond near the Savannah River Site in Aiken, South Carolina between July 17 and July 22, 1998. No radioactive or chemical contamination is known to exist in this pond. The animals were then transported to Colorado State University where they were maintained in a temperature-controlled greenhouse with natural lighting. Animal care procedures followed in this study are in accordance with Colorado State University Animal Care and Use Committee guidelines.

Blood samples were collected from the dorsal coccygeal vein in the turtles' tails. The methods followed were essentially as described by Haskell and Pokras (22), with a few variations. I fabricated a device to immobilize the turtle's tail with an elastic cord in a straight, and fully extended position. Use of this device allowed me to have both hands free, and it prevented movement of the tail during blood collection. To ensure sterility of the sample, the tail was washed with betadine, followed by a wash with ethanol. This wash procedure was repeated twice more, and the last application of betadine was allowed to contact the turtle's skin for five minutes before application of the last ethanol wash. The bacterial contamination that I found to be very frequent in cultures before I instituted this wash protocol was greatly reduced with this procedure. I also noted that it

was much easier to collect blood samples during the warmest part of the day (approximately 11:00 AM –1:00 PM) as opposed to the early morning. This was most likely due to more rapid circulation when temperatures were warmer. One to three ml of blood was collected using a five ml syringe containing a few drops of sodium heparin and equipped with a 25 gauge, 5/8 inch needle. Additional sodium heparin was added to the cultures (approximately 10 units ml^{-1} whole blood) to prevent clotting, as the few drops in the syringe prevented immediate clotting, but did not always prevent clotting over the several days the samples were cultured. Samples were always processed immediately following collection.

I set up all cultures in 15 ml conical centrifuge tubes tilted at a 45° angle to facilitate gas exchange. Previous work with human lymphocytes concluded that cells entered the cell cycle much more readily if they were concentrated in a relatively small volume of culture medium, as occurs when cells settle to the bottom of centrifuge tubes, rather than diluted in flasks or petri dishes with high surface areas (23). Furthermore, I observed that turtle lymphocytes attach to and stretch out on the surfaces of polystyrene culture vessels which have a tissue culture coating. This contrasts with mammalian lymphocytes, which do not attach. A fraction of turtle lymphocytes even attached to uncoated polystyrene dishes. Therefore I used centrifuge tubes, which had smaller surface areas per unit volume.

Culture conditions included incubation at 29°C, the preferred body temperature of *T. scripta* (24) in a 5% CO_2 environment. Cellgro complete, serum free (CSF) culture medium (Mediatech, Herndon, Virginia) was added to the blood sample in a ratio of 5:1 (medium volume:blood volume), unless otherwise noted. Gentamycin (Gibco BRL,

Grand Island, Illinois, final concentration 25 μg ml^{-1}) and fungizone (Gibco BRL, final concentration 0.5 μg ml^{-1}) were added to the cultures to impede the growth of bacterial or fungal contamination. Other culture conditions were varied in the following experiments, as described.

At the end of the incubation period, colcemide (Gibco BRL, final concentration of 0.15 μg ml^{-1}) was applied to block cells in mitosis prior to fixation. The duration of this colcemide block was six hours for the small culture volume experiments, and 12 hours for all other experiments.

The fixation procedure consisted of the following standardized protocol: 1) cell cultures were centrifuged; 2) the supernatant was discarded, and the cell pellet was resuspended in 800 μl 0.075 M KCl and incubated for 15 minutes at 37°C; 3) 200 μl fixative (3:1 methanol/glacial acetic acid) was added to the hypotonic solution and mixed; 4) cells were centrifuged, the supernatant was discarded, and cells in the pellet were dispersed by agitation; 5) one ml of fixative was added dropwise to the cells while they were agitated to prevent clumping; 6) cells were then centrifuged and carried through two additional fixation steps. Fixed cells were dropped onto clean, cold, wet glass slides.

The number of post-stimulation mitoses undergone by cells was determined by the use of differential chromatid staining, essentially as described by Benn and Perle (25). Briefly, bromodeoxyuridine (BrdU) was added to the cultures at a concentration of 10^{-4} M at the start of the incubation period. Following fixation and slide preparation, cells were stained with Hoechst 33258 (0.5 μg ml^{-1}) for 10 minutes at room temperature. The slides were rinsed briefly in phosphate buffered saline (PBS) then in distilled water, and

mounted in MacIlvaine's buffer (pH 7.5). They were then placed on wet paper towels and exposed to a black light (40 W m^{-2}) for 30 minutes. Finally, the slides were rinsed in distilled water, incubated in 2x SSC at 65°C for 15 minutes and stained for approximately seven minutes in 10% giemsa. With this procedure, cells which had completed one round of DNA synthesis in the presence of BrdU and entered the first post-stimulation mitosis showed two identically stained chromatids for each chromosome. Cells which completed two rounds of DNA synthesis showed "harlequin" stained chromosomes i.e., one chromatid was stained much more lightly (26).

Time period from stimulation to the first mitosis:

Experiments referred to below as Experiments MP1 and MP2 were designed to determine the time required from stimulation into the cell cycle until the first wave of mitotic cells in the population, i.e., the time of the first peak in mitotic index (mitotic peak, or MP).

In experiment MP1, a 2.5 ml blood sample was collected and aliquotted into cultures consisting of 0.5 ml whole blood plus 2.5 ml CSF medium. Cultures were stimulated with phytohemagglutinin-M form (PHA) (Gibco BRL, final concentration of 2%) and lipopolysaccharides (LPS) (Sigma, St. Louis, Missouri, final concentration of 55 $\mu g\ ml^{-1}$). The first colcemide block began at 48 hours after the addition of mitogens to the cell cultures, and lymphocyte separation and fixation was performed 12 hours later, followed by slide preparation and giemsa staining. Cell collection was continued over four 12 hour periods spanning 48-96 hours post-stimulation. One thousand cells were scored to determine the mitotic index from each treatment.

In experiment MP2, I repeated this experiment with the first collection period beginning at 72 hours post-stimulation, and the last period ending at 132 hours. Blood from the same turtle was used for both experiments. Following fixation and giemsa staining, cells were scored until either 2500 cells had been counted, or 25 mitotic cells had been observed and the mitotic index was determined (MI = number of mitotic cells / number of mitotic plus interphase cells).

Comparison of separated lymphocytes (SL) vs. whole blood cultures:

Lymphoprep ficoll (Nycomed Pharma, Oslo, Norway) with a density of 1.077 ± 0.001 g ml^{-1} was used for all lymphocyte separations. A volume of ficoll equal to the blood volume to be separated was added to a centrifuge tube, and the blood was carefully layered on top of the ficoll. The sample plus ficoll was then centrifuged at 200 g for 20 minutes at room temperature. Following centrifugation, the blood had separated into a layer of erythrocytes at the bottom of the tube with the ficoll layered on top of the erythrocytes. A thin buffy layer of putative lymphocytes collected at the interface between the ficoll and the overlying plasma. Cells in the buffy layer were collected, fixed, dropped onto microscope slides, and stained with Wright's stain. Lymphocyte identity was then verified by cell morphology.

In the experiment subsequently referred to as SL, a 2.5 ml blood sample was collected from one turtle, and 0.5 ml of whole blood was cultured with approximately 2.5 ml of CSF medium. Lymphocytes from another 0.5 ml of whole blood were separated and following centrifugation, the lymphocytes in the buffy layer, as well as the plasma fraction (the majority of which consists of serum) were collected. The combined volume

of this material was approximately 0.2-0.3 ml, and this was cultured with approximately 2.7 ml of CSF medium, as was used with the whole blood. The plasma fraction made up slightly more than half the volume of whole blood, and cultures were established so that the plasma made up approximately 10% of the total culture volume. So, for example, if 0.5 ml of whole blood, containing approximately 0.2-0.3 ml of plasma, was used in a treatment, the culture volume was adjusted to 3.0 ml by the addition of culture medium. Therefore, both cultures, one containing whole blood and the other containing isolated lymphocytes plus plasma, contained approximately the same concentration of turtle plasma.

The two cultures were stimulated with PHA (2%) and LPS (0.55 $\mu g\ ml^{-1}$) and incubated for 72 hours, at which time colcemide was added. Lymphocytes were isolated from the whole blood culture using two ficoll separations twelve hours later and both cultures were fixed. Slides were prepared and stained with 10% giemsa for seven minutes. One thousand cells were then scored and the mitotic index was determined.

Comparison of cultures with large or small volumes:

In the experiment subsequently referred to as SV1 (small volume), three small-volume cultures (1.0, 0.5, and 0.25 ml) were established with separated lymphocytes. Turtle plasma concentrations in all cultures were kept constant at 10%, and PHA (2%) and LPS (0.55 $\mu g\ ml^{-1}$) were used to stimulate the cultures. Culture incubation and fixation was identical to that followed in experiment SL. One thousand cells were scored from each treatment.

Three 1 ml whole-blood cultures were used in experiment SV2, and subjected to three different incubation environments: 1) a culture was maintained in a sealed centrifuge tube in a dry incubator; 2) a culture was maintained in the same dry incubator environment, but the centrifuge cap was loosened to allow gas exchange (and evaporation); 3) a culture was maintained in a humid environment with a loosened cap. The humid environment was created by incubating the culture inside a plastic container with a few centimeters of water in the bottom. After allowing the air in the container to equilibrate with the 5% CO_2 atmosphere in the incubator, the container was sealed to raise the humidity. Cells were harvested over a 6 hour collection period, from 93-99 hours post stimulation. At the end of the incubation period, the cultures were centrifuged at 200 g for 5 minutes, and the cell pellet was resuspended in a small volume (approximately 0.5 ml) of culture media. This suspension was then layered on top of approximately 0.5 ml of ficoll in a 1 ml glass centrifuge tube, and centrifuged at 200 g for 20 minutes at room temperature. Cells from the buffy layer were then collected, fixed, and stained with a solution of antifade containing 4,6-diamidino-2-phenylindole (DAPI). Cells were then scored for mitotics until 25 mitotics had been observed.

Comparison of different mitogenic agents:

In this experiment, subsequently referred to as experiment M (mitogens), PHA, LPS, pokeweed mitogen, and concanavalin A were used in a titration series to stimulate lymphocytes in 1 ml whole blood cultures. Combinations or mixtures were also tested. A 1.8 ml blood sample was collected from a single turtle, and this sample was aliquotted (0.2 ml each) into nine 1 ml cultures which were shared between experiments M and

MED. All cultures were established so that turtle plasma concentration was 10%. Cells in this experiment, were cultured in CSF medium. All combinations of 0.5, 1.0, and 2.0 times the manufacturer-recommended concentration of PHA (2%) and the optimal LPS concentration for stimulation of alligator lymphocytes (55 μg ml^{-1}) (21) were tested (there was no manufacturer recommendation for LPS concentration). The manufacturer-recommended-concentration of pokeweed mitogen (1%) plus LPS, and the recommended concentration of concanavalin A (9 μg ml^{-1}) plus LPS was also tested. Cultures were maintained in a humid environment for 90 hours, at which time colcemide was added. The collection period for all cultures was 12 hours, followed by lymphocyte separation in 1 ml glass centrifuge tubes, fixation, slide preparation, DAPI staining and cell scoring. Cells were scored until 25 mitotic cells or 2500 total cells were counted.

Experiment MED – cell culture media:

Aliquots of blood from the same sample used in experiment M (above) were used for experiment MED. Two cultures containing αMEM (minimum essential medium) cell culture medium and stimulated with PHA (2%) and LPS (55 μg ml^{-1}) were used in this experiment. One culture contained 10% fetal bovine serum (FBS) and the other contained 20% FBS. With the exception of the culture media, conditions were identical between experiments M and MED and these two experiments were run concurrently, so that the mitotic index values from the treatments in this experiment could be directly compared with that from the culture using the same mitogen concentrations in experiment M.

Comparison of turtle vs. fetal bovine sera:

For comparison of lymphocyte cultures with autologous turtle serum vs. FBS, subsequently referred to as experiment TS (turtle serum), a 2.0 ml blood sample was collected from a single turtle, and aliquotted into twelve 1 ml cultures (with CSF medium) which were shared between experiment TS, and the experiments described below as IL-2, and C, which compare the effects of added interleukin-2 and calyculin A. All these experiments were run concurrently. All cultures were stimulated with PHA (2%) and LPS (55 $\mu g\ ml^{-1}$) and were incubated in a humid environment for 90 hours, followed by a 12 hour collection period with colcemide, lymphocyte separation, cell fixation, slide preparation and cell scoring. Cells were scored until 25 mitotic cells or 2500 total cells had been counted.

Three cultures were used in experiment TS for specific comparison of autologous turtle serum with FBS. Whole blood volumes were varied across treatments to give different concentrations of turtle plasma. A 5% turtle plasma culture was established by the addition of 83 µl whole blood to 917 µl CSF medium. A 10% plasma culture contained 167 µl whole blood and 833 µl medium, and a 20% plasma culture contained 334 µl blood and 667 µl medium.

I also tested the possible efficacy of adding interleukin-2 (IL-2) to the cultures. All cultures and conditions used in this experiment were identical to the 10% turtle plasma culture (experiment TS), but with the addition of human, recombinant IL-2 (Sigma, St. Louis, Missouri). Three cultures were used in this experiment containing 0.175, 0.35, or 0.70 ng ml^{-1} of IL-2 (1 ng = 2.4 U). These concentrations represent 0.5, 1.0, and 2.0 times the manufacturer-specified EC_{50}, defined as the effective concentration

of growth factor that elicits a 50% increase in cell growth in a cell-based bioassay. Slides were stained with DAPI, and 2500 cells from each treatment were scored.

Finally, to test the possible use of calyculin A to induce premature chromosome condensation in cycling cells, I set up another series of cultures along with the turtle serum and IL-2 series, but to this series I added calyculin A (Sigma, stock concentration =10 $\mu g\ ml^{-1}$ in ethanol). Three cultures were used in this experiment. Calyculin A was added to these cultures (50, 100, or 200 nM) 1 hour prior to cell fixation. Cultures were then kept in a 37°C waterbath until fixation. Lymphocyte separation, cell fixation, slide preparation and staining were as described for experiment TS. Slides were stained with DAPI, and 2500 cells from each treatment were scored.

Results and discussion:

The results of all the experiments for all the conditions tested are summarized in Table 4.1. The calculated uncertainties for MI values are one standard deviation due to counting statistics for a Poisson distribution. The experiments which were run concurrently and which used aliquots from a common blood sample are boxed together in Table 4.1. Results from identical treatments between separate experiments were sometimes quite variable, even when blood samples from the same animal were used (for example, treatment M-2 from experiment M and the 10% turtle serum treatment from experiment TS). Therefore, the results of culture conditions or parameters were compared only within a given experiment.

Table 4.1: Comparison of *T. scripta* lymphocyte mitotic indices for varying culture conditions.

Treatment/ Condition[a]	N	I	M	MI (%)	V (ml)	Mitogen[b] (concentration)	Collection (hours)	Medium[c]
Experiment MP1 – mitotic peak								
MP1-1	1000	1000	0	0.00±0.00	3	PHA (2%), LPS (0.55 μg ml^{-1})	48-60	CSF
MP1-2	1000	995	5	0.50±0.22	3	PHA (2%), LPS (0.55 μg ml^{-1})	60-72	CSF
MP1-3	1000	996	4	0.40±0.20	3	PHA (2%), LPS (0.55 μg ml^{-1})	72-84	CSF
MP1-4	1000	980	20	2.0±0.45	3	PHA (2%), LPS (0.55 μg ml^{-1})	84-96	CSF
Experiment SL – separated lymphocytes								
Sep. lymphocytes	1000	994	6	0.60±0.24	3	PHA (2%), LPS (0.55 μg ml^{-1})	72-84	CSF
Experiment MP2 – mitotic peak								
MP2-1	2500	2487	13	0.52±0.14	3	PHA (2%), LPS (0.55 μg ml^{-1})	72-84	CSF
MP2-2	1862	1837	25	1.3±0.27	3	PHA (2%), LPS (0.55 μg ml^{-1})	84-96	CSF
MP2-3	1668	1642	26	1.6±0.31	3	PHA (2%), LPS (0.55 μg ml^{-1})	96-108	CSF
MP2-4	2500	2493	7	0.28±0.11	3	PHA (2%), LPS (0.55 μg ml^{-1})	108-120	CSF
MP2-5	2500	2495	5	0.20±0.09	3	PHA (2%), LPS (0.55 μg ml^{-1})	120-132	CSF
Experiment SV2 – small volume cultures								
SV2-1	5362	5337	25	0.47±0.09	1	PHA (2%), LPS (0.55 μg ml^{-1})	93-99	CSF
SV2-2	7413	7388	25	0.33±0.07	1	PHA (2%), LPS (0.55 μg ml^{-1})	93-99	CSF
SV2-3	8907	8882	25	0.28±0.06	1	PHA (2%), LPS (0.55 μg ml^{-1})	93-99	CSF
Experiment M – mitogens								
M-1	2500	2494	6	0.24±0.10	1	PHA (0.5%), LPS (0.55 μg ml^{-1})	90-102	CSF
M-2	2500	2478	22	0.88±0.19	1	PHA (2%), LPS (0.55 μg ml^{-1})	90-102	CSF
M-3	2500	2486	14	0.56±0.15	1	PHA (4%), LPS (0.55 μg ml^{-1})	90-102	CSF
M-4	2500	2497	3	0.12±0.07	1	PHA (2%), LPS (0.275 μg ml^{-1})	90-102	CSF
M-5	2500	2490	10	0.40±0.13	1	PHA (2%), LPS (1.1 μg ml^{-1})	90-102	CSF
M-6	2500	2500	0	0.00±0.00	1	PWM (1%), LPS (0.55 μg ml^{-1})	90-102	CSF
M-7	2500	2484	16	0.64±0.16	1	ConA (9 μg ml^{-1}), LPS (0.55 μg ml^{-1})	90-102	CSF

Experiment MED – culture media								
MD-1	2500	2492	8	0.32±0.11	1	PHA (2%), LPS (0.55 μg ml^{-1})	90-102	αMEM
MD-2	2500	2485	15	0.60±0.15	1	PHA (2%), LPS (0.55 μg ml^{-1})	90-102	αMEM
Experiment TS – turtle serum								
5% turtle serum	2500	2485	15	0.60±0.15	1	PHA (2%), LPS (0.55 μg ml^{-1})	90-102	CSF
10% turtle serum	2500	2492	8	0.32±0.11	1	PHA (2%), LPS (0.55 μg ml^{-1})	90-102	CSF
20% turtle serum	2500	2491	9	0.36±0.12	1	PHA (2%), LPS (0.55 μg ml^{-1})	90-102	CSF
Experiment IL2 – interleukin 2								
IL2 (0.175 ng ml^{-1})	2500	2495	5	0.20±0.09	1	PHA (2%), LPS (0.55 μg ml^{-1})	90-102	CSF
IL2 (0.35 ng ml^{-1})	2500	2492	8	0.32±0.11	1	PHA (2%), LPS (0.55 μg ml^{-1})	90-102	CSF
IL2 (0.70 ng ml^{-1})	2500	2497	3	0.12±0.07	1	PHA (2%), LPS (0.55 μg ml^{-1})	90-102	CSF
Experiment C – calyculin A								
Calyculin A (50 nM)	2500	2500	0	0.00±0.00	1	PHA (2%), LPS (0.55 μg ml^{-1})	90-102	CSF
Calyculin A (100 nM)	2500	2499	1	0.04±0.04	1	PHA (2%), LPS (0.55 μg ml^{-1})	90-102	CSF
Calyculin A (200 nM)	2500	2500	0	0.00±0.00	1	PHA (2%), LPS (0.55 μg ml^{-1})	90-102	CSF

N=total number of cells scored; I=number of interphase cells scored; M=number of mitotic cells scored; MI=mitotic index; V=culture volume.

Boxed sections indicate experiments conducted concurrently with aliquots from a common blood sample.

a: SV-1=sealed culture, no gas exchange; SV-2=dry environment, gas exchange; SV-3=humid environment, gas exchange
Differences between treatments in experiments MP1, MP2, M and MD are listed in table; IL2=interleukin-2

b: PHA=phytohemagglutinin; LPS=lipopolysaccharides; PWM=pokeweed mitogen; ConA=concanavalin A

c: CSF=complete, serum free medium; MEM=minimum essential medium

Time for the first post-stimulation mitosis:

The results of experiments MP1 and MP2 to determine the optimal period over which to apply colcemide to obtain the maximum number of first division mitotic cells are summarized in Figure 4.1. The first collection interval began at 48 hours after the addition of mitogens to the cultures. This time period was selected as a first estimate because the first peak in the mitotic index occurs at 48 hours in humans. No mitotic cells were observed (MI = 0) in the first collection period, 48-60 hours. A few mitotic cells began to appear in the 60-72 hour collection period (MI = 0.50±0.22%), held relatively constant (MI = 0.40±0.20%) through the 72-84 hour collection period, and increased dramatically in the 84-96 hour collection period to a high of 2.0±0.45%.

Since I did not see a peak in MI in the first series of intervals spanning 48-96 hours post-stimulation, but a rather constant increase, I could not conclude that I had determined the peak period of first division cells. In the second experiment, using blood from the same turtle, two collection periods, 72-84 hours and 84-96 hours, were included as in the first experiment but collection periods of 96-108 hours, 108-120 hours, and 120-132 hours were also studied. The differences in MI values between the two experiments for the 72-84 hours and 84-96 hours collection times were within the range of counting uncertainty. The MI values for the 72-84 hour period was 0.50±0.10 %. This was followed by a broad peak including the 84-96 hours collection period (MI = 1.3±0.27 %), and the 96-108 hour collection period (MI = 1.5±0.30 %). This peak was followed by a rapid decline (MI = 0.16±0.08 %) at 120-132 hours. The MI for the two peak periods was nearly identical, therefore I concluded that the peak was centered at 96 hours,

between the two collection periods and subsequent experiments utilized a twelve hour collection period from 90-102 hours.

I was also interested in determining whether I was observing cells in their first post-stimulation mitosis or whether they were in their second (or later) generation. I made this determination by culturing the cells in the presence of bromodeoxyuridine (BrdU). In cells that have gone through one mitosis in the presence of BrdU, the chromosomes have two unifilarly labeled chromatids (one DNA strand BrdU substituted, the other not, in each chromatid), which appear darkly stained with the differential chromatid staining technique used (26). After the second mitosis in the continuous presence of BrdU, one chromatid will be unifilarly labeled, and will appear dark, while the other chromatid will be bifilarly labeled and will appear light. If BrdU is added to the cultures at the time of stimulation, it can be determined whether mitotic cells are in their first or second post-stimulation mitosis. In experiment MP1 all mitotic cells were in their first mitosis. All mitotic cells collected prior to 96 hours in experiment MP2 were first-division cells, and a very small number of second-division cells (4% of all mitotic cells scored) began to appear in the 96-108 hour collection period (data not shown). Therefore, it can be concluded that greater than 96% of the mitotic cells appearing in the peak between 84 and 108 hours were in the first post-stimulation mitosis.

Separated lymphocytes vs. whole blood cultures:

The next technical issue I addressed was the effective isolation of turtle lymphocytes. It is difficult to do cytogenetic studies for species with nucleated erythrocytes which are not lysed and eliminated during fixation, as is the case for

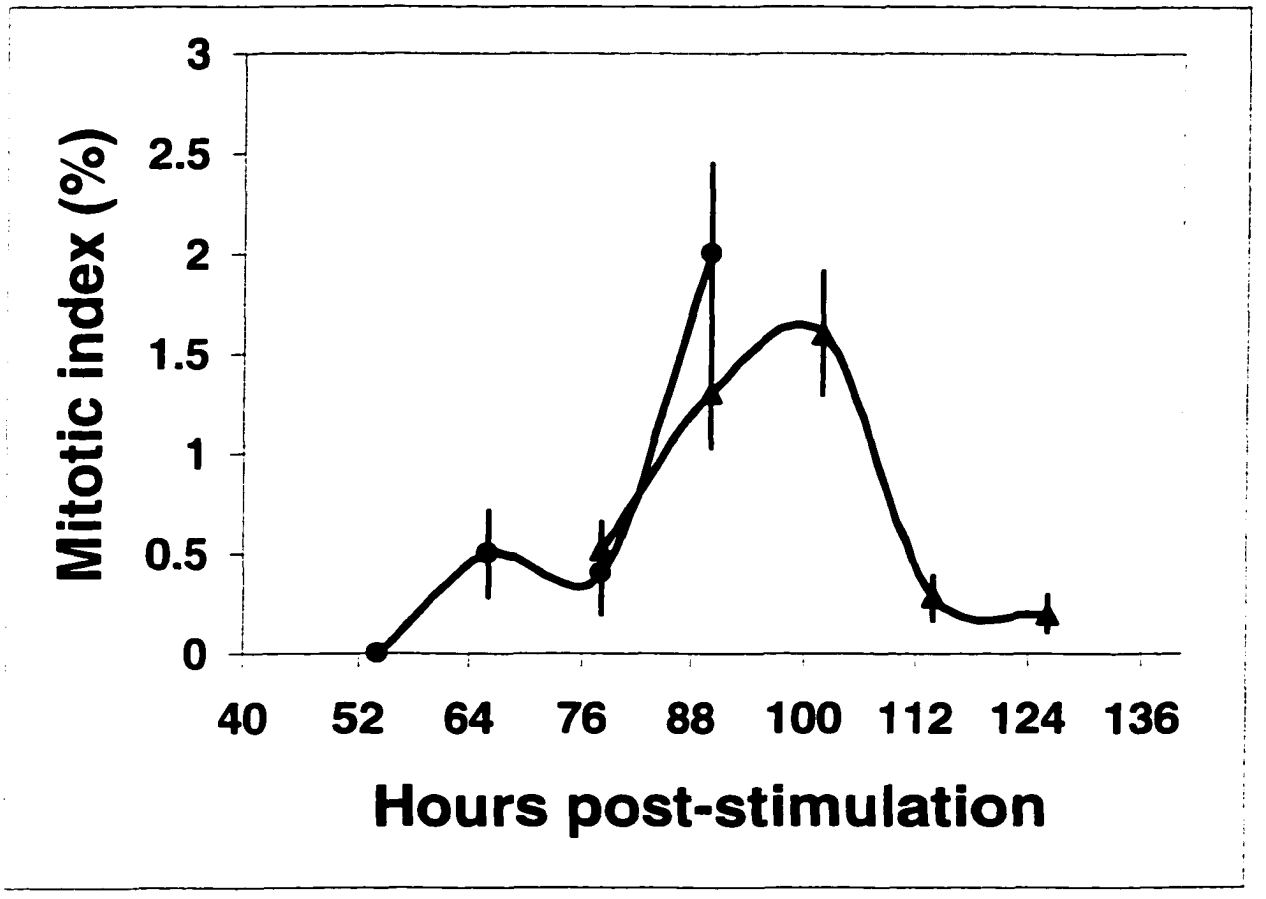

Figure 4.1:
Turtle lymphocyte mitotic index vs. time after stimulation. The data points in the graph indicate the midpoint of the collection period, for instance the point at 66 hours indicates the mitotic index of the cells collected during the 60-72 hour collection period. Error bars indicate one standard deviation due to counting statistics for a Poisson distribution. Data from two separate experiments (denoted by ● and ▲) were included, however blood samples from the same animal were used for both experiments and all culture conditions except length of incubation period were identical.

anucleate erythrocytes of mammals. Commercial ficoll centrifugation medium is available for the separation of lymphocytes from mammalian whole blood. However, it was unknown whether the ficoll density which is optimal for use with mammalian blood would also be optimal for reptilian blood.

To verify that the buffy layer did indeed contain lymphocytes, I isolated cells from this layer and identified them by cell morphology. These results confirmed that commercial ficoll used for mammalian lymphocyte isolation was suitable for isolation of turtle lymphocytes as well.

I included the plasma fraction in separated lymphocyte cultures because previous studies have indicated that alligator lymphocytes were capable of stimulation into the cell cycle only when they were fed with alligator serum, rather than fetal bovine serum (which is typically used with mammalian cell culture) (21). Furthermore, these studies found that a serum concentration of approximately 10% of the culture volume was superior to lower concentrations.

After determining the adequacy of the separation protocol for isolation of turtle lympyocytes, the next experiments I performed were designed to determine whether lymphocyte isolation should be performed prior to, or following mitogenic stimulation and culture incubation. The advantage of isolating lymphocytes prior to the incubation period is that very little hemolysis of erythrocytes has occurred. I noted that if whole blood was cultured and lymphocyte isolation was performed at the end of the incubation period, a fraction of the erythrocytes sometimes hemolyzed, making separation of these cells from lymphocytes difficult. In some cases, the ficoll separation procedure had to be

performed twice, and even then, some erythrocytes remained. Since erythrocytes are largely unresponsive to mitogenic stimulation, and they are difficult to distinguish from interphase lymphocytes using conventional giemsa or DAPI staining, the presence of a variable number of erythrocytes could confound measurements of the mitotic index. This difficulty could be avoided if lymphocytes were isolated immediately after sample collection, and prior to incubation.

Another advantage of separation prior to incubation is that the various samples for experiments could be divided into many experimental treatments. In order to perform the lymphocyte separation, enough lymphocytes to form a visible buffy layer must be present. I found that the minimum volume of whole blood necessary to yield a visible buffy layer was approximately 0.5 ml if a 15 ml centrifuge tube is used in the separation protocol. Therefore, if separation was performed after incubation, each experimental treatment required 0.5 ml of whole blood. The maximum volume of blood I was able to collect from a given turtle was approximately 2.5 ml, and a sample volume of 1.0 ml was more common. This severely limited the number of aliquots available from a sample. If, on the other hand, the separation was performed prior to incubation, the separated lymphocytes could be aliquotted into numerous small-volume treatments. I addressed this issue by centrifuging all blood cells out of whole blood cultures at the end of incubation, resuspending the cell pellet in a small volume of culture medium, and performing the separation procedure in small diameter, 1 ml glass centrifuge tubes, instead of the larger diameter 15 ml tubes. This had the effect of making the buffy coat thicker, and therefore easier to visualize.

I designed an experiment to compare mitotic indices of lymphocytes isolated from the same sample either before or after incubation. This experiment was performed in conjunction with the first experiment to locate the peak in first post-stimulation mitosis (experiment MP1), the results of which are described below. This experiment consisted of comparing the MI values from two 3 ml cultures from the same blood sample treated identically, except that in one sample, the lymphocytes were isolated prior to incubation, and in the other sample separation was performed following incubation. The MI values for these two samples were similar (Table 4.1), indicating that for these culture conditions, separating lymphocytes either before or following incubation has no impact on MI value. The MI for the separated lymphocyte culture (0.60±0.24%) was similar to that for the corresponding whole blood culture in experiment MP1 (treatment MP1-3, MI = 0.40±0.20%).

Culture volume conditions:

The next logical step was to test various concentrations of different mitogens, but these experiments required several treatments from the same blood sample (to minimize interindividual variation). Therefore, I designed an experiment to determine optimal conditions for small volume cultures which would require smaller aliquots of whole blood. I first attempted to establish separated lymphocyte cultures in 1.0, 0.5, and 0.25 ml volumes. None of these cultures were successful (MI=0), despite repeated attempts. I hypothesize that this was due to the influence of evaporation on the osmolarity, pH, and/or oxygen tension of the cultures. Previous work with human lymphocytes has revealed that isolated lymphocytes are much more sensitive to changes in these

parameters than are lymphocytes in whole blood cultures, where erythrocytes provide a buffering effect (23). Due to the cylindrical shape of the centrifuge tubes, the fluid surface areas of the cultures were approximately the same regardless of volume therefore I would expect the absolute rate of water loss by evaporation to be similar. The result would then be a larger relative change in osmolarity and nutrient concentrations with time in small vs. larger culture volumes.

To test this hypothesis, I set up cultures in three different environments. The first culture was established in a humid environment, with the centrifuge tube cap loosened to allow gas exchange. Presumably, this culture would experience minimal changes due to either cell respiration or evaporation. The second culture was established in a dry environment with gas exchange. This culture would be expected to suffer effects of evaporation. The last culture was established in a dry environment with the cap tightened to prevent gas exchange. This culture would experience changes due to cell respiration, such as pH variances, but not effects due to evaporation. The whole-blood culture maintained in a humid environment with gas exchange had the highest MI value, 0.47±0.09 %, followed by the culture in the dry environment with gas exchange 0.33±0.07 %, and the culture in the dry environment with no gas exchange 0.28±0.06 % (Table 4.1). Apparently, changes in pH, osmolarity, oxygen tension, or some other physical or chemical parameters can be caused by either evaporation or cell respiration, as the culture in the humid environment with free gas exchange had the highest MI value. This supports my evaporation hypothesis. However, cell respiration may be marginally more important than evaporation, as the culture in which gas exchange was prevented had a somewhat lower MI value than the culture in the dry environment with free gas

exchange. While the performance of small volume (1 ml) cultures can be improved by using whole blood cultures in a humid environment, 3 ml cultures consistently had three- or four-fold higher MI values, all other factors being equal.

Comparison of different mitogens:

The next experiment tested the mitogenic activity of different concentrations of PHA and LPS. PHA stimulates nearly all T-lymphocytes (which form the majority of the lymphocyte population), while LPS stimulates B-lymphocytes, as well as many other types of cells (27). These mitogens were selected for a titration series because they were found to be optimal in the stimulation of alligator lymphocytes (21). This was the most closely related species to turtles for which I had information on mitogenic response of lymphocytes.

I also tested the performance of manufacturer-recommended concentrations of two other common T-lymphocyte mitogens, pokeweed mitogen and concanavalin A (con A), in combination with LPS, though a full titration series was not performed. Turtle lymphocytes were found to be completely unresponsive to pokeweed mitogen. The recommended concentration of con A performed almost as well as the optimal concentration of PHA. The difference in the mitotic indices of cultures containing these two mitogens was within counting error. This response profile is similar to that reported for alligators: PHA gave the best mitogenic response, followed by con A, while pokeweed mitogen gave the poorest response (21).

With the LPS concentration held constant at 55 μg ml^{-1}, the highest MI value (0.88±0.19%) was obtained with the manufacturer-recommended concentration of PHA (2%). At 0.5% PHA, MI=0.24±0.10% and at 4% PHA, MI=0.56±0.15% (Table 4.1).

The concentration of LPS found to be optimal in stimulation of alligator lymphocytes also gave the highest MI value in turtle lymphocytes. When the PHA concentration was held to 2% and the LPS concentration was varied, the MI values for turtle lymphocytes for LPS concentrations of 0.275, 0.55 (optimal for alligator), and 1.1 μg ml^{-1} were 0.12±0.07%, 0.56±0.15%, and 0.40±0.13%, respectively (Table 4.1).

There were no mitotic cells observed in the pokeweed mitogen-stimulated culture, while the MI for the con A culture was 0.64±0.16%.

Comparison of culture media and sera:

I next examined the ability of two different cell culture media to support lymphocyte proliferation, and the influence of the concentration of FBS was also investigated. The two media tested were CSF medium, and αMEM, which is commonly used in mammalian cell culture. When αMEM is used, FBS must be added to support cell proliferation. It was critical that this serum be heat inactivated (heated to 56°C for 30 minutes) when used with turtle lymphocytes. I made numerous attempts to culture turtle lymphocytes in serum which had not been inactivated, and none of these attempts were successful, most likely due to the presence of an inhibitory complement component. Cuchens and Clem (1979) found that the concentration of FBS used was irrelevant to success in culturing alligator lymphocytes, but I did not find this to be the case with turtle lymphocytes. Doubling the FBS concentration nearly doubled the mitotic index of

cultured lymphocytes. However, neither of the αMEM cultures with FBS (either 10% or 20%) performed as well as the cultures with CSF medium containing autologous turtle plasma.

The MI values for the 10% and 20% FBS were 0.32±0.11 and 0.60±0.15, respectively (Table 4.1). These values are both lower than the culture from experiment M, which contained CSF medium containing autologous turtle plasma and the same mitogen concentrations (treatment M-2, MI = 0.88±0.19).

Regarding the use of turtle serum, while Cuchins and Clem found that the FBS concentration had no impact on stimulation of alligator lymphocytes cultured in MEM, the concentration of alligator serum did have an effect, with 10% alligator serum being more effective than 5%. This was not the case for turtle lymphocytes cultured in CSF medium containing autologous turtle plasma. The MI value decreased when the turtle serum concentration was increased from 5% (MI = 0.60±0.15) to 10% (MI = 0.32±0.11), but remained essentially unchanged when the serum concentration was increased from 10% to 20% (MI = 0.36±0.12)(Table 4.1). A possible explanation is that increasing the serum concentration dilutes the medium concentration. CSF medium is designed to contain all the growth factors and nutrients needed to support a much higher fraction of proliferating cells than are normally found in *in vivo*. Therefore, dilution of this medium with additional serum lowers the concentrations of the growth factors and nutrients, and this may lead to a lower proliferating fraction in the cultured cell population.

Regarding IL-2, my early attempts at turtle lymphocyte culture were plagued with two problems: first, I failed to stimulate the lymphocytes into the cell cycle and second, the lymphocytes suffered high levels of apoptosis (cell suicide), as revealed by flow

cytometry (data not shown). In the hope of enhancing lymphocyte stimulation and reducing apoptosis, I experimented with the addition of IL-2 to the lymphocyte cultures. This lymphokine has been shown to reduce lymphocyte apoptosis under certain conditions (28). Furthermore, IL-2 is widely recognized as a T-lymphocyte growth factor (29-32) and IL-2 also plays a role in the activation of B- and other types of lymphocytes (27,29,33). The effect of IL-2 on lymphocytes appears to be determined by the IL-2 concentration, the competency of the lymphocytes to enter the cell cycle, and many other factors. While IL-2 can sometimes rescue lymphocytes from apoptosis, under other conditions it can also induce apoptosis (34), and over the range of IL-2 concentrations I tested, it appears that IL-2 had the latter effect or no effect at all on turtle lymphocytes. IL-2 had no effect when added in a concentration equal to the EC_{50} for human lymphocytes (EC_{50} = 0.35 ng ml^{-1}, MI = 0.32±0.11), as the MI value was equal to that from a similar culture run concurrently, but without the addition of IL-2 (experiment TS). The MI value is somewhat lower at one half the IL-2 EC_{50} (MI = 0.20±0.09), and still lower at twice the EC_{50} (MI = 0.12±0.07)(Table 4.1).

Human recombinant IL-2 is commercially available, while turtle IL-2 is not. It is possible that the human version of this lymphokine is at least partially inactive in turtles. It is also possible that at a different concentration, human IL-2 would have a more positive effect on turtle lymphocyte proliferation.

Finally, I examined the possibility of inducing premature chromosome condensation (PCC) in turtle lymphocytes. Conventional methods of achieving PCC involve the fusion of mitotic "inducer" cells to interphase cells using Sendai virus (35-37) or polyethylene glycol (38). Unfortunately, induction of PCC in lymphocytes by fusion

typically suffers from low yields of cells with condensed chromosomes, usually because of a low incidence of fusion (39). Recently, calyculin A has been shown to induce PCC in human lymphocytes, possibly by interfering with serine/threonine phosphatases (40). Using calyculin A, yields of cells with condensed chromosomes have been reported as high as 30-60% (40). I performed several experiments on turtle fibroblasts to determine the optimal concentration of calyculin A which might produce such an effect in turtle cells (data not shown). None of these experiments were very encouraging, although 200 nM concentrations did produce a level of PCC that was somewhat higher than other concentrations ranging from 25-800 nM. Durante, *et. al.* (1998) recommended a calyculin A concentration of 50 nM for human lymphocytes. Therefore, in my calyculin A experiment with turtle lymphocytes, I included treatments spanning the range from 50-200 nM. Regarding the mitotic index (not the PCC index) in the presence of calyculin A, I found that the MI in all lymphocyte cultures not only failed to increase, but actually decreased. No mitotic cells were observed in the 50 nM and 200 nM treatments (MI=0.00±0.00), and only one was observed in the 100 nM treatment (MI=0.04±0.04).

It may be that calyculin A interfered with the cell cycle arresting action of colcemide, but it does not appear to have had this effect in Durante's work with human lymphocytes and it is difficult to imagine how this could occur. It is also possible that either the calyculin A, or the one hour incubation at 37°C involved in the PCC procedure caused apoptosis in mitotic lymphocytes. Incubation temperatures as high as 36°C have been shown to render turtle epithelial cells incapable of growth (41). It is unknown however, whether these elevated temperatures actually cause apoptosis, or whether a one hour exposure would be sufficient to cause the demise of mitotic lymphocytes.

Conclusion:

There are several important differences between the culture techniques suitable for turtle lymphocytes compared to those typically employed for human or other mammalian lymphocytes. A failure to recognize these differences could be a major obstacle to the inclusion of turtles (and most other reptiles) in cytogenetic and immunologic studies. Taken as a whole, the results of this series of experiments identify lymphocyte culture conditions which should allow the incorporation of turtles into cytogenetic and immunologic studies more readily. Such studies with turtles will provide valuable insights in applications as diverse as ecological risk assessment, comparative genomics and immunology, ecotoxicology and environmental biodosimetry.

Acknowledgements:

The authors would like to thank Dianne Vannais and Dr. Elizabeth McNiel of the Colorado State University Department of Radiological Health Sciences for their valuable suggestions and insights throughout the course of this study. I would also like to thank Dr. Terry Campbell of the Colorado State University Veterinary Teaching Hospital for assistance in lymphocyte identification.

This work was supported by the Department of Energy grant RR267-055/4895914 to University of Georgia, Savannah River Ecology Laboratory and subcontract to Colorado State University, and a grant from the NIH, National Cancer Institute, 5 T32 CA09236 to Colorado State University.

REFERENCES

1. Meyers-Schone, L., Shugart, L. R., Beauchamp, J. L, and Walton, B. T., Comparison of two freshwater turtle species as monitors of radionuclide and chemical contamination: DNA damage and residue analysis. *Environmental Toxicology and Chemistry* **12**, 1487-1496 (1993).

2. Meyers-Schone, L. and Walton, B. T., Turtles as monitors of chemical contaminants in the environment. *Reviews of Environmental Contamination and Toxicology* **135**, 93-153 (1994).

3. Dickerson, R. L., Hooper, M. J., Gard, N. W., Cobb, G. P., and Kendall, R. J., Toxicological foundations of ecological risk assessment: biomarker development and interpretation based on laboratory and wildlife species. *Environmental Health Perspectives* **102 Suppl 12**, 65-69 (1994).

4. Ayres, M., Sampaio, M. M., Barros, R. M. S., Dias, L. B, and Cunha, O. R., A karyological study of turtles from the Brazilian Amazon region. *Cytogenetics* **8**, 401-409 (1969).

5. Barros, R. M., Ayres, M., Sampaio, M. M., Cunha, O., and Assis, F., Karyotypes of two subspecies of turtles from the Amazon region of Brazil. *Caryologia* **25**, 463-469 (1972).

6. Bickham, J. W., A cytosystematic study of turtles in the genera *Clemmys, Mauremys* and *Sacalia*. *Herpetologica* **31**, 198-204 (1975).

7. Bickham, J. W. and Baker, R. J., Karyotypes of some neotropical turtles. *Copeia* **1976**, 703-708 (1976).

8. Bickham, J. W., Meiotic analysis of four species of turtles. *Genetica* **46**, 193-198 (1976).

9. Bickham, J. W., Bull, J. J., and Legler, J. M., Karyotypes and evolutionary relationships of trionychoid turtles. *Cytologia* **48**, 177-183 (1983).

10. Rhodin, A. G. J., Karyotypic analysis of the *Podocnemis* turtles. *Copeia* **1978**, 723-728 (1978).

11. Sampaio, M. M., Barros, R. M., Ayres, M, and Cunha, O. R., A karyological study of two species of tortoises from the Amazon region of Brazil. *Cytologia* **36**, 199-204 (1969).

12. Stock, A. D., Karyological relationships in turtles (Reptilia: Chelonia). *Canadian Journal of Genetics & Cytology* **15**, 859-868 (1972).

13. Bickham, J. W. and Baker, R. J., Chromosome homology and evolution of emydid turtles. *Chromosoma* **54**, 201-219 (1976).

14. Bickham, J. W., The karyotype and chromosomal banding patterns of the green turtle (*Chelonia Mydas*). *Copeia* **1980**, 540-543 (1980).

15. Bickham, J. W., Two-hundred-million-year-old chromosomes: deceleration of the rate of karyotypic evolution in turtles. *Science* **212**, 1291-1293 (1981).

16. Bull, J. J. and Legler, J. M., Karyotypes of side-necked turtles (Testudines: Pleurodira). *Canadian Journal of Zoology* **58**, 828-841 (1980).

17. Carr, J. L., Bickham, J. W., and Dean, R. H., The karyotype and chromosomal banding patterns of the Central American river turtle *Dermatemys Mawii*. *Herpetologica* **37**, 92-95 (1981).

18. Sites, J. W., Bickham, J. W., Haiduk, M. W., and Iverson, J. B, Banded karyotypes of six taxa of kinosternid turtles. *Copeia* 692-698 (1979).

19. Depledge, M. H., Genotypic toxicity: implications for individuals and populations. *Environmental Health Perspectives* **102 Suppl 12**, 101-104 (1994).

20. Cuchens, M. A. and Clem, L. W., Phylogeny of lymphocyte heterogeneity. IV. evidence for T-like and B-like cells in reptiles. *Developmental and Comparative Immunology* **3**, 465-475 (1979).

21. Cuchens, M. A. and Clem, L. W., Phylogeny of lymphocyte heterogeneity. III. mitogenic responses of reptilian lymphocytes. *Developmental and Comparative Immunology* **3**, 287-297 (1979).

22. Haskell, A. and Pokras, M. A., Nonlethal blood and muscle tissue collection from redbelly turtles for genetic studies. *Herpetological Review* **25**, 11-12 (1994).

23. McFee, A. F., Sayer, A. M., Salomaa, S. I., Lindholm, C., and Littlefield, Methods for improving the yield and quality of metaphase preparations for FISH probing of human lymphocyte chromosomes. *Environmental & Molecular Mutagenesis* **29**, 98-104 (1997).

24. Spotila, J. R., Foley, R. E., and Standora, E. A., Thermoregulation and climate space of the slider turtle, In *Life History and Ecology of the Slider Turtle* (Gibbons, J. W., Eds.), pp. 288-298. Smithsonian Institution Press, Washington, D.C., (1990).

25. Benn, P. A. and Perle, M. A., Chromosome staining and banding techniques, In *Human Cytogenetics: A practical Approach* (Rooney, D. E. and Czepulkowski, B. H., Eds.), pp. 91-118. Oxford University Press, New York, (1992).

26. Perry, P. and Wolff, S., New Giemsa method for the differential staining of sister chromatids. *Nature* **251**, 156-158 (1974).

27. Stites, D. P., Terr, A. I., and Parslow, T. G, *Medical Immunology*. Appleton & Lange, Stamford, CT, (1997).

28. Adachi, Y., Oyaizu, N., Than, S., McCloskey, T. W., and Pahwa, S., IL-2 rescues in vitro lymphocyte apoptosis in patients with HIV infection. *Journal of Immunology* **157**, 4184-4193 (1996).

29. Gomez, J., Gonzalez, A., Martinez, A., and Rebollo, A., IL-2-induced cellular events. *Critical Reviews in Immunology* **18**, 185-220 (1998).

30. Nelson, B. H. and Willerford, D. M., Biology of the interleukin-2 receptor. *Advances in Immunology* **70**, 1-81 (1998).

31. Paul, W. E., Pleiotropy and redundancy: T cell-derived lymphokines in the immune response. *Cell* **57**, 521-524 (1989).

32. Smith, K. A., Interleukin-2: inception, impact, and implications. *Science* **240**, 1169-1176 (1988).

33. Schorle, H., Holtschke, T., Hunig, T, Schimpl, A., and Horak, I., Development and function of T cells in mice rendered interleukin-2 deficient by gene targeting. *Nature* **352**, 621-624 (1991).

34. Lenardo, M., Chan, K. M., Hornung, F., McFarland, H., Siegel, R., Wang, J., and Zheng, L., Mature T lymphocyte apoptosis--immune regulation in a dynamic and unpredictable antigenic environment. *Annual Review of Immunology* **17**, 221-253 (1999).

35. Johnson, R. T., Rao, P. N, and Hughes, S. D., Mammalian cell fusion III. A HeLa cell inducer of premature chromosome condensation active in cells from a variety of animal species. *Journal of Cellular Physiology* **76**, 151-157 (1970).

36. Johnson, R. T., Rao, P. N, and Hughes, S. D., Mammalian cell fusion: induction of premature chromosome condensation in interphase nuclei. *Nature* **226**, 717-722 (1970).

37. Rao, P. N and Johnson, R. T., Mammalian cell fusion: I. Studies on the regulation of DNA synthesis and mitosis. *Nature* **225**, 159-164 (1970).

38. Okayasu, R., Cheong, N., and Iliakis, G., Technical note: comparison of yields and repair kinetics of interphase chromosome breaks visualized by Sendai-virus or PEG-mediated cell fusion in irradiated CHO cells. *International Journal of Radiation Biology* **64**, 689-694 (1993).

39. Pantelias, G. E. and Maillie, H. D., The use of peripheral blood mononuclear cell prematurely condensed chromosomes for biological dosimetry. *Radiation Research* **99**, 140-150 (1984).

40. Durante, M., Furusawa, Y., and Gotoh, E., Technical report: a simple method for simultaneous interphase-metaphase chromosome analysis in biodosimetry. *International Journal of Radiation Biology* **74**, 457-462 (1998).

41. Clark, H. F and Karzon, D. T., Terrapene heart (TH-1), a continuous cell line from the heart of the box turtle Terrapene carolina. *Experimental Cell Research* **48**, 263-268 (1967).

Chapter 5

Chromosome Translocations In *T. Scripta:* *The Dose-Rate Effect and* In Vivo *Lymphocyte Radiation Response*

Abstract:

Using a whole-chromosome FISH painting probe we previously developed for chromosome-1 of the yellow-bellied slider turtle (*Trachemys scripta*), I investigated the dose-rate effect for radiation-induced symmetrical translocations in *T. scripta* fibroblasts and lymphocytes. The dose-rate below which no reduction in effect per unit dose is observed with further dose protraction was approximately 23 cGy hr^{-1}.

I estimated the whole-genome spontaneous background level of complete, apparently simple symmetrical translocations in *T. scripta* lymphocytes to be approximately $1.20x10^{-3}$ /cell projected from aberrations occurring in chromosome-1. Similar spontaneous background levels reported for humans are some 5- to 30-fold higher, ranging from about $6x10^{-3}$ to $3.4x10^{-2}$ per cell. This relatively low background level for turtles would be a significant advantage for resolution of effects at low doses and dose-rates.

I also chronically irradiated turtles over a range of doses from 0-8 Gy delivered at approximately 5.5 cGy hr^{-1}, and constructed a lymphocyte dose-response curve for complete, apparently simple symmetrical translocations (Y_T) suitable for use with animals chronically exposed to radiation in contaminated environments. The best fit calibration curve (not constrained through the zero dose estimate was of the form $Y_{as} = c + aD + bD^2$, where Y_{as} was the number of apparently simple symmetrical translocations per cell, D was the dose (Gy), a = (0.0058±0.0009), b = (-0.00033±0.00011), and c = (0.0015±0.0013). With additional whole-chromosome probes to improve sensitivity, environmental biodosimetry using stable chromosome translocations could provide a

practical and genetically relevant measurement endpoint for ecological risk assessments and biomonitoring programs.

Introduction:

A large number of sites around the United States are contaminated with radionuclides (1), and many similar sites exist around the world. Aquatic and terrestrial organisms inhabiting a variety of these sites at former nuclear weapons production facilities and waste disposal areas are chronically exposed to varying levels of ionizing radiation, yet it is difficult to calculate or directly measure the biologically relevant doses these organisms are receiving (2). Much of the early work in comparative radiobiology involved measuring acute mortality (such as LD50 values for various animals and plants), which is a relatively insensitive indicator of radiation-induced damage and is not directly applicable to the chronic exposures organisms experience in contaminated environments. More sensitive indicators of integrated dose and biologically relevant effects are needed. Molecular cytogenetic techniques widely used in humans and a few other mammalian species could provide such indicators (3).

I have previously reported the development of a whole-chromosome-specific fluorescence *in situ* hybridization (FISH) probe for chromosome-1 of the yellow-bellied slider turtle (*Trachemys scripta*) (4). I believe that this was the first report of a whole-chromosome probe for a reptilian species. I used this probe to determine the dose-response relationship for chromosome aberration induction in cultured *T. scripta* fibroblasts acutely irradiated *in vitro* with ^{137}Cs gamma rays. I then developed culture techniques for turtle lymphocytes that allowed direct measurement of aberration

induction in turtle cells irradiated *in vivo*. These studies were designed to assess the potential usefulness for application in environmental biodosimetry, i.e., the application of biodosimetric techniques developed in humans to organisms exposed to radionuclide-contaminated environments, and took the first steps toward making these techniques relevant to biomonitoring applications.

Turtles (and other organisms) inhabiting contaminated environments are nearly always subjected to chronic, low dose-rate exposures, rather than the acute, high dose-rate exposures typical of many laboratory studies and accidental exposures. Many previous studies with other organisms and various endpoints of biological damage have shown that the biological effectiveness per unit dose is generally reduced as the intensity of exposure or the dose-rate of sparsely ionizing radiation is reduced (e.g. (5-12)). Furthermore, it has also been shown that below a critical dose-rate, further dose protraction does not result in a further reduction in effect per unit dose (6,8,10,12). Identification of this critical dose-rate is important because it is the response to chronic, low dose-rate exposures that is of concern for radiological protection for humans as well as other species.

In the current study I take the next steps toward bringing biodosimetric techniques to ecologically relevant field investigations. First, to minimize the number of experimental animals required, I examined the dose-response of *T. scripta* fibroblasts subjected to chronic *in vitro* exposure to ^{137}Cs gamma rays over a range of dose-rates to estimate the lower range limit to the dose-rate effect. I hypothesize that the dose-rate effect in *T. scripta* will be similar to that previously observed in various other organisms, that is, a reduction in effect per unit dose with a plateau at higher dose-rates due to

saturation, and a plateau at lower dose-rates due to the dominance of one-hit radiation interactions. Similar data were then obtained for *T. scripta* lymphocytes but using a single dose delivered *in vivo* at two different low dose rates in the range determined for fibroblast cultures. Finally, I construct a complete *in vivo* dose-response curve for lymphocytes from turtles irradiated at a low dose-rate. I hypothesize that the shape of this curve will be linear, as has been observed for various endpoints in other organisms subjected to low dose-rate irradiation.

Materials and Methods:

Experimental animals and cell lines:

All animals included in this study were adult yellow-bellied slider turtles (*T. scripta*). They were captured with hoop traps from a farm pond near Jackson, South Carolina between July 17 and July 22, 1998. No radioactive or chemical contamination is known to exist in this pond. The animals were then transported to Colorado State University where they were maintained in a temperature-controlled greenhouse with natural lighting. Animal care procedures followed in this study are in accordance with Colorado State University Animal Care and Use Committee guidelines.

The fibroblasts used in this study were low-passage cells from a fibroblast line of *T. scripta* cells established by primary explant from embryos. The embryo donor was a gravid female from an uncontaminated pond in the same vicinity of Jackson, SC.

Irradiation:

Continuous, low-dose-rate irradiation was delivered in a specially designed irradiator. This unit consisted of a shielded warm room into which one to twelve 0.148 TBq (nominal) ^{137}Cs sources (Amersham, Arlington Heights, VA) could be removed or inserted from a remote location. The sources were arranged around the circumference of an 80 cm circle in a horizontal plane. Cell cultures or turtles in plastic tubs were then placed on horizontal shelves above the source-plane. The exposure-rate can be controlled in this unit by either varying shelf height above the source-plane, or by varying the number of sources inserted. In the experiments described here, all twelve sources were inserted, and shelf-height was varied to yield the desired exposure-rates. Nominal exposure rates were measured at varying heights above the source plane using a Victoreen R chamber. Calibration of this chamber was traceable to the National Institute of Standards and Technology. Variations in dose-rate uniformity across the horizontal field were less than 10%. These measurements were taken in 1990, and values were decay-corrected to the time of this study.

Approximately 30 minutes prior to irradiation, contact-inhibited fibroblast cultures in T-150 flasks were gassed with 5% CO_2, 2% O_2 for approximately two minutes. The caps on the culture flasks were then tightened and the cultures were placed inside an airtight 7.8 L plastic container. The container was then gassed for approximately five minutes prior to sealing the lid. The cultures were placed in the irradiator at the appropriate shelf-height. Fibroblast culture irradiation was performed at 29°C (the preferred body temperature of *T. scripta* (13)).

Irradiation of the experimental animals was conducted similarly. The animals were placed in the same plastic containers used for fibroblast irradiation (one animal per container), but holes were drilled in the container lids to allow air exchange. A few cm of water was placed in the bottom of each container to prevent dehydration. Food was also added to the containers, and the animals appeared to be eating normally. Once inside these containers, the animals could only move perhaps 10-20 cm in any direction, thus ensuring a reasonably consistent exposure rate.

Prior to irradiation, all turtles were moved to the irradiation chamber anteroom (which is exposed only to background radiation), where they remained until the end of all irradiations except for the period they spent in the irradiator. The irradiations spanned a period of approximately 6 days, during which the animals were scheduled in and out of the radiation field to give the appropriate total dose. The total dose was controlled by the length of the irradiation period. Irradiation of turtles was performed at room temperature (approximately 25°C), and free air exchange was allowed between the irradiator and anteroom to ensure that the temperature did not vary. The turtles were irradiated continuously, with the exception of daily cleanings of their plastic containers (approximately 10 minutes/cleaning). The light cycle was controlled both in the irradiator and in the anteroom to mimic natural conditions as closely as possible (approximately 12 hours light alternated with 12 hours dark).

Cell culture:

Fibroblasts were grown to confluence in T-150 tissue culture flasks. The incubation environment consisted of a humidified atmosphere of 5% CO_2 in air at 29°C.

The fibroblasts were cultured in αMEM with 10% fetal bovine serum. Gentamycin (Gibco BRL, Grand Island, Illinois, final concentration 25 $\mu g\ ml^{-1}$) and fungizone (Gibco BRL, final concentration 0.5 $\mu g\ ml^{-1}$) were added to the cultures to impede the growth of bacterial or fungal contamination. To prepare cultures for irradiation, T-150 flasks were inoculated with $1x10^6$ cells 7 days before irradiation. These cultures reached confluence after approximately 3-4 days, after which growth is stopped or at least severely reduced. The degree of cell cycling in these nominally "contact-inhibited" cultures was measured in the fibroblast cultures by the addition of bromodeoxyuridine (BrdU) (10^{-4} M) to two replicate cultures established in parallel with the unirradiated experimental control cultures. At the conclusion of the irradiation of experimental treatments (approximately 200 hours after the addition of BrdU), the (unirradiated) cultures containing BrdU were immediately fixed and labeled with mouse monoclonal anti-BrdU (Amersham Pharmacia Biotech, Piscataway, NJ) followed by anti-mouse Ig, fluorescein-linked whole antibody (from sheep) (Amersham Pharmacia Biotech). One-thousand cells from each replicate were then scored using a fluorescence microscope equipped with a FITC filter to determine the proportion of cells which entered or remained in S-phase during the incubation period.

Prior to this experiment, the efficacy of the BrdU antibody system in this cell line was tested by growing log-phase fibroblasts in the presence of BrdU, then staining with the fluorescein-conjugated antibody system (data not shown). As expected, a large fraction of the cell population (presumably the fraction that was cycling), incorporated BrdU and was differentially stained by the antibodies. There was also a fraction of the population which was not stained (presumably the fraction that was not cycling).

Therefore, it appears that this system is effective in detecting cells which have undergone DNA synthesis in the presence of BrdU.

Whole blood (1-3 ml) was collected from the dorsal coccygeal vein in the animals' tails into 3 cc syringes containing a few drops of sodium heparin. An additional 10 U sodium heparin ml^{-1} whole blood was added, and the blood was mixed with complete serum-free medium (Mediatech, Herndon, VA) in a ratio of 1 ml blood/11 ml medium. Blood is approximately 50% plasma, thus the cultures contained approximately 4-5% turtle plasma, but no bovine or other serum products. Gentamycin (Gibco BRL, final concentration 25 $\mu g\ ml^{-1}$) and fungizone (Gibco BRL, final concentration 0.5 $\mu g\ ml^{-1}$) were added to the cultures to impede the growth of bacterial or fungal contamination. Lymphocytes were stimulated with phytohemagglutinin M-form (PHA) (Gibco BRL, final concentration 2%) and lipopolysaccharides (LPS) (Sigma, St. Louis, Missouri, final concentration of 55 $\mu g\ ml^{-1}$). Three ml cultures were set up in 15 ml centrifuge tubes. These cultures were maintained in a 29°C incubator in a humid, 5% CO_2 environment. Colcemide (Gibco BRL, final concentration 0.15 $\mu g\ ml^{-1}$) was applied at 90 hours post-stimulation to block cells in their first post-stimulation mitosis. At approximately 111 hours post-stimulation, lymphocytes were separated from the cultures by centrifuging in a ficoll gradient at 200 g for 20 minutes at room temperature. Lymphoprep ficoll (Nycomed Pharma, Oslo, Norway) with a density of 1.077 ± 0.001 g ml^{-1} was used for all lymphocyte separations. Separation was carried out to remove erythrocytes, which are nucleated in reptiles, and which are not eliminated by the fixation procedure. Following separation, lymphocytes were swelled in 0.075 M hypotonic solution (30 minutes, 37°C), and fixed in three changes of 3:1 methanol/glacial acetic

acid. Both pre- and post-irradiation samples were collected from each animal and the samples were treated identically.

Fluorescence in situ hybridization (FISH):

FISH was carried out as described previously (4), with some modifications. Approximately 40 µl of the hybridization mixture which contained 50% formamide, 10% dextran sulfate, about 300 ng of PCR biotin-labeled probe and 5 µg of turtle cot DNA was denatured in a thermal cycler for 10 minutes at 84°C, reannealed for 45 minutes at 37°C, and the probe hybridization mixture was then placed on the slide (denatured as described below), covered by a 22 x 50 mm coverslip and sealed with rubber cement. Hybridization then proceeded for at least 2 days at 37°C in a dry slide box. The target slides onto which the hybridization probe was placed were prepared by denaturing the chromosomes on slides in 70% formamide in 2 x saline sodium citrate (SSC) at pH 7.0 for 2 minutes at 68°C. After this, the slide was quickly transferred first to ice cold 70% ethanol, then 90% and then 100% ethanol (1.5 minutes each) and finally air dried. After probe hybridization to the denatured chromosomes, the coverslips were removed, the slides were washed in two changes of 50% formamide in 2 x SSC, pH 7.0, at 45°C to remove loosely bound or hybridized DNA and then were washed twice more in 2 x SSC and 3 times in PN buffer for 3 minutes each, also at 45°C. For probe detection, PN buffer containing 5% non-fat dry milk was applied for 30 minutes at room temperature (to block the probe from binding to extraneous sites and increasing background), and a solution of 5 µg ml^{-1} fluorescein-avidin (Vector Laboratories, Burlingame, CA) in 0.1 M sodium bicarbonate, 0.15 M NaCl was applied (approximately 5 µl cm^{-2} of the slide) and the slide

was incubated for 15 minutes at 37° C. The slide was then rinsed in 3 changes of PN buffer at 45° C for 3 minutes each. Biotinylated anti-avidin D (Vector Laboratories) in water (5 μg ml^{-1}) was then applied and the slide was incubated for 15 minutes at 37° C. This was followed by the same PN wash cycle, another layer of block and fluorescein-avidin, and another PN wash cycle. For microscopy, the slides were counterstained with a solution of antifade containing 4,6-diamidino-2-phenylindole (DAPI) at a concentration of 0.62 μg μl^{-1} and propidium iodide (PI) at a concentration of 0.5 μg μl^{-1} under a coverslip. Slides were then viewed under a fluorescence microscope with appropriate excitation and emission filters.

Aberration scoring:

Aberrations were scored according to the PAINT nomenclature system (14), with minor modification. Apparently simple interchange aberrations were defined as those in which both of the chromosomes involved were bicolored and had had only one color junction each (two such chromosomes were considered one complete exchange). Bicolored chromosomes containing more than one color junction were defined as complex (15). A complete translocation was defined as one in which two bicolored chromosomes were visible in the cell. If only one bicolored chromosome was visible, the translocation was defined as incomplete even though many of these were probably hidden complete translocations which appeared incomplete because of the resolution of the detection system (16-18). Finally, symmetrical translocations were defined as those in which each bicolored chromosome had exactly one centromere, while asymmetrical translocations were defined as those in which a bicolored chromosome had two

centromeres and was accompanied by a bicolored acentric fragment for complete translocations, or by a painted acentric fragment or no visible fragment for incomplete translocations).

Results:

Verification of fibroblast contact inhibition:

Contact-inhibited cultures set up as described earlier were incubated in the presence of BudR for approximately 200 hours followed by fixation and preparation for detection of BudR incorporation. One-thousand cells were scored from each replicate BudR control culture. In the first replicate, 52 cells were BudR-positive, indicating that 5.2% of the cell population had incorporated BudR during S-phase during the period of about 8 days when the irradiated cultures were being exposed. The results in the second replicate were similar, with 41 cells (4.1%) being BudR-positive.

Fibroblast dose-rate effect:

The interchange aberration frequencies for turtle fibroblasts irradiated with 10 Gy of ^{137}Cs gamma rays at various dose-rates are listed in Table 5.1 and illustrated in Figure 5.1. Error bars in Figure 5.1 reflect the standard deviation due to Poisson counting statistics. Each data point in Figure 5.1 represents the frequency of symmetrical translocations detected in an independent fibroblast culture, and two identical replicates were irradiated at each dose-rate. The aberration frequencies from an acutely (high dose-rate) irradiated fibroblast culture from a previous study conducted in this laboratory (4) are also listed in Table 5.1 and plotted in Figure 5.1. The acutely irradiated culture

Table 5.1. Chromosomal aberrations* involving *T. scripta* chromosome 1 as determined by FISH whole chromosome painting at the first mitosis after 10 Gy of ^{137}Cs gamma rays delivered at various dose-rates to G_0 fibroblast cultures.

			Interchange aberrations total (%)			
			Symmetrical		Asymmetrical†	
Dose-rate (cGy hr^{-1})	# cells scored	Total color junctions (%)	Apparently simple	Complex or incomplete	Apparently simple	Complex or incomplete
0	500	0 (0.00)	0 (0.00)	0 (0.00)	0 (0.00)	0 (0.00)
0	500	2 (0.40)	0 (0.00)	0 (0.00)	1 (0.20)	0 (0.00)
5.1	400	56 (14.0)	16 (4.00)	12 (3.00)	1 (0.25)	10 (2.50)
5.1	300	15 (5.00)	5 (1.67)	1 (0.33)	2 (0.67)	0 (0.00)
9.3	196	35 (17.9)	12 (6.12)	2 (1.02)	1 (0.51)	7 (3.57)
9.3	309	32 (10.4)	10 (3.24)	3 (0.97)	2 (0.65)	5 (1.62)
22.8	300	39 (13.0)	12 (4.00)	6 (2.00)	2 (0.67)	5 (1.67)
22.8	300	41 (13.7)	12 (4.00)	4 (1.33)	5 (1.67)	3 (1.00)
69.1	300	49 (16.3)	14 (4.67)	9 (3.00)	2 (0.67)	10 (3.33)
69.1	292	79 (27.1)	32 (11.0)	8 (2.74)	1 (0.34)	5 (1.71)
20880#	*561*	*369 (65.8)*	*111 (19.8)*	*32 (5.7)*	*47 (8.4)*	*2 (0.36)*

* Interstitial and terminal deletions not scored.

† Centromeres were frequently obscured as a result of the FISH procedure. This leads to a bias resulting in a deficiency of asymmetrical (dicentric) aberrations with a corresponding excess of the symmetrical counterpart.

Data point included from ref. (4).

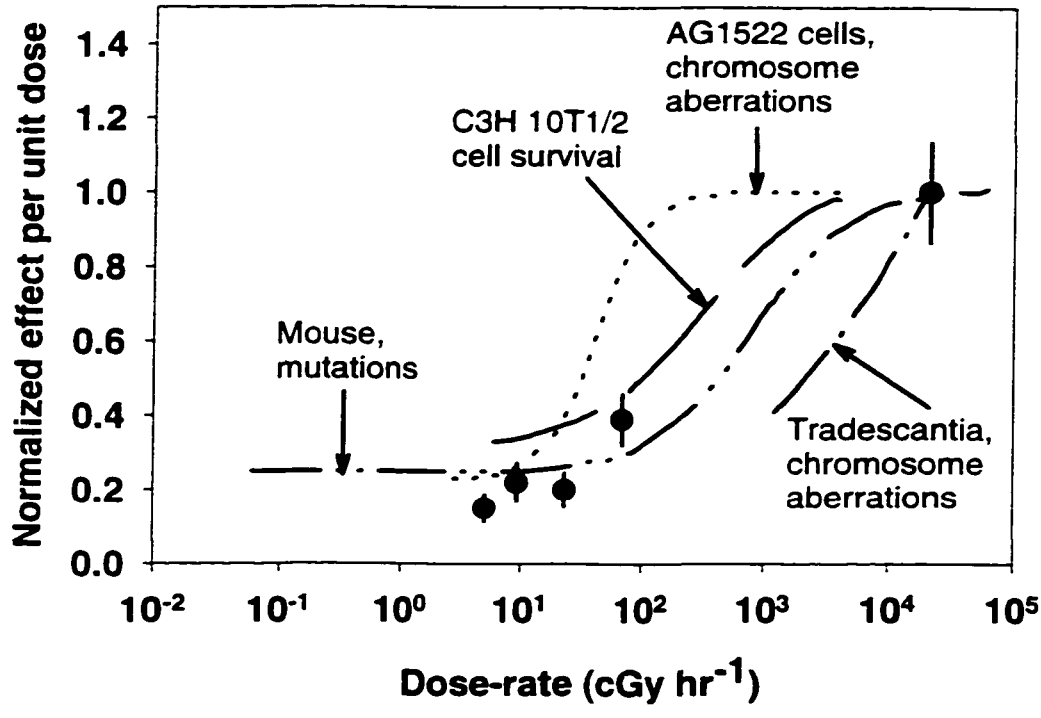

Figure 5.1:

Comparison of the dose-rate effect observed for radiation-induced symmetrical translocations in *T. scripta* fibroblasts (●) with the dose-rate effect observed in other organisms using a variety of biological endpoints. These include mutations in mice (11,19), survival of murine C3H 10T1/2 cells (12), chromosome aberrations in human AG1522 fibroblasts (6,7), and chromosome exchanges in *Tradescantia* microspores observed by Giemsa staining (10). All data has been normalized by dividing each observation by the maximum effect observed in each study. The curves are 5-factor sigmoid fits to the normalized data, except for the *Tradescantia* curve, which is a second order polynomial fit. Error bars on *T. scripta* data represent propagated errors due to Poisson counting statistics (one standard deviation).

also received 10 Gy, used the same cell-line, and was handled identically to the cultures in this study but the dose was delivered at a high dose-rate where the exposure required only 3 minutes instead of 8 days in the case of the lowest dose rate included in the current study. This point is included for comparative purposes.

Regression analysis was employed to determine whether there was a plateau in the symmetrical exchange frequency for the 10 Gy dose as the dose-rates were reduced from 22.8 to 9.3 to 5.1 cGy hr^{-1}. The first regression was performed on the data for all dose-rates included in this experiment (69.1, 22.8, 9.3, and 5.1 cGy hr^{-1}). The 95% confidence interval on the slope of this regression line did not include zero: $y = (0.00071 \pm 0.00029)*DR + (0.030 \pm 0.011)$; $r^2=0.49$, DR=dose-rate (cGy hr^{-1}), uncertainties are standard errors. A second regression was performed on the data for lowest 3 dose-rates (22.8, 9.3, and 5.1 cGy hr^{-1}). The 95% confidence interval on the slope of this regression line did include zero: $y = (0.00034 \pm 0.00079)*DR + (0.034 \pm 0.011)$; $r^2=0.044$.

In addition, the nonparametric Kruskal-Wallis test (20) was performed to test for differences between the symmetrical translocation frequencies between all the dose-rates considered, and again between only the lowest three dose-rates. There was no significant difference between the effects per unit dose observed for the lowest three dose-rates, but there was a significant increase at the highest dose-rate (69.1 cGy hr^{-1}).

Lymphocyte dose-rate effect:

To determine whether the plateau in the dose-rate effect also applied for lymphocytes irradiated *in vivo*, the aberration frequency in lymphocytes was compared between one turtle who received 8 Gy at a dose-rate of 16.3 cGy hr^{-1}, and two turtles who

received the same dose at 5.5 cGy hr^{-1}. The results are summarized in Table 5.2. The symmetrical translocation frequency in the animal receiving 16.3 cGy hr^{-1} was 0.025±0.0071 translocations/cell, while that for the two animals receiving 5.5 cGy hr^{-1} was 0.029±0.0080 and 0.026±0.0068 translocations/cell.

Background symmetrical exchange frequency in lymphocytes:

The data on symmetrical exchange frequency in unirradiated turtles was used to estimate the spontaneous background level of these aberrations in these animals. For this estimate, the pre-irradiation samples from all turtles were combined with the post-sham-irradiated samples from the two sham-irradiated turtles. Only one complete, apparently simple symmetrical exchange was observed in a combined total of 4919 lymphocytes scored. All zero dose lymphocyte data are presented in Table 5.2.

Lymphocyte dose-response:

The dose-response data for turtles irradiated at 5.5 cGy hr^{-1} over a range of total doses from 0-8 Gy are summarized in Table 5.2 and the values are plotted in Figure 5.2. The data plotted in Figure 5.2 are the net symmetrical translocation frequencies (frequency after irradiation – frequency before irradiation) for each turtle, however the symmetrical translocation frequency before irradiation was zero in all of the pre-irradiation samples. Figure 5.2 also shows the least squares regression line: Y_{AS} = (0.0041±0.0014) + (0.0031±0.00035)*D; where Y_{AS} is the complete, apparently simple symmetrical translocation frequency per cell, and D is the dose in Gy (r^2 = 0.91, n = 10,

Table 5.2. Chromosomal aberrations* involving *T. scripta* chromosome 1 as determined by FISH whole chromosome painting at the first mitosis before and after 0-8 Gy of ^{137}Cs gamma rays delivered to lymphocytes *in vivo* at 5.5 cGy hr^{-1}.

			Interchange aberrations total (%)			
			Symmetrical		Asymmetrical†	
Dose (Gy)	# cells scored	Total color Junctions (%)	Apparently simple	Complex or incomplete	Apparently simple	Complex or incomplete
0	300	0 (0.00)	0 (0.00)	0 (0.00)	0 (0.00)	0 (0.00)
0	600	3 (0.50)	1 (0.17)	1 (0.17)	0 (0.00)	0 (0.00)
0	500	0 (0.00)	0 (0.00)	0 (0.00)	0 (0.00)	0 (0.00)
0	489	0 (0.00)	0 (0.00)	0 (0.00)	0 (0.00)	0 (0.00)
0	300	0 (0.00)	0 (0.00)	0 (0.00)	0 (0.00)	0 (0.00)
1	319	8 (2.51)	2 (0.63)	1 (0.31)	1 (0.31)	1 (0.31)
0	300	0 (0.00)	0 (0.00)	0 (0.00)	0 (0.00)	0 (0.00)
1	700	18 (2.57)	5 (0.71)	1 (0.14)	2 (0.29)	3 (0.43)
0	300	0 (0.00)	0 (0.00)	0 (0.00)	0 (0.00)	0 (0.00)
2	700	22 (3.14)	10 (1.43)	2 (0.29)	0 (0.00)	0 (0.00)
0	300	0 (0.00)	0 (0.00)	0 (0.00)	0 (0.00)	0 (0.00)
2	213	14 (6.57)	3 (1.41)	3 (1.41)	2 (0.94)	1 (0.47)
0	400	0 (0.00)	0 (0.00)	0 (0.00)	0 (0.00)	0 (0.00)
4	300	16 (5.33)	6 (2.00)	2 (0.67)	0 (0.00)	2 (0.67)
0	500	0 (0.00)	0 (0.00)	0 (0.00)	0 (0.00)	0 (0.00)
4	700	48 (6.86)	11 (1.57)	12 (1.71)	5 (0.71)	4 (0.57)
0	300	0 (0.00)	0 (0.00)	0 (0.00)	0 (0.00)	0 (0.00)
8	453	33 (7.28)	13 (2.87)	3 (0.66)	0 (0.00)	4 (0.88)
0	300	0 (0.00)	0 (0.00)	0 (0.00)	0 (0.00)	0 (0.00)
8	550	37 (6.73)	14 (2.55)	6 (1.09)	1 (0.18)	1 (0.18)
0	330	0 (0.00)	0 (0.00)	0 (0.00)	0 (0.00)	0 (0.00)
8#	511	36 (7.05)	13 (2.54)	2 (0.39)	4 (0.78)	0 (0.00)

Dashed lines denote individual turtles. For each turtle, the first line is pre-irradiation data, and the second line is post-irradiation data.

* Interstitial and terminal deletions not scored.

† Centromeres were frequently obscured as a result of the FISH procedure. This leads to a bias resulting in a deficiency of asymmetrical (dicentric) aberrations with a corresponding excess of the symmetrical counterpart.

Dose-rate =16.3 cGy hr^{-1}

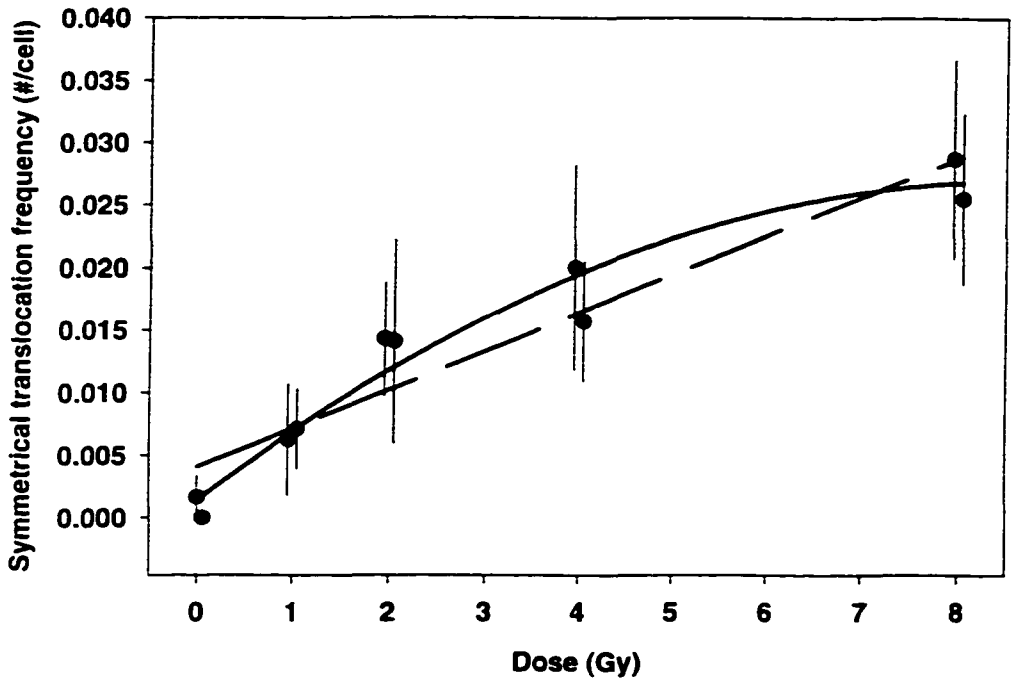

Figure 5.2:

Dose-response curve for *T. scripta* lymphocytes continuously exposed to ^{137}Cs gamma rays *in vivo*. All irradiations were carried out at 25°C at a dose-rate of 5.5 cGy hr^{-1}. Each datapoint represents the net frequency (frequency after irradiation – frequency before irradiation) of apparently simple, complete symmetrical translocations involving chromosome 1, but no translocations were observed in any pre-irradiation sample. Datapoints are offset for clarity. Error bars represent 1 standard deviation based on Poisson counting statistics. The least square regression is shown (dashed line), however a linear-quadratic curve (solid line) gave a significantly better fit to the data ($\alpha = 0.05$).

uncertainties for each coefficient are standard errors). A significantly better fit (as determined by an F-test (21)) is given by a second-order polynomial, $Y_{AS} = (0.0015 \pm 0.0013) + (0.0058 \pm 0.0009)*D - (0.00033 \pm 0.00011)*D^2$, ($r^2 = 0.96$, $n = 10$). The improvement was significant at $\alpha = 0.05$, but not at $\alpha = 0.01$.

Discussion and conclusions:

Dose-rate effect:

It is well known from numerous studies using diverse endpoints in a variety of organisms that for sparsely ionizing radiation, there is a reduction in the effect of a given dose when the dose-rate is lowered or the dose is fractionated or otherwise protracted in time (22). The dose-rate effect generally applies over a range of dose-rates between a few Gy hr^{-1} down to a few cGy hr^{-1}. At the low end, there often appears to be a minimum dose-rate, below which further reductions in dose-rate result in no further diminution of response per unit dose *i.e.* a plateau is reached (5-12,19).

The dose-rate effect for the production of chromosomal aberrations in *Tradescantia* microspores was first described by Sax (10). This effect has since been observed, for example, in the survival of human (5,6,23) and murine (12) fibroblasts, in the induced frequency of unstable aberrations in human lymphocytes (24-30) and in mutation induction in mice (11). The only study of dose protraction for stable translocations detected by FISH that I am aware of was recently conducted in murine lymphocytes and this study involved fractionating the dose over time rather than reducing the dose-rate (31). A comparison of the dose-rate effect data from this study to that observed for a variety of endpoints in a variety of organisms is illustrated in Figure 5.1.

Because different endpoints were used, data from the original studies were normalized by dividing each data value by the maximum observed effect. For the case where cell killing was the biological effect (12), survival values were converted to the corresponding lethal events per cell to facilitate the comparison. I observed a dose-rate effect for symmetrical translocations in *T. scripta* fibroblasts similar to that observed for radiation-induced mutations in mice (11,19), chromosome aberrations in human AG1522 fibroblasts (6,7) and in *Tradescantia* microspores (10), and for survival of mouse C3H 10T1/2 cells (12).

A study of the dose-rate effect for symmetrical translocations induced in turtle cells was necessary to ensure the accuracy of the calibration curve constructed in this study using chronic irradiation. If the dose-rate used in the laboratory study was not in the minimum dose-rate plateau, then low dose-rate or protracted doses received by turtles in the field would be underestimated, as illustrated in Figure 5.3.

In an effort to more closely mimic *in vivo* conditions, the fibroblast cultures were irradiated in a 2% oxygen environment. While this oxygen level would be considered at the low end of the normal range for mammalian systems where 2-5% normal tissue oxygen tensions are typical (32), the 2% level is not unrealistic for turtles due to their diving behavior. It is well documented that turtles have an extraordinary ability to survive in hypoxic, or even anoxic conditions. Ultsch and Jackson (33) subjected *Chrysemys picta*, an emydine species closely related to *T. scripta*, to forced submergence in anoxic water at 3°C, where they survived for over 6 months. While *T. scripta* can survive long anoxic or hypoxic periods, they do not subject themselves to such extreme conditions voluntarily. *T. scripta* can be found as far north as Michigan (34),

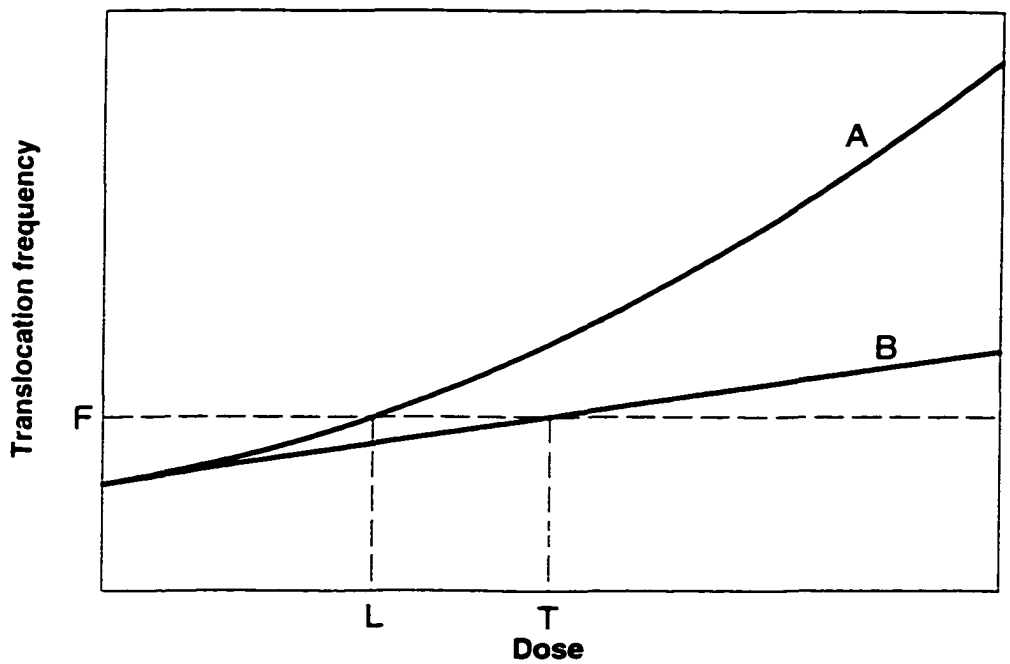

Figure 5.3:
Hypothetical curves showing a curvilinear dose-response relationship resulting from administration of the dose at a dose-rate where the dose-rate-dependent component is greater than zero (curve A), and a linear relationship resulting from administration of the dose at a chronic dose-rate where the dose-rate-dependent component has disappeared (curve B). Assume a turtle receives a dose from a contaminated environment, resulting in a symmetrical translocation frequency, F. Using curve A as a calibration curve for such an animal would result in an erroneously low estimate of dose (L), while the true dose received (T) would be obtained by using curve B.

where they are most likely subjected to hypoxia during overwintering in frozen ponds and slow-moving streams. But over much of *T. scripta*'s geographic range, winters are much milder and water bodies do not typically freeze. In such habitats, turtles are typically active in the warm seasons, but are semi-dormant in winter. Nevertheless, they have free access to air, even in winter, and do surface to breathe and even bask on warm days.

Most voluntary dives by *T. scripta* and other emydine turtles are of short enough duration [5-6 minutes for *T. scripta* at 20-25°C (35)] to be entirely aerobic (36). However, even during periods of short-term submergence, oxygen stores are rapidly depleted. Jackson (37) found that after approximately 15 minutes of submergence in 24°C water, average blood oxygen content (in samples obtained from cardiac puncture) in *T. scripta* had dropped to approximately 2% (from 6% before submergence). A minimum value of approximately 0.75% was reached after 45 minutes, where it remained for the duration of the study (4 hours). Similarly, Crocker (38) found that arterial blood in *C. picta* had an oxygen content of only 0.22% after 6 hours of submersion in 20°C water. As observed in both humans (32) and mice (39), pO_2 in normal tissues is clearly lower than in blood vessels in the immediate vicinity. I felt that irradiating cultures in a 2% oxygen environment was an appropriate balance between full aerobic conditions and complete anoxia.

A concern for lowering the oxygen tension would, of course, be whether the pO_2 I chose, or more importantly the typical pO_2 levels in critical tissues of turtles, would be low enough to affect radiosensitivity. For the following reason, I would not expect the O_2 level of 2% used in this study to appreciably affect radiosensitivity. A general

formulation often used to describe radiosensitivity as a function of oxygen tension is: $r = (m[O_2]+k) / ([O_2]+k)$; where $[O_2]$ is the oxygen concentration required to increase the radiosensitivity above that for anoxic cells by the factor, r, which approaches a maximum value, m, at high oxygen concentrations (40,41). The value of k is the concentration of oxygen where the radiosensitivity is half way between the minimum and maximum sensitivities. Since the maximum, m, usually refers to the maximum oxygen enhancement ratio and has a value of about 3.0, and k generally corresponds to around 0.4%, I would expect relative radiosensitivity to be 2.67 for the 2% O_2 level I used compared to 2.85 to 2.92 for the 5-10% O_2 levels that might represent the highest expected values for normal mammalian tissues.

Of course, the turtle fibroblasts in culture, like any cells, respire and utilize oxygen. At 22°C, Chinese hamster cells consume about $4x10^{-18}$ moles of O_2 per cell per second (42). This corresponds to $(8.64x10^4) * (4x10^{-18}$ moles of O_2 per cell per day) = $3.46x10^{-13}$ moles O_2 per cell per day or for a culture containing $3.75x10^6$ cells, the culture consumption would be $1.3x10^{-6}$ moles d^{-1} or about 1.3 μmoles d^{-1}. Our T-150 flasks contain about 755 cc of the 2% O_2 gas mixture, or 15.1 cc O_2. Since a gas occupies 22.4 L $mole^{-1}$ at STP, or about 27 L $mole^{-1}$ in Fort Collins, CO, this corresponds to 15.1/27,000 moles O_2 or 559 μmoles. For the longest radiation exposures of 8 days at the lowest dose-rate used, only 10.4 μmoles would be consumed by the cells. This would result in a fractional reduction of oxygen by only 10.4/559 = 0.019, or from 2% to 1.86%. In turn, this would decrease the relative radiosensitivity from about 2.67 for 2% O_2, to about 2.65 for 1.86% O_2, i.e. the radiosensitivity would be expected to change by only about 0.75%.

Statistical analysis of results:

The regression analyses and the nonparametric Kruskal-Wallis test both indicated a plateau when the lowest three dose-rates (5.1, 9.3 and 22.8 cGy hr^{-1}) were analyzed, but not when the highest dose-rate (69.1 cGy hr^{-1}) was included. Several conclusions can be drawn from these results, namely: (1) a dose-rate effect was observed, with decreases in effect for a given dose with protraction of the dose; (2) the plateau of the dose-rate effect begins at a dose-rate between 69.1 and 22.8 cGy hr^{-1}, and no further reductions in effect per unit dose were seen at lower dose-rates; (3) the presence of a plateau in the dose-rate effect would indicate that irradiation at the lower dose-rates experienced by turtles in contaminated environments would not be expected to result in a dose-response relationship significantly different from that observed in this study, unless the dose-rate effect in turtles operates differently from that observed in all other organisms studied previously.

Further evidence that the 5.5 cGy hr^{-1} dose-rate used for lymphocyte irradiation in this study is low enough to be contained in the plateau region of the dose-rate effect was provided by the irradiation of one animal at 16.3 cGy hr^{-1}. This is nearly three times the dose-rate used for the turtles in the dose-response experiment, yet the induced frequency of symmetrical exchanges in the turtle receiving the higher dose-rate was nearly identical to the two animals receiving the same dose (8 Gy) at the lower dose-rate of 5.5 cGy hr^{-1} (Table 5.2). This result, especially when combined with the fibroblast results and what is generally known about dose-rate effects in other systems, suggests that the dose-rate used in this study yielded a calibration curve which should be appropriate for use with animals

receiving lower dose-rate environmental exposures. I cannot, of course, rule out other complicating factors without observations at much lower dose-rates under field conditions, but I should have a reasonable approximation with the present results.

Background level of symmetrical translocations in T. scripta lymphocytes:

One of the most significant disadvantages of using symmetrical translocations, as opposed to dicentrics, for retrospective biodosimetry is that the background frequency of symmetrical translocations in humans is up to 10 times higher than that for dicentrics (43). A further complication is the apparent correlation in humans between individual age and background symmetrical translocation frequency (43). Background symmetrical translocations are most likely caused by endogenous biological processes rather than exposure to environmental clastogens such as man-made pollutants or natural sources of ionizing radiation (44). One of the most significant potential sources of symmetrical translocations is free radical damage resulting from oxygen metabolism (45-48).

In contrast to mammals, a very low frequency of symmetrical translocations was observed in *T. scripta* lymphocytes. The full-genome equivalent background frequency was (1.20 ± 1.20) x 10^{-3} complete, apparently simple, symmetrical translocations per cell. Background estimates for humans range from 7.30×10^{-3} (49) to 3.39×10^{-2} (50) translocations/cell, (original human data was converted to full genome equivalent using chromosome length measurements (51) and the formula provided by Lucas (52)). Only complete translocations involving two bicolored chromosomes were included and counted as a single event. Based on these values, the background frequency in *T. scripta* is only 4-16% of that seen in humans. It should be noted that there is a large uncertainty

associated with all of these values, as they are based on a very small number of observed symmetrical translocations. Nevertheless, it appears that the background symmetrical exchange frequency in *T. scripta* lymphocytes is appreciably lower than that in human lymphocytes. A major issue in radiation protection, both for humans and for other organisms in the environment is the detection and quantification of effects at very low doses. Even though turtles are more radioresistant than humans by a factor of about 2 (4), and would therefore appear to be a less sensitive indicator species for biodosimetry, the "background noise" of aberrations can be much more of a limiting factor for this purpose than absolute sensitivity. A 5- to 30-fold lower background aberration frequency for turtles may in fact make them a more sensitive organism for purposes of detection of protracted, low-level effects.

There are several plausible explanations for a lower background aberration frequency in *T. scripta*. First, the turtle's resting metabolic rate is a fraction of that of mammals largely due to the fact that turtles are ectothermic, while mammals are endothermic. Furthermore, the turtle metabolic rate is depressed when they dive (37,38) or hibernate (53,54), so the difference is even more pronounced during the significant portion of their lives turtles spend underwater. As a result of their lower metabolic rate, turtle chromosomes might be expected to be exposed to less damage from reactive oxygen species (ROS) resulting from oxygen metabolism. In spite of their much lower exposure to ROS-damage, *T. scripta* has cellular levels of protective antioxidants similar to those of humans (55,56).

I therefore conclude that the low background frequency of symmetrical translocations in *T. scripta* is a significant advantage for environmental biodosimetry studies, especially at low doses and dose-rates typical of contaminated environments.

Dose-response of turtle lymphocytes irradiated in vivo at a low dose-rate:

As shown in Figure 5.2, the complete symmetrical translocation frequency increased with dose. A weighted linear regression gave a good fit to the data, as expected since the dose was administered at a low dose-rate. However, the linear regression appears to overestimate the spontaneous background frequency of symmetrical translocations. In fact, it would appear that a curvilinear fit, with a flattening of the curve at higher doses provides a better fit to the data. A curvilinear dose-response would be expected if saturation was approached at higher doses, but the aberration frequency was quite low, even at the highest dose tested. Saturation does not appear to be occurring, and it is difficult to envision another justification for a curvilinear fit. It should be noted that since the frequency of translocations was low, there are substantial errors associated with each data point. This being the case, it is difficult to state with any degree of confidence whether a slight flattening of the curve at higher doses is occurring. Nevertheless, the curvilinear fit represents the best fit to the data, and should therefore be used as the calibration curve for environmental biodosimetry until more data becomes available.

A complication for determination of symmetrical translocation frequency is that centromeres are often obscured by the harsh denaturation treatments involved in the FISH procedure, which leads to a mis-scoring of some asymmetrical translocations as

symmetrical unless a pancentromeric probe is also used (57). This is especially problematic for the *T. scripta* genome because of the presence of several microchromosomes, the centromeres of which are difficult to detect even under the best of circumstances. Definitive identification of translocations as symmetrical or asymmetrical will be possible once a pancentromeric probe becomes available. Classical theory predicts that symmetrical and asymmetrical translocations should occur in equal frequency (58), as has been observed in several studies (49,59-63), but some recent studies have noted an excess of symmetrical translocations even when centromeres are readily visible, either by use of a pancentromeric probe or when DAPI staining allows positive centromere identification (64-67). Still, an unknown portion of the excess symmetrical translocations observed in this study are almost certainly due to misclassification of some asymmetrical translocations as symmetrical.

The dose-response relationship depicted in Figure 5.2 (solid curve) represents a calibration curve which, to a first approximation, should be suitable for use with turtles from contaminated environments who have received unknown doses of sparsely ionizing radiation. A few improvements would make this methodology practical for use on a routine basis in biomonitoring and ecological risk assessment.

First, it will be necessary to determine the persistence of symmetrical translocations in *T. scripta* lymphocytes over much longer times. It has previously been assumed that since these aberrations do not explicitly result in the loss of genetic material, they should be stable over time, as suggested by several studies (60,68-71). However, some recent studies suggest that there is at least some initial loss of symmetrical translocations, followed by a plateau above control values (72-75). I plan to

resample the animals used in this study periodically to determine the stability of symmetrical translocations frequencies over much longer periods.

As mentioned previously, the development of a centromere-specific probe would allow for unequivocal discrimination of symmetrical and asymmetrical translocations. This would have important ramifications for the determination of translocation persistence, since asymmetrical translocations are unstable and disappear over time. If a fraction of the aberrations scored as symmetrical translocations are actually asymmetrical, it could appear that symmetrical translocations are declining when this is not in fact occurring, or at least any such decline could be overestimated.

The most important improvement to this methodology would be the development of probes for additional *T. scripta* chromosomes. In this species, 2n = 50, and chromosome 1 represents approximately 17% of the *T. scripta* genome (as determined by measuring DAPI and chromomycin fluorescence on identical chromosomes and also by chromosome length measurements). Probes for the five largest chromosomes would allow 56% of the genome to be painted, while the largest 10 chromosomes would cover 80% of the genome. Additional probes and perhaps multiplex fluorescence *in situ* hybridization (mFISH) could provide some advantage in this regard (76).

The results of this study demonstrate that using whole-chromosome FISH probes for environmental biodosimetry represents a promising new methodology for conducting exposure assessments for organisms inhabiting radionuclide-contaminated environments. Environmental biodosimetry using stable chromosome translocations is clearly feasible, and would provide a genetically relevant measurement endpoint for ecological risk assessments. With the modest improvements discussed above, this methodology could

result in more precise and ecologically meaningful risk assessments and biomonitoring programs.

Acknowledgements:

The authors would like to thank Dr. Phil Chapman of the Colorado State University Department of Statistics for advice on statistical procedures. This work was supported by the Department of Energy grant RR267-055/4895914 to University of Georgia, Savannah River Ecology Laboratory and subcontract to Colorado State University, and a grant from the NIH, National Cancer Institute, 5 T32 CA09236 to Colorado State University.

REFERENCES

1. Wolbarst, A. B., Blom, P. F., Chan, D, Cherry, R. N. Jr., Doehnert, M., Fauver, D., Hull, H. B., MacKinney, J. A., Mauro, J., Richardson, A. C. B., and Zaragoza, L., Sites in the United States contaminated with radioactivity. *Health Physics* **77**, 247-260 (2000).

2. Whicker, F. W., Shaw, G., Voigt, G., and Holm, E, Radioactive contamination: the state of the science and its application to predictive models. *Environmental Pollution* **100**, 133-149 (2000).

3. Whicker, F. W. and Bedford, J. S., Environmental impact of radioactive releases. In *Proceedings of an International Symposium on Environmental Impact of Radioactive Releases* pp. 561-567. International Atomic Energy Agency, Vienna, (1995).

4. Ulsh, B. A., Muhlman-Diaz, M., Whicker, F. W., Hinton, T. G., Congdon, J. D, and Bedford, J. S., Chromosome translocations in turtles: a biomarker in a sentinel animal for ecological dosimetry. *Radiation Research* **153**, 752-759 (2000).

5. Bedford, J. S. and Hall, E. J., Survival of HeLa cells cultured *in vitro* and exposed to protracted gamma-irradiation. *International Journal of Radiation Biology* **7**, 377-383 (1963).

6. Bedford, J. S. and Cornforth, M. N., Relationship between the recovery from sublethal X-ray damage and the rejoining of chromosome breaks in normal human fibroblasts. *Radiation Research* **111**, 406-423 (1987).

7. Cornforth, M. N., Bailey, S. M., and Goodwin, E. H., Radiation induced chromosomal aberrations in noncycling human fibroblasts under limiting low dose rates: implications concerning initial slopes and models of saturable repair. In *Forty first Annual Meeting of the Radiation Research Society* (1993).

8. Hall, E. J. and Bedford, J. S., A comparison of the effects of acute and protracted gamma-radiation on the growth of seedlings of *Vicia faba* Part I. Experimental observations. *International Journal of Radiation Biology* **8**, 467-474 (1964).

9. Purrott, R. J. and Reeder, E. J., Chromosome aberration yields induced in human lymphocytes by 15 MeV electrons given at a conventional dose-rate and in microsecond pulses. *International Journal of Radiation Biology & Related Studies in Physics, Chemistry & Medicine* **31**, 251-256 (1977).

10. Sax, K., The time factor in X-ray production of chromosome aberrations. *Proceedings of the National Academy of Sciences of the United States of America* **25**, 225-233 (1939).

11. Searle, A. G., Mutation induction in mice, In *Advances in Radiation Biology* (Lett, J. T., Adler, H., and Zelle, M., Eds.), pp. 131-207. Academic Press, San Diego, CA, (1974).

12. Wells, R. L. and Bedford, J. S., Dose-rate effects in mammalian cells. IV. Repairable and nonrepairable damage in noncycling C3H 10T 1/2 cells. *Radiation Research* **94**, 105-134 (1983).

13. Spotila, J. R., Foley, R. E., and Standora, E. A., Thermoregulation and climate space of the slider turtle, In *Life History and Ecology of the Slider Turtle* (Gibbons, J. W., Eds.), pp. 288-298. Smithsonian Institution Press, Washington, D.C., (1990).

14. Tucker, J. D., Morgan, W. F., Awa, A. A., Bauchinger, M., Blakey, D., Cornforth, M. N., Littlefield, L. G., Natarajan, A. T., and Shasserre, C., A proposed system for scoring structural aberrations detected by chromosome painting. *Cytogenetics & Cell Genetics* **68**, 211-221 (1995).

15. Savage, J. R. and Simpson, P. J., FISH "painting" patterns resulting from complex exchanges. *Mutation Research* **312**, 51-60 (1994).

16. Deng, W. and Lucas, J. N., Combined FISH with pan-telomeric PNA and whole chromosome-specific DNA probes to detect complete and incomplete chromosomal exchanges in human lymphocytes. *International Journal of Radiation Biology* **75**, 1107-1112 (1999).

17. Kodama, Y., Nakano, M., Ohtaki, K., Delongchamp, R., Awa, A. A., and Nakamura, N., Estimation of minimal size of translocated chromosome segments detectable by fluorescence in situ hybridization. *International Journal of Radiation Biology* **71**, 35-39 (1997).

18. Wu, H., George, K., and Yang, T., Estimate of true incomplete exchanges using fluorescence in situ hybridization with telomere probes. *International Journal of Radiation Biology* **73**, 521-527 (1998).

19. Russell, W. L., The effect of radiation dose rate and fractionation on mutation in mice, In *Repair from Genetic Radiation Damage* (Sobels, F. H., Eds.), pp. 205-217. The MacMillan Company, New York, (1963).

20. Walpole, R. E. and Myers, R. H., *Probability and Statistics for Engineers and Scientists*. Macmillan Publishing Company, New York, NY, (1989).

21. Snedecor, G. W., *Statistical Methods*. The Iowa State University Press, Ames, IA, (1956).

22. National Council on Radiation Protection and Measurements. *Influence of dose and its distribution in time on dose-response relationships for low-LET radiations*. 64, National Council on Radiation Protection and Measurements, Oxford and New York, (4-1-1980).

23. Mitchell, J. B., Bedford, J. S., and Bailey, S. M., Dose-rate effects in plateau-phase cultures of S3 HeLa and V79 cells. *Radiation Research* **79**, 552-567 (1979).

24. Bauchinger, M., Schmid, E., and Dresp, J., Calculation of the dose-rate dependence of the dicentric yield after Co γ-irradiation of human lymphocytes. *International Journal of Radiation Biology* **35**, 229-233 (1979).

25. Bauchinger, M., Quantification of low-level radiation exposure by conventional chromosome aberration analysis. *Mutation Research* **339**, 177-189 (1995).

26. Brewen, J. G. and Luippold, H. E., Radiation-induced human chromosome aberrations: *in vitro* dose rate studies. *Mutation Research* **12** , 305-314 (1971).

27. Edwards, A. A. and Lloyd, D. C., On the prediction of the dose-rate effects for dicentric production in human lymphocytes by X- and γ-rays. *International Journal of Radiation Biology* **37**, 89-92 (1980).

28. Liniecki, J., Bajerska, A., Wyszynsja, K, and Cisowska, B., Gamma-radiation-induced chromosomal aberrations in human lymphocytes: dose-rate effects in stimulated and non-stimulated cells. *Mutation Research* **43**, 291-304 (1977).

29. Lloyd, D. C. and Edwards, A. A., Chromosome aberrations in human lymphocytes: effect of radiation quality, dose, and dose rate, In *Radiation-Induced Chromosome Damage in Man* (Ishihara, T. and Sasaki, M. S., Eds.), pp. 23-49. Alan R. Liss, Inc., New York, (1983).

30. Lloyd, D. C., Purrott, R. J., Dolphin, G. W., Bolton, D, and Edwards, A. A., The relationship between chromosome aberrations and low LET radiation dose to human lymphocytes. *International Journal of Radiation Biology* **28**, 75-90 (1999).

31. Tucker, J. D., Sorensen, K. J., Chu, C. S., Nelson, D. O., Ramsey, M. J., Urlando, C., and Heddle, J. A., The accumulation of chromosome aberrations and Dlb-1 mutations in mice with highly fractionated exposure to gamma radiation. *Mutation Research* **400**, 321-335 (1998).

32. Vaupel, P., Schlenger, K., Knoop, C., and Hockel, M., Oxygenation of human tumors: evaluation of tissue oxygen distribution in breast cancers by computerized O2 tension measurements. *Cancer Research* **51**, 3316-3322 (1991).

33. Ultsch, G. R. and Jackson, D. C., Long-term submergence at 3 degrees C of the turtle Chrysemys picta bellii in normoxic and severely hypoxic water. I. Survival, gas exchange and acid-base status. *Journal of Experimental Biology* **96**, 11-28 (1982).

34. Ernst, C. H., Systematics, taxonomy, variation, and geographic distribution of the slider turtle, In *Life History and Ecology of the Slider Turtle* (Gibbons, J. W., Eds.), pp. 57-67. Smithsonian Institution Press, Washington, D.C., (1990).

35. Bagatto, B. and Henry, R. P., Excercise and forced submergence in the pond slider (Trachemys scripta) and softshell turtle (Apalone ferox): influence on bimodal gas exchange, diving behaviour and blood acid-base status. *Journal of Experimental Biology* **202**, 267-278 (1999).

36. Gatten, R. E. Jr., Anaerobic metabolism in freely diving painted turtles (Chrysemys picta). *Journal of Experimental Zoology* **216**, 377-385 (1981).

37. Jackson, D. C., Metabolic depression and oxygen depletion in the diving turtle. *Journal of Applied Physiology* **24**, 503-509 (1968).

38. Crocker, C. E., Ultsch, G. R., and Jackson, D. C., The physiology of diving in a north-temperate and three tropical turtle species. *Journal of Comparative*

Physiology - B, Biochemical, Systemic, & Environmental Physiology **169**, 249-255 (1999).

39. Vaupel, P., Is there a critical tissue oxygen tension for bioenergetic status and cellular pH regulation in solid tumors? *Experientia* **52**, 464-468 (1996).

40. Deschner, E. E and Gray, L. H., Influence of oxygen tension on X-ray induced chromosomeal damage in Ehrlich Ascites tumor cells irradiated in vitro and in vivo. *Radiation Research* **11**, 115-147 (1959).

41. Howard-Flanders, P. and Alper, T., The sensitivity of microorgansims to irradiation uder controlled gas conditions. *Radiation Research* **7**, 518-540 (1957).

42. Whillans, D. W. and Rauth, A. M., An experimental and analytical study of oxygen depletion in stirred cell suspensions. *Radiation Research* **84**, 97-114 (1980).

43. Lucas, J. N., Deng, W., Moore, D., Hill, F., Wade, M., Lewis, A., Sailes, F, Kramer, C., Hsieh, A., and Galvan, N, Background ionizing radiation plays a minor role in the production of chromosome translocations in a control population. *International Journal of Radiation Biology* **75**, 819-827 (1999).

44. Tucker, J. D., Spruill, M. D., Ramsey, M. J., Director, A. D., and Nath, J., Frequency of spontaneous chromosome aberrations in mice: effects of age. *Mutation Research* **425**, 135-141 (1999).

45. Adelman, R., Saul, R. L., and Ames, B. N., Oxidative damage to DNA: relation to species metabolic rate and life span. *Proceedings of the National Academy of Sciences of the United States of America* **85**, 2706-2708 (1988).

46. Ames, B. N. and Gold, L. S., Endogenous mutagens and the causes of aging and cancer. *Mutation Research* **250**, 3-16 (1991).

47. Ames, B. N. and Shigenaga, M. K., Oxidants are a major contributor to aging. *Annals of the New York Academy of Sciences* **663**, 85-96 (1992).

48. Richter, C., Park, J. W., and Ames, B. N., Normal oxidative damage to mitochondrial and nuclear DNA is extensive. *Proceedings of the National Academy of Sciences of the United States of America* **85**, 6465-6467 (1988).

49. Finnon, P., Moquet, J. E., Edwards, A. A., and Lloyd, D. C., The ^{60}Co gamma ray dose-response for chromosomal aberrations in human lymphocytes analysed by FISH; applicability to biological dosimetry. *International Journal of Radiation Biology* **75**, 1215-1222 (1999).

50. Barquinero, J. F., Cigarran, S., Caballin, M. R., Braselmann, H., Ribas, M., Egozcue, J., and Barrios, L., Comparison of X-ray dose-response curves obtained by chromosome painting using conventional and PAINT nomenclatures. *International Journal of Radiation Biology* **75**, 1557-1566 (1999).

51. NIH/CEPH Collaborative Mapping Group, A comprehensive genetic linkage map of the human genome. *Science* **258**, 67-86 (1992).

52. Lucas, J. N., Awa, A., Straume, T., Poggensee, M., Kodama, Y., Nakano, M., Ohtaki, K., Weier, H. U., Pinkel, D., and Gray, J., Rapid translocation frequency analysis in humans decades after exposure to ionizing radiation. *International Journal of Radiation Biology* **62**, 53-63 (1992).

53. Ultsch, G. R., Ecology and physiology of hibernation and overwintering among freshwater fishes, turtles, and snakes. *Biological Reviews* **64**, 435-516 (1989).

54. Ultsch, G. R., Carwile, M. E., Crocker, C. E., and Jackson, D. C., The physiology of hibernation among painted turtles: the Eastern painted turtle Chrysemys picta picta. *Physiological & Biochemical Zoology* **72**, 493-501 (1999).

55. Storey, K. B., Metabolic adaptations supporting anoxia tolerance in reptiles: recent advances. *Comparative Biochemistry & Physiology - B: Comparative Biochemistry* **113**, 23-35 (1996).

56. Willmore, W. G. and Storey, K. B., Antioxidant systems and anoxia tolerance in a freshwater turtle Trachemys scripta elegans. *Molecular & Cellular Biochemistry* **170**, 177-185 (1997).

57. Straume, T. and Lucas, J. N., A comparison of the yields of translocations and dicentrics measured using fluorescence in situ hybridization. *International Journal of Radiation Biology* **64**, 185-187 (1993).

58. Lucas, J. N., Chen, A. M., and Sachs, R. K., Theoretical predictions on the equality of radiation-produced dicentrics and translocations detected by chromosome painting. *International Journal of Radiation Biology* **69**, 145-153 (1996).

59. Boei, J. J. and Natarajan, A. T., Combined use of chromosome painting and telomere detection to analyse radiation-induced chromosomal aberrations in mouse splenocytes. *International Journal of Radiation Biology* **73**, 125-133 (1998).

60. Fernandez, J. L., Campos, A., Goyanes, V., Losada, C., Veiras, C., and Edwards, A. A., X-ray biological dosimetry performed by selective painting of human chromosomes 1 and 2. *International Journal of Radiation Biology* **67**, 295-302 (1995).

61. Finnon, P., Lloyd, D. C., and Edwards, A. A., Fluorescence in situ hybridization detection of chromosomal aberrations in human lymphocytes: applicability to biological dosimetry. *International Journal of Radiation Biology* **68**, 429-435 (1995).

62. Kanda, R. and Hayata, I., Comparison of the yields of translocations and dicentrics measured using conventional Giemsa staining and chromosome painting. *International Journal of Radiation Biology* **69**, 701-705 (1996).

63. Lindholm, C., Luomahaara, S., Koivistoinen, A., Ilus, T., Edwards, A. A., and Salomaa, S., Comparison of dose-response curves for chromosomal aberrations established by chromosome painting and conventional analysis. *International Journal of Radiation Biology* **74**, 27-34 (1998).

64. Barquinero, J. F., Knehr, S., Braselmann, H., Figel, M., and Bauchinger, M., DNA-proportional distribution of radiation-induced chromosome aberrations analysed by fluorescence in situ hybridization painting of all chromosomes of a human female karyotype. *International Journal of Radiation Biology* **74**, 315-323 (1998).

65. Bauchinger, M., Schmid, E., Zitzelsberger, H., Braselmann, H., and Nahrstedt, U., Radiation-induced chromosome aberrations analysed by two-colour fluorescence in situ hybridization with composite whole chromosome-specific DNA probes and a pancentromeric DNA probe. *International Journal of Radiation Biology* **64**, 179-184 (1993).

66. Dominguez, I., Boei, J. J., Balajee, A. S., and Natarajan, A. T., Analysis of radiation-induced chromosome aberrations in Chinese hamster cells by FISH using chromosome-specific DNA libraries. *International Journal of Radiation Biology* **70**, 199-208 (1996).

67. Knehr, S., Huber, R., Braselmann, H., Schraube, H., and Bauchinger, M., Multicolour FISH painting for the analysis of chromosomal aberrations induced by

220 kV X-rays and fission neutrons. *International Journal of Radiation Biology* **75**, 407-418 (1999).

68. Gebhart, E., Neubauer, S., Schmitt, G., Birkenhake, S., and Dunst, J., Use of a three-color chromosome in situ suppression technique for the detection of past radiation exposure. *Radiation Research* **145**, 47-52 (1996).

69. Lloyd, D. C., Moquet, J. E., Oram, S., Edwards, A. A., and Lucas, J. N., Accidental intake of tritiated water: a cytogenetic follow-up case on translocation stability and dose reconstruction. *International Journal of Radiation Biology* **73**, 543-547 (1998).

70. Lucas, J. N., Hill, F. S., Burk, C. E., Cox, A. B., and Straume, T., Stability of the translocation frequency following whole-body irradiation measured in rhesus monkeys. *International Journal of Radiation Biology* **70**, 309-318 (1996).

71. Salassidis, K., Georgiadou-Schumacher, V., Braselmann, H., Muller, P., Peter, R. U., and Bauchinger, M., Chromosome painting in highly irradiated Chernobyl victims: a follow-up study to evaluate the stability of symmetrical translocations and the influence of clonal aberrations for retrospective dose estimation. *International Journal of Radiation Biology* **68**, 257-262 (1995).

72. Matsumoto, K., Ramsey, M. J., Nelson, D. O., and Tucker, J. D., Persistence of radiation-induced translocations in human peripheral blood determined by chromosome painting. *Radiation Research* **149**, 602-613 (1998).

73. Spruill, M. D., Nelson, D. O., Ramsey, M. J., Nath, J., and Tucker, J. D., Lifetime persistence and clonality of chromosome aberrations in the peripheral blood of mice acutely exposed to ionizing radiation. *Radiation Research* **153**, 110-121 (2000).

74. Tucker, J. D., Breneman, J. W., Briner, J. F., Eveleth, G. G., Langlois, and Moore, D. H., Persistence of radiation-induced translocations in rat peripheral blood determined by chromosome painting. *Environmental & Molecular Mutagenesis* **30**, 264-272 (1997).

75. Xiao, Y., Darroudi, F., Grigorova, M., and Natarajan, A. T., Induction and persistence of chromosomal exchanges in mouse bone marrow cells following whole-body exposure to X-rays. *International Journal of Radiation Biology* **75**, 1119-1128 (1999).

76. Speicher, M. R., Gwyn, Ballard S., and Ward, D. C., Karyotyping human chromosomes by combinatorial multi-fluor FISH. *Nature Genetics* **12**, 368-375 (1996).